

MASTER

The correction of temperature variations in a radiometer

van Gestel, J.C.A.M.

Award date:
1990

[Link to publication](#)

Disclaimer

This document contains a student thesis (bachelor's or master's), as authored by a student at Eindhoven University of Technology. Student theses are made available in the TU/e repository upon obtaining the required degree. The grade received is not published on the document as presented in the repository. The required complexity or quality of research of student theses may vary by program, and the required minimum study period may vary in duration.

General rights

Copyright and moral rights for the publications made accessible in the public portal are retained by the authors and/or other copyright owners and it is a condition of accessing publications that users recognise and abide by the legal requirements associated with these rights.

- Users may download and print one copy of any publication from the public portal for the purpose of private study or research.
- You may not further distribute the material or use it for any profit-making activity or commercial gain

EINDHOVEN UNIVERSITY OF TECHNOLOGY

FACULTY OF ELECTRICAL ENGINEERING

TELECOMMUNICATIONS DIVISION EC

**THE CORRECTION OF TEMPERATURE
VARIATIONS IN A RADIOMETER.**

by **J.C.A.M. van Gestel**

Graduation Thesis

performed January 1990 – October 1990

Graduation professor: Prof. dr. ir. G. Brussaard

Supervisors: dr. ir. M.H.A.J. Herben

ir. P.J.I. de Maagt

**The faculty of Electrical Engineering of the Eindhoven
University of Technology does not accept any responsibility
for the contents of training and graduation reports.**

ABSTRACT

Research has been done in order to correct temperature variations in a total power radiometer. This radiometer type is compared with other radiometer types currently being used. The temperature dependence of several radiometer parts is analyzed. It appears that the diode, theoretically and practically, is the main cause of radiometer parameter variations due to temperature variations. Software is developed to process the measured data and translate these into radiometer parameters. Also a program is written that can correct for temperature variations. This program only works adequately if the temperature dependence of the parameters is measured accurately. Some initial measurements were performed with the best possible experimental set-up presently available at EUT. Still, a more accurate set-up should be made, in order to define the temperature dependence of the local and overall parameters. The accuracy of such a set-up comes close to the best realizable set-up, especially for the temperature measurements.

CONTENTS.

ABSTRACT.	1
1. INTRODUCTION.	5
2. DIFFERENT RADIOMETER TYPES.	6
2.1 The total power radiometer.	7
2.2 The Dicke radiometer.	8
2.3 The noise injection radiometer.	10
3. SENSITIVITY IN RADIOMETERS.	12
3.1 The variance of the output signal.	12
3.2 Deriving the autocorrelation of the square-law detector output.	13
4. ANALYSIS OF THE RADIOMETER PARTS.	16
4.1 The detector diode.	16
4.1.1 Characteristics of diode detectors.	16
4.1.2 Different diode types.	20
4.1.3 The diode as used in the radiometer.	21
4.2 The mixer.	25
4.2.1 Characteristics of mixers.	26
4.2.2 Diode mixers.	29
4.2.3 The mixer as used in the radiometer.	30
4.3 The oscillator.	31
4.3.1 Characteristics of oscillators.	31
4.3.2 An example: the negative impedance oscillator.	32
4.3.3 The oscillator as used in the radiometer.	34
4.4 The amplifiers.	34
4.4.1 Characteristics of amplifiers.	34
4.4.2 The amplifiers as used in the radiometer.	38
4.5 The video amplifier.	39
4.5.1 Characteristics of video amplifiers.	40
4.5.2 The video amplifier as used in the radiometer.	41

5. TEMPERATURE DEPENDENCE OF THE RADIOMETER PARAMETERS.	43
5.1 A mathematical model for a total power radiometer.	43
5.2 The radiometer on a block diagram level.	44
5.3 The receiver noise temperature.	45
5.4 The overall gain.	46
5.5 The effect of a local temperature change.	47
6. WRITING PROGRAMS FOR SIMULATION/CORRECTION OF THE RADIOMETER OUTPUT.	50
6.1 The procedure Tempdependence.	50
6.2 The procedure Radiometer.	52
6.3 The function Rectemp.	54
6.4 The programs.	54
7. MEASUREMENTS.	58
7.1 The measurement setup.	58
7.1.1 The radiometer.	58
7.1.2 Using the chart recorder.	59
7.1.3 Using a temperature stabilized environment.	61
7.1.4 Temperature sensors.	61
7.1.5 Calibrating the thermocouples.	62
7.1.6 Local heating/cooling.	63
7.2 Results.	65
7.2.1 Overall temperature change.	65
7.2.2 Local temperature changes.	68
7.3 Measuring the IF/video unit after its repair.	69
7.3.1 Reproducibility of sweep measurements.	71
7.3.2 Conversion factor and receiver noise temperature	71
7.3.3 Hysteresis effects.	76
8. CONCLUSIONS AND RECOMMENDATIONS.	80
REFERENCES.	81

APPENDICES.

A1. S-parameters of a two-port network.	84
A2. Example of the use of S-parameters in the microwave region.	85
B. Multiple reflections.	86
C. The calibration curves of the thermocouples.	88
D. The program texts.	90
E. Specifications of the semiconductor components in the IF/video unit.	125
E1. The data sheets of the A1 amplifier.	126
E2. The data sheets of the GPD201 amplifier.	131
E3. The data sheets of the HSCH Schottky diode.	134
E4. The data sheets of the video amplifier.	138

1.INTRODUCTION.

Because of the growing need of telecommunications with geostationary satellites, more transmission capacity is needed. A way to increase this capacity is the use of higher frequency bands. Above 14 GHz (the current limit of practical civil exploitation), the quality of the satellite link is limited by propagation effects, especially attenuation by the atmosphere. Therefore, it is necessary to explore new frequency bands by propagation research. The most relevant parameter of a propagation path that has to be measured is the propagation loss. There is a relation between the attenuation on a propagation path in a certain frequency band and the thermal noise received at the same path and in the same frequency band [1]. A radiometer, which is a highly sensitive microwave receiver and antenna, is capable of measuring thermal noise and therefore capable of providing relevant information about the propagation loss.

The classical design of the radiometer needs a very accurate temperature stabilization and continuous calibration to a reference source. The temperature stabilization is done externally, by keeping the radiometer environment at a well-defined physical temperature. A new approach to the design of radiometers will be investigated by application of modern methods, especially the use of sensors and on-line data processing. This could lead to much more compact and less expensive systems.

In chapter 2, the three most used radiometer types are discussed. In chapter 3, an expression for the radiometer sensitivity is derived. In chapter 4, the temperature dependence of the semiconductor components in the radiometer is discussed. In chapter 5, general expressions are derived for the temperature dependence of the global and local temperature dependence of the radiometer parameters. In chapter 6, the programs that simulate the behavior of the radiometer and process the measured data are discussed. In chapter 7, the measurements are presented and conclusions are drawn in chapter 8.

2. DIFFERENT RADIOMETER TYPES.

In this chapter three different radiometer types will be discussed: the total power radiometer, the Dicke switched radiometer and the noise-injection radiometer. Before the different types are discussed, the idealized radiometer is analyzed .

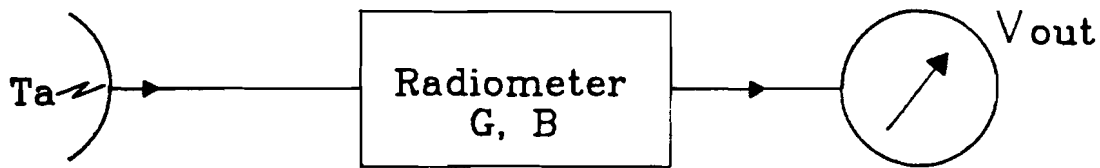


Figure 2.1: The idealized radiometer.

The radiometer selects a portion of the available output power in a certain frequency band from the antenna. The available output power is the maximum output power for an input signal matched with the antenna. The power selected is the available noise power P_a . Here this power is represented by the available noise temperature T_a , which is related to P_a as:

$$P_a = kBT_a \quad (2.1)$$

Where k is Boltzmann's constant. This portion is specified as that power in a certain bandwidth B around a given center frequency. It is amplified with gain G and will be

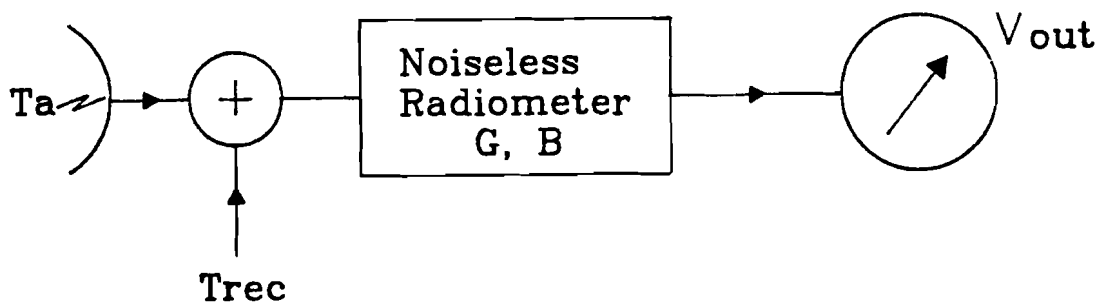


Figure 2.2: A "real" radiometer.

presented on a display (Figure 2.1). It shows [2,3]:

$$V_{\text{out}} = c G P_a = c G k B T_a \quad (2.2)$$

Here k is Boltzmann's constant and c is a linearity constant. Unfortunately, the receiver itself will generate noise, here represented by the receiver noise temperature T_{rec} (Figure 2.2). The antenna signal and the receiver noise are independent, so they will add on a power base. Because the noise sources are independent, they can not be detected separately. The meter now displays:

$$V_{\text{out}} = c k B G (T_a + T_{\text{rec}}) \quad (2.3)$$

2.1 The total power radiometer.

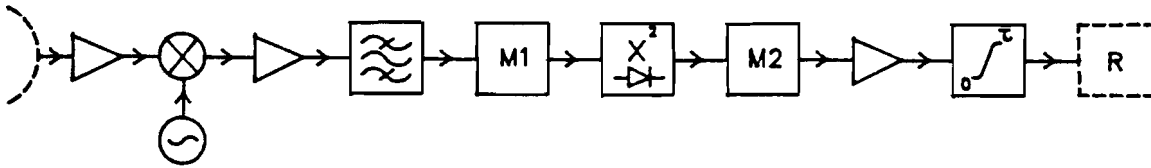


Figure 2.3: A total power radiometer.

The scheme of the total power radiometer is the closest to the idealized radiometer scheme. It also consists of an antenna, an amplifying system, and an output indicating system. The system can be represented as given in the block diagram of figure 2.3. The gain in this radiometer is established by the multiplication of the transfer functions of the different parts and represented in this diagram by G_{if} , G_{rf} and G_{vid} . Of course, the gain also includes the losses from the different non-amplifying parts (filters, the mixer, waveguide, matching losses). The frequency selectivity is established by a filter with a bandwidth B_{if} (centered around a given frequency) and by the frequency selectivity of the RF amplifier that has a bandwidth B_{rf} . B_{rf} is usually larger than B_{if} , so the resulting bandwidth is B_{if} . Then the microwave power has to be detected. Using microwave semiconductor diodes, there are two options to choose as a detector type:

the linear detector and the square-law detector. It is very attractive to use the square-law detector: the output voltage will be proportional to the input noise power and therefore to the input temperature. The input signal for the detector should be amplified before it is applied to the detector. This is to get the signal at such a level, that the diode can operate as a square-law or linear detector. Cheaper amplifiers are available for IF signals. To achieve good detection characteristics, the input signal to the radiometer should be amplified before it is applied to the diode detector. At present radio frequency (RF) amplifiers with good performance (high gain, low noise figure) are too expensive for $RF = 30 \text{ GHz}$. This frequency is one of the frequencies that are of interest for propagation research with the Olympus satellite as performed on EUT. Therefore it is necessary to convert the RF signal down to an intermediate frequency (IF), so that IF amplifiers can be used. The device that converts the frequency down is a mixer. To find the mean of the signal, coming from the detector, an integrator can be used. With a longer integration time the signal can be smoothed more. The output voltage will be a (slow-changing, pseudo) DC signal, and can be expressed as:

$$V_{\text{out}} = c k B G (T_a + T_{\text{rec}}) \quad (2.4)$$

V_{out} is totally dependent on T_{rec} and G . These can not be regarded as stable enough to satisfy reasonable requirements of absolute accuracy.

The sensitivity of the total power radiometer will be derived in chapter 3, but for the sake of completeness be stated here:

$$\Delta T = (T_a + T_{\text{rec}}) \sqrt{\frac{1}{B \tau} + \left[\frac{\Delta G}{G}\right]^2} \quad (2.5)$$

The major problem of this scheme is that its temperature dependent gain varies with time. In the absence of any gain variations, it would be the radiometer with the best sensitivity ΔT .

2.2 The Dicke radiometer.

To reduce the instability problems of the existing radiometers of his time, R.H. Dicke

proposed a scheme [4] in 1946 for reducing the effects of gain fluctuations in a radiometer. Instead of using the radiometer to measure the antenna temperature directly, the difference between this and some reference temperature is measured.

The receiver input is switched at a constant rate between the antenna and a reference load, with a constant noise temperature T_{ref} . Now the output is proportional to the temperature difference between the antenna and the reference load. The block diagram is shown in figure 2.4. Again an expression for V_{out} can be found:

$$V_{out} = c k B \{G(T_a + T_{rec}) - G(T_{ref} + T_{rec})\} \quad (2.6)$$

This can be reduced to:

$$V_{out} = c k B G(T_a - T_{ref}) \quad (2.7)$$

Note that the sensitivity to gain and noise temperature instabilities is greatly reduced in this radiometer type, especially if the reference temperature T_{ref} is chosen closely to the expected available noise temperature T_a .

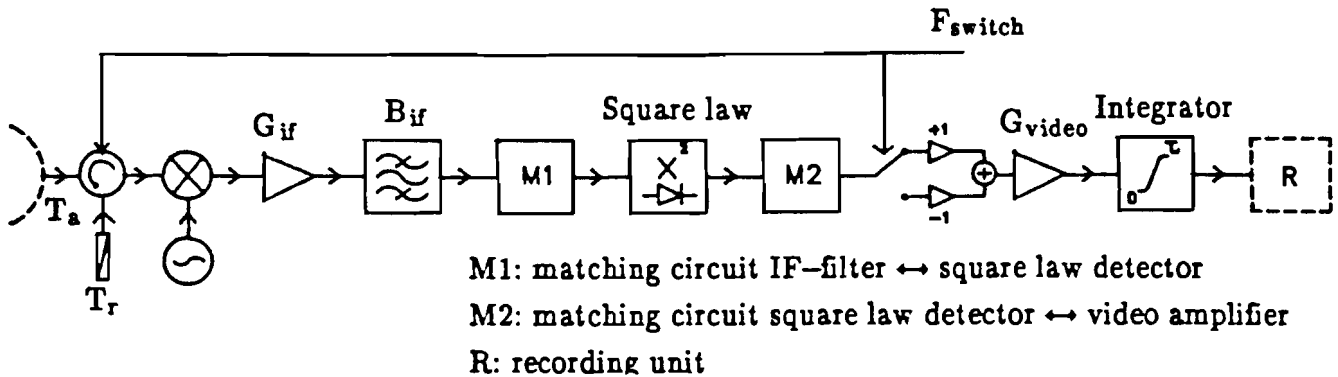


Figure 2.4: The Dicke radiometer.

The switching frequency has to be chosen high enough, so that G is constant while V_{out} is being determined. Now T_{rec} has been eliminated and only changes in G will influence the results. Using equation (2.7), the available noise temperature is found to be:

$$T_a = T_{ref} + \frac{V_{out}}{c k B G} \quad (2.8)$$

The sensitivity ΔT of the Dicke switched radiometer will be:

$$\Delta T = \frac{\sqrt{2(T_a + T_{rec})^2 + 2(T_{ref} + T_{rec})^2}}{\sqrt{B \tau}} \quad (2.9)$$

2.3 The noise-injection radiometer.

From equation (2.7) it can be seen, that the output of a Dicke switched radiometer is zero if the reference temperature and the antenna temperature are equal. If a way is found to keep the reference temperature the same as the antenna temperature, there is a radiometer of which the output is not dependent on G or T_{rec} . The noise-injection radiometer is designed according to this principle [2]. Figure 2.5 shows, how the output noise temperature T_{inj} of a variable noise generator is added to the antenna signal T_a , so that the resultant input T_a' to the radiometer is equal to the reference temperature T_{ref} . A serve loop adjusts T_{inj} to maintain the zero output condition. From equation (2.7) it follows:

$$V_{out} = c k B G (T_a' - T_{ref}) = 0 \quad (2.10)$$

and as:

$$T_a' = T_a + T_{inj} \quad (2.11)$$

T_a satisfies:

$$T_a = T_{ref} - T_{inj} \quad (2.12)$$

T_{ref} is a known constant. T_{inj} has to be known to find T_a . The accuracy with which T_a is determined is independent of the accuracy of the Dicke switched radiometer. It is only dependent on the accuracy of T_{inj} and T_{ref} . The sensitivity of the noise-injection radiometer is found using (2.9). See also [2].

$$\Delta T = \frac{\sqrt{2(T_a' + T_{rec})^2 + 2(T_{ref} + T_{rec})^2}}{\sqrt{B \tau}} \quad (2.13)$$

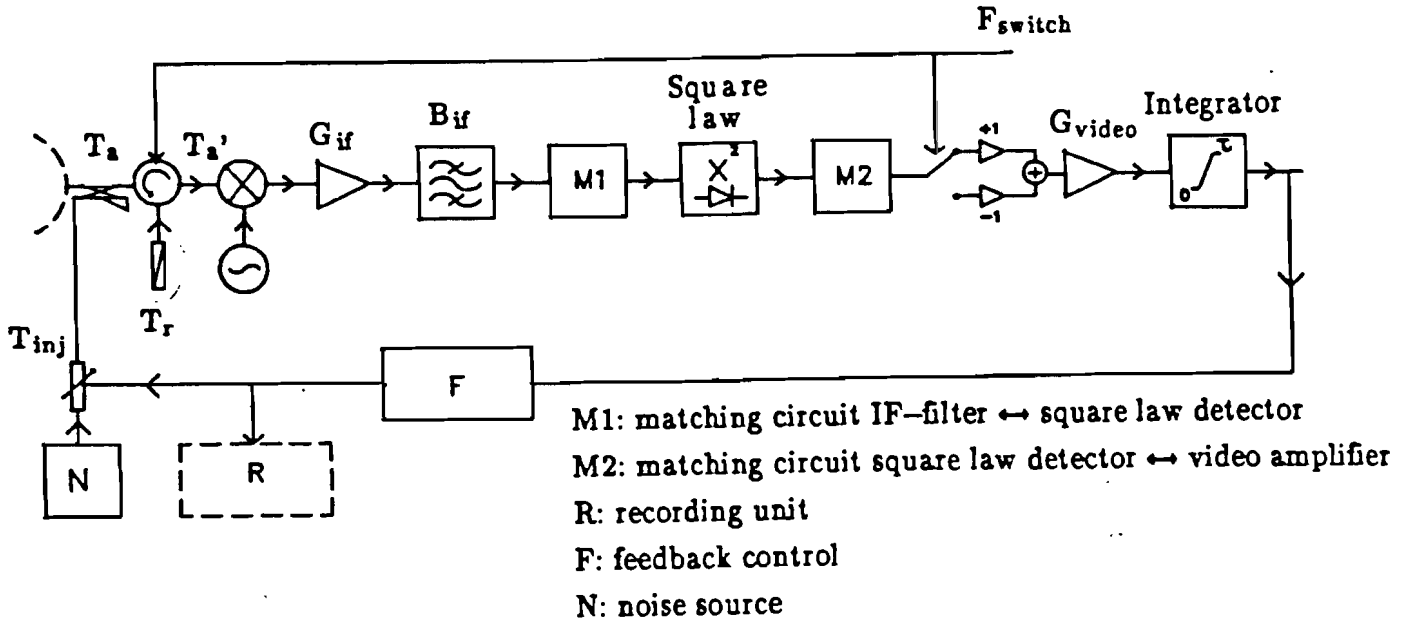


Figure 2.5: A noise-injection radiometer.

But, as T_a' is equal to T_{ref} , equation (2.13) reduces to:

$$\Delta T = 2 \frac{T_{ref} + T_{rec}}{\sqrt{B\tau}} \quad (2.14)$$

The noise-injection radiometer is the design that is expected to have the best sensitivity, because ΔT is insensitive to gain variations [2,3]. The output is independent of gain and noise temperature fluctuations. The sensitivity when no gain variations occur, is not as good as the sensitivity of the total power radiometer, though. Furthermore, this scheme is very complex and therefore very expensive.

3. SENSITIVITY IN RADIOMETERS.

Radiometer sensitivity, ΔT , is the smallest available input noise temperature that can be detected from the radiometer output. This figure is taken to equal the uncertainty in measuring the off-source noise power output referred to the system input.

The radiometer is assumed to be perfectly linear before the diode detector, the predetection circuits serving only to increase the predetector signal and to set the bandwidth. The derivation of ΔT is really the analysis of the output of a detector, the input of which is bandlimited white noise. The standard deviation σ_p of the output voltage of the integrator then equals:

$$\sigma_p = c k B G \Delta T \quad (3.1)$$

The average input power $\overline{P_i}$ at the square-law detector equals:

$$\overline{P_i} = k B G_{pre} (T_a + T_{rec}) \quad (3.2)$$

Here G_{pre} represents the gain before the detector.

3.1 The variance of the output signal.

The samples of the random signal are taken very close together relative to the spacing between independent samples. The variance for integration over a time τ is given by [5,6]:

$$\sigma_p^2 = \frac{2}{\tau} \int_0^{\tau} \left(1 - \frac{t}{\tau}\right) R_{sf}(t) dt \quad (3.3)$$

To find the variance of the output signal from the integrator, the autocovariance $R_{sf}(\tau)$ of the integrator input has to be calculated. The autocovariance is defined as:

$$R_{sf}(\tau_c) = R_{int}(\tau_c) - \overline{V_{int}}^2 \quad (3.4)$$

Where R_{int} is the autocorrelation of the integrator input signal and $\overline{V_{\text{int}}^2}$ is the square mean of this signal. If the voltage gain between the detector and the integrator is taken to be G_{post} , the autocovariance of the integrator input equals:

$$R_{sf}(\tau_c) = G_{\text{post}}^2 (R_{sqo}(\tau_c) - \overline{V_{sqo}}^2) \quad (3.5)$$

$\overline{V_{sqo}}$ is the mean power at the output of the square-law detector. $\overline{V_{sqo}}$ relates to $\overline{P_i}$ as $\overline{V_{sqo}} = c \overline{P_i}$. Now the autocorrelation $R_{sqo}(\tau)$ of the output signal of the square-law detector has to be found.

3.2 Deriving the autocorrelation of the square-law detector output.

At the input of the square-law detector, there is a bandlimited white noise signal. In this observation, the signal is assumed to be an ideal bandpass signal. The spectrum of this signal is given in figure 3.1.

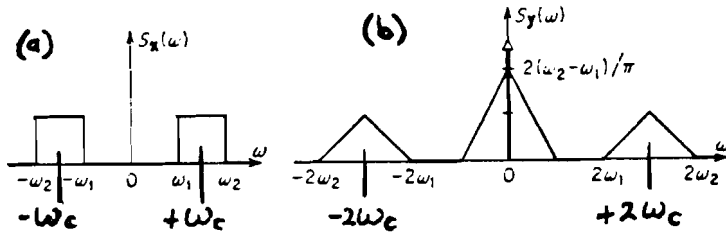


Fig. 3.1a: The power spectrum of the input signal for the square-law device.

b: The power spectrum of the output signal of the square-law device.

The autocorrelation function of such an ideal bandpass white noise signal is:

$$R_{sqi}(\tau_c) = \overline{P_i} \frac{\sin(\pi B \tau_c)}{\pi B \tau_c} \cos(\omega_c \tau_c) \quad (3.6)$$

Here ω_c is the center angular frequency of the IF signal. Because the input $x(t)$ is Gaussian, the autocorrelation R_{sqo} of the output of the square-law detector can be found with [7]:

$$\begin{aligned} R_{sqo}(\tau_c) &= c^2 E\{x^2(t+\tau_c)x^2(t)\} \\ &= c^2 (E\{x^2(t+\tau_c)\}E\{x^2(t)\} + 2E\{x(t+\tau_c)x(t)\}) \end{aligned} \quad (3.7)$$

$$R_{sqo}(\tau_c) = c^2 (R_{sqi}^2(0) + 2R_{sqi}^2(\tau_c)) \quad (3.8)$$

hence the autocorrelation of the output signal is:

$$R_{sqo}(\tau_c) = c^2 (\overline{P_i}^2 \frac{\sin^2(\pi B \tau_c)}{(\pi B \tau_c)^2} (1 + \cos(2\omega_c \tau_c)) + \overline{P_i}^2) \quad (3.9)$$

Now, if the higher frequency components ($\omega \geq \omega_c$) are eliminated, the autocovariance of this signal is:

$$R_{sf}(\tau_c) = G_{post}^2 (R_{sqo}(\tau_c) - \overline{V_{sqo}}^2) = G_{post}^2 (\overline{V_{sqo}}^2 \frac{\sin^2(\pi B \tau_c)}{(\pi B \tau_c)^2}) \quad (3.10)$$

If this is used in equation (3.4), the term t/τ can be considered negligible over the region where the autocovariance function is of significant size in the integrand, so (3.3) may be approximated by:

$$\sigma_p^2 \approx \frac{2 G_{post}^2 \overline{V_{sqo}}^2}{\tau} \int_0^\tau \frac{\sin^2(\pi B t)}{(\pi B t)^2} dt \quad (3.11)$$

This can be integrated analytically to obtain:

$$\sigma_p^2 \approx \frac{G_{post}^2 \overline{V_{sqo}}^2}{\pi B \tau} \left[\frac{\cos(2\pi B \tau) - 1}{\pi B \tau} + 2 \text{Si}(2\pi B \tau) \right] \quad (3.12)$$

Here $\text{Si}(x)$ is the sine-integral function. If $B\tau \gg 1$, the first term in the square brackets is negligible, the second term is approximately π . Now equation (3.12) reduces to:

$$\sigma_p^2 \approx \frac{G_{post}^2 \overline{V_{sqo}}^2}{B \tau} = \frac{c^2 G_{post}^2 \overline{P_i}^2}{B \tau} \quad (3.13)$$

Using (3.1) and (3.2), and knowing $G = G_{\text{post}}G_{\text{pre}}$, it is found that:

$$\Delta T \triangleq \sigma_p \approx \frac{T_a + T_{\text{rec}}}{\sqrt{B\tau}} \quad (3.14)$$

Equation (3.14) only accounts for the measurement uncertainty due to noise fluctuations and does not incorporate receiver gain fluctuations. The root mean square uncertainty in T_a due to system gain variations may be defined as [6]:

$$\Delta T_g = (T_a + T_{\text{rec}}) \left[\frac{\Delta G}{G} \right] \quad (3.15)$$

When naming the ΔT of eq. (3.14) ΔT_n , it is found that:

$$\begin{aligned} \Delta T &= \sqrt{(\Delta T_n)^2 + (\Delta T_g)^2} \\ &= (T_a + T_{\text{rec}}) \sqrt{\frac{1}{B\tau} + \left[\frac{\Delta G}{G} \right]^2} \end{aligned} \quad (3.16)$$

4. ANALYSIS OF THE RADIOMETER PARTS.

As it has already been mentioned in chapter 2, the radiometer consists of several functional parts. In this chapter, an analysis of these parts is made, especially for the temperature dependent characteristics of these parts. It will specifically refer to the actual use in a total power radiometer

4.1 The detector diode.

To detect a microwave signal, a steady or baseband signal whose amplitude is related to that of the original signal has to be produced. To achieve this, the input signal should be applied to a non-linear device. For this device, usually a diode is used.

It is very important that a good detector diode is chosen. The most important parameters that will be discussed here, are the voltage sensitivity γ , the linearity constant k , the tangential signal sensitivity TSS, the video resistance R_v , the nominal detectable signal NDS, and the noise corner frequency. The following diode types will be discussed: the Schottky-barrier, the tunnel and the PIN.

4.1.1 Characteristics of diode detectors.

A. The current-voltage characteristics.

An ideal diode follows the diode equation:

$$I_d = I_s \left(\exp \frac{qV}{n kT} - 1 \right) \quad (4.1)$$

According to equation (4.1), a detector diode can be represented by several constants, the most important are n , the ideality factor, greater than one, but close to unity and I_s , the saturation current. In this equation I_d is the diode current, V the voltage across the diode junction, q is the charge of an electron, k is Boltzmann's constant and T is the temperature in Kelvins.

B. Video resistance (R_v).

The equivalent circuit of a diode is shown in figure 4.1, where L_p and R_s are a series inductance and series resistance, respectively; C_p is the package capacitance, C_j and R_j the

junction capacitance and junction resistance, respectively. R_s , R_j and C_j are dependent on diode material and the junction property. The video resistance is defined as the sum of the diode series resistance and the junction resistance:

$$R_v = R_s + R_j \quad (4.2)$$

The junction resistance is the dynamic resistance of the diode, and it is a function of the DC bias current. It can be obtained by differentiating the diode current–voltage relationship. It is given by:

$$R_j = \frac{dV}{dI_d} = \frac{n k T}{q (I_d + I_s)} \quad (4.3)$$

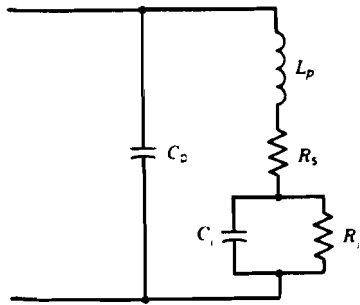


Figure 4.1: Equivalent circuit of a diode detector.

C. Voltage sensitivity (γ).

Voltage sensitivity specifies the slope of the output voltage V_o versus the input power P_i of the detector diode:

$$V_o = \gamma P_i \quad (4.4)$$

γ is only defined for the square law mode of the detector. The value of γ depends on the load resistance, R_l (see figure 4.5), the signal level and the frequency of the input signal. The signal level must be kept in the square law range of the diode. With a higher input signal level, the diode will operate in the linear detection mode, or will even get to saturation (Figure 4.2). A high value of γ means better sensitivity.

D. The linearity constant (k_d).

As follows from figure 4.2, the diode can also operate in a linear detection mode. Then a linearity constant k_d is defined:

$$V_o = k_d V_i \quad (4.5)$$

Here V_i is the input voltage and V_o is the output voltage. In this mode, it is important that the signal level is kept in the linear range.

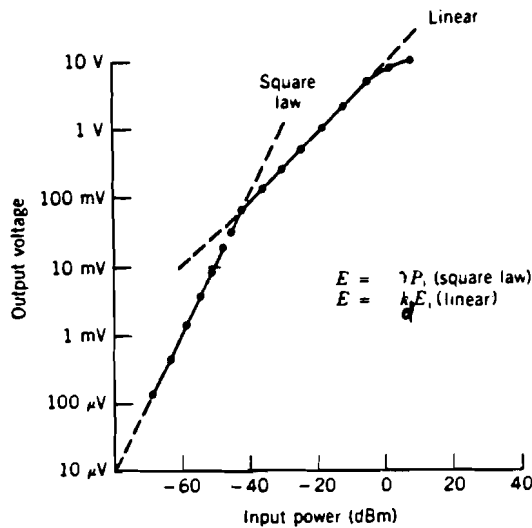


Figure 4.2: Ranges of square-law and linear behavior in a diode detector.

E. Nominal detectable signal (NDS).

NDS is that input IF power level that must be applied to the detector diode that the video power from the detector is 3 dB higher than the video noise level. Besides this it is defined as exactly that microwave power required to produce an output power equal to the noise power [8]. This means that the noise, generated by the detector can be expressed by a noise source with power level NDS at the input of a detector, that does not produce noise. The noise that is generated by the detector will add an extra DC component to the output voltage of the square-law detector. In a well-dimensioned system, NDS is negligible to the input signal of the diode. Also, video frequency noise adds to the random variations at the output of the square-law detector. The noise voltage is given by [12]

$$U_n = \sqrt{2 \sqrt{4kTR_{eq}B}} \quad (4.5a)$$

Here R_{eq} is the equivalent noise resistance of the diode. The diode behaves like a noisy resistor with value R_{eq} .

F. Tangential signal sensitivity (TSS).

TSS is the most common sensitivity rating for diodes. A tangential signal is defined on an oscilloscope display as a pulse whose bottom level coincides with the top level of the noise on either side of the pulse (see figure 4.3). In order to eliminate the subjectivity of the TSS measurement, diode manufacturers define the TSS signal level as the signal level at the input of the diode generating a video output signal which is 8 dB greater than the video noise level.

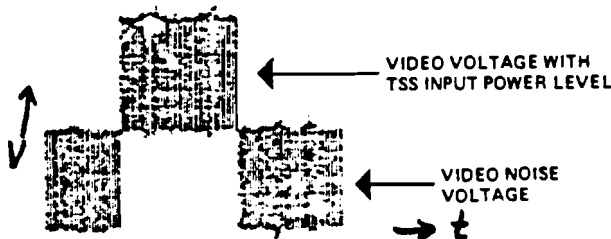


Figure 4.3: Representation of a TSS measurement.

signal [9]. For square law detectors, this places TSS approximately 4dB over NDS.

G. Noise corner frequency.

The presence of a series resistance in the diode substrate makes the effective noise output comparable to resistor noise at high frequencies. The ratio of diode noise power to resistor noise power, the noise temperature ratio, is close to unity at frequencies above a few megahertz. At lower frequencies, diode noise gradually increases and soon reaches an inverse frequency behavior. This excess noise contribution is called flicker noise or $1/f$ noise. There is a frequency at for which the $1/f$ noise line crosses unity noise temperature ratio. This frequency is called the noise corner frequency. The noise corner frequency is

dependent on the type of diode and the bias current. That is, it increases with an increasing bias current [10].

4.1.2 Different diode types.

A. The Schottky–barrier diode.

A Schottky diode uses a barrier, this is a metal to semiconductor junction, to form the diode. In an n–type Schottky–barrier diode, the current flow consists of the majority carriers (electrons). This means that this device can switch very rapidly from forward to reverse bias without minority carrier (holes) effects. The current–voltage characteristics resemble that of a pn–junction, except for the following differences:

- the reverse breakdown voltage is lower,
- the reverse leakage current is higher with the same resistivity of the used n–material,
- the forward voltage of a specific forward current is generally lower for a Schottky diode.(see figure 4.4).

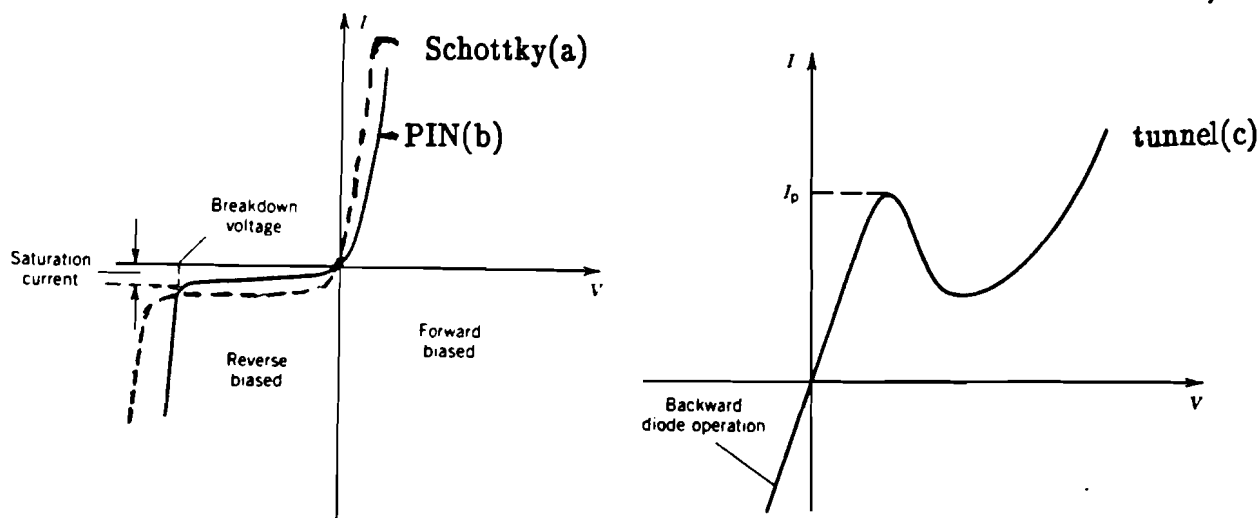


Figure 4.4: The voltage–current curves for a Schottky (a), PIN (b) and tunnel (c) diode.

All Schottky diodes have a lower noise corner frequency than pn junction diodes [11].

B. The tunnel diode.

A tunnel diode is a pn junction device whose doping level is made purposely high. This produces a very narrow junction across which electrons can tunnel easily. The tunneling

phenomenon is a majority carrier (electrons) effect. The tunneling time of carriers through a potential energy barrier is governed by the quantum transition probability per unit time. The tunneling time is very short, permitting the use of tunnel diodes well into the millimeter wave range. The current-voltage curve of a typical tunnel diode is shown in figure 4.6b. When a tunnel diode operates as a detector, it is often biased at a voltage somewhat lower than the voltage corresponding to the peak current I_p . However, a bias voltage in a tunnel diode is not critically required.

C. The PIN-diode.

A PIN-diode is a pn-junction with between the p⁺-region and the n⁺-region an intrinsic layer, also called the i-region. The PIN-diode structure is equivalent to that of a pn-junction in series with a very high resistance formed by the intrinsic semiconductor. It should still have a high resistance according to this model, even when forward biased, but in practice this is not so. As soon as it is forward biased, a current I_d appears because holes pass from the p⁺- to the i-region and electrons from the n⁺-region to the i-region. Before this, the intrinsic region contained practically no free carriers, and has a high resistance, but by the injection of these free carriers the resistivity decreases. This implies, that the series resistance decreases, too. It can be shown that the resistance is dependent on the steady voltage, applied to the diode [12].

4.1.3. The diode as used in the radiometer.

For the radiometer, it is very useful to have an output signal (voltage) with a linear relation to the input noise power. In order to achieve this, the detector will have to operate in the square law mode. In order to use this square law detector, several conditions have to be satisfied. In general, like for any other device, there should be no reflections, or the least possible reflections at both terminals of the detector. Next to this, the input signal should be at a sufficient level, in order to operate the diode as a square-law detector. The input impedance of the diode does not match with 50 Ohms. To match the input signal of the diode, an active diode input match was made [13]. The total circuit is displayed in figure 4.5.

The part of the circuit left of the dashed line is the diode input match. From [13] it can be seen that the gain of this circuit is equal to:

$$G_{\min} = \left| \frac{\frac{Y_{21}}{R_c + R_v}}{\frac{R_c R_v}{R_c R_v} - Y_{22}} \right| \quad (4.8)$$

For $Y_{21} = 33 \exp(j5\pi/6)$ and $Y_{22} = 1.1 \exp(j0.49\pi)$ it can be found that the influence of the video resistance of the diode, R_v , and R_c is negligible, because they both have a resistance of a few $k\Omega$'s. Then it follows:

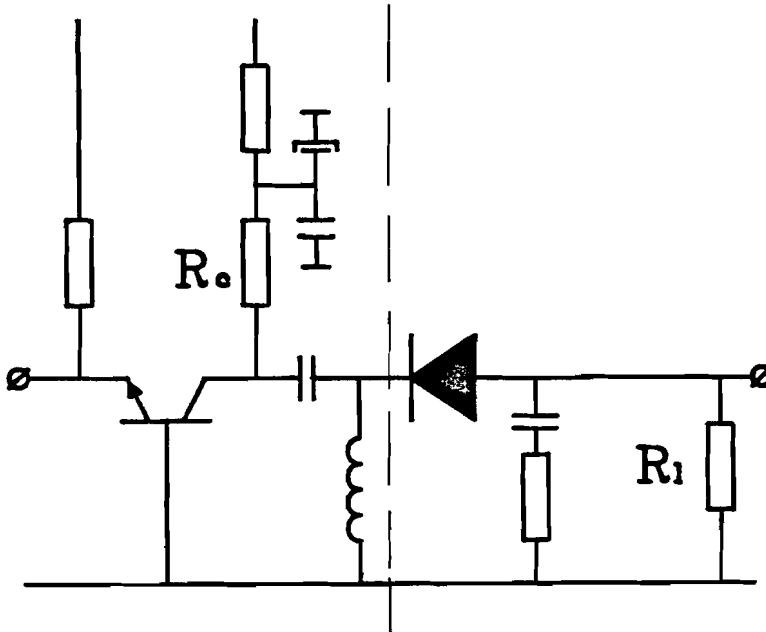


Fig 4.5 The diode detector circuit, with input match and load resistance.

$$G_{\min} = 30 \text{ or } G_{\min} = 14.8 \text{ dB}$$

For a zero bias schottky diode detector, the junction resistance R_j can be written as (eq. 4.3, $I_d = 0$, zero bias):

$$R_j = \frac{nkT}{q(I_s)} \quad (4.9)$$

Where the saturation current I_s is calculated from [14]:

$$I_s = AA^* T^2 \exp\left[\frac{-q\phi}{kT}\right] \quad (4.10)$$

Here A is the diode area and A^* is the modified Richardson constant [16], k is Boltzmann's constant, T is the temperature, ϕ is the barrier voltage and q is the charge of an electron.

If we take $c_1 = AA^*$ and $\phi=0.5$, $n=1$ [14], the video resistance is (eq. 4.2):

$$R_v = R_j + R_s = \frac{\exp(5800/T)}{11600 T c_1} + R_s \quad (4.11)$$

The series resistance is proportional to the physical temperature. The typical value of the series resistance at $T = 298\text{K}$ is 15Ω [15], so:

$$R_s = \frac{15 T}{298} = \frac{T}{19.9} \quad (4.12)$$

This all results in:

$$R_v = \frac{\exp(5800/T)}{11600 c_1 T} + \frac{T}{19.9} \quad (4.13)$$

The basic voltage sensitivity, $\gamma_0 = \beta R_v$ (where β is the current sensitivity of the diode and assumed to be constant as a function of the temperature) for is degraded by the diode parasitics to:

$$\gamma = \frac{\beta R_v}{1 + \omega^2 C^2 R_s R_v} \quad (4.14)$$

And the load resistance reduces this with:

$$\frac{R_1}{R_1 + R_v} \quad (4.15)$$

Resulting in a voltage sensitivity:

$$\gamma = \frac{R_1}{R_1 + R_v} \times \frac{\beta R_v}{1 + \omega^2 C^2 R_s R_v} \quad (4.16)$$

The function seems to reach a maximum for a certain temperature. In order to find this

maximum, the derivative of γ with respect to T can be taken and set equal to zero.

$$\frac{d\gamma}{dT} = 0 \quad (4.17)$$

When calculating this, it comes to the equation:

$$-R_1 \left(1 + \exp \left[\frac{5800}{T} \right] + \left[\frac{5800}{T} \right] \right) + \frac{\omega^2 C^2 \exp(11600/T)}{19.9 (11600)^2 c_1} = 0 \quad (4.18)$$

This equation still contains 4 variables: R_1 , C , c_1 and T . C and c_1 can be chosen by picking a suitable diode. Usually, I_s is given for a diode at a certain temperature, so c_1 can be calculated from equation (4.10). In theory, R_1 can be chosen to get the temperature at which γ reaches its maximum in the range of the temperature at which it operates, but in practice, it is chosen to be equal to R_v , so that R_1 has the lowest possible noise contribution [13]. At the temperature at which γ reaches a maximum, γ has low sensitivity to temperature changes. In order to get the maximum in the operating temperature range, a lower load resistance is needed, which causes γ to degrade quite much, according to equation (4.15). This means a trade-off can be made for absolute γ and the noise contribution of the load resistance towards the sensitivity of γ towards temperature. The result comes closer to the performance of a tunnel diode or to a biased Schottky diode, for which the latter the video resistance is dependent on the bias current rather than the saturation current (eq. 4.3).

In the actual circuit, the diode is chosen to be an HSCH 3486 of Hewlett-Packard. For this diode, the following specifications are known at $T = 25^\circ \text{C}$ (298 K) [15]

$$2\text{k}\Omega < R_v < 8\text{k}\Omega$$

$$\gamma > 7.5 \text{ mV}/\mu\text{W}$$

$$C = 0.3 \text{ pF}$$

$$I_s = 1.0 \mu\text{A}$$

Further, the load resistance has a value of $4.7 \text{ k}\Omega$. From (4.15) it follows that R_v increases with temperature. The specifications of the diode are far from well-defined. This means that the specifications can vary for various individual detector diodes of this type. Therefore the temperature variations can not be known until they are measured. From these typical values, the diode voltage sensitivity can be calculated as a function of the temperature. A plot of the normalized voltage sensitivity as function of the temperature is

shown in figure 4.5a. It appears that, for these specifications, the diode voltage sensitivity could have a maximum close to the temperature range in which the radiometer operates.

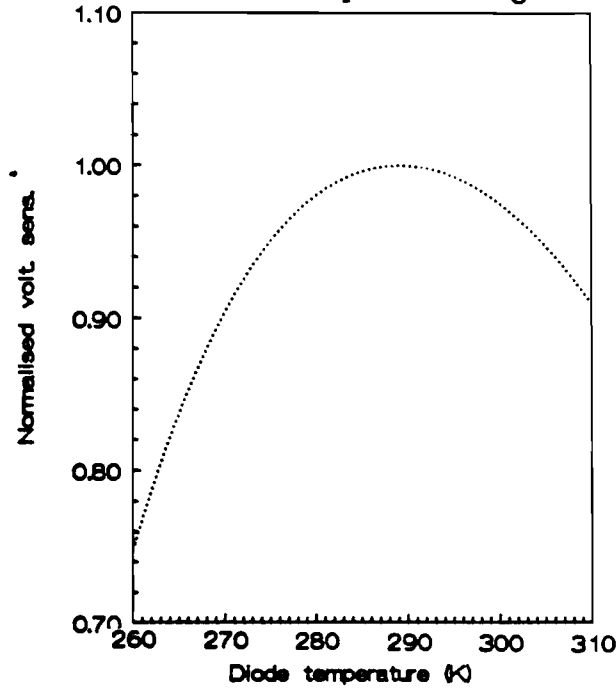


Figure 4.5a: Calculated voltage sensitivity as function of the temperature.

4.2 The Mixer.

In order to convert the 30 GHz RF signal to a frequency of 100MHz, the Rf signal needs to be mixed with a local oscillator signal of 29.9 GHz. The most common way to mix two signals is to apply them to a device with non-linear current-voltage characteristics. A convenient way to describe the transfer characteristics is by the use of power series [12]:

$$V_o = \sum_{m=1}^{\infty} K_m V_i^m \quad (4.19)$$

The first term is linear and K_1 is the small signal gain; the second term is quadratic and produces the second harmonic. K_m are other constants in this power series. V_i can be taken as the sum of two sinusoidal input voltages $V_i = V_{lo} + V_{rf}$, where V_{lo} has a frequency f_{lo} and V_{rf} has a frequency f_{rf} :

$$V_o = K_1(V_{lo} + V_{rf}) + K_2(V_{lo} + V_{rf})^2 + \sum_{n=3}^{\infty} K_n(V_{lo} + V_{rf})^n \quad (4.20)$$

V_{lo} is the local oscillator (LO) voltage and V_{rf} is the radio frequency signal (RF) voltage.

Equation (4.20) becomes:

$$\begin{aligned}
 V_o = & \underbrace{[K_1 V_{10} + K_2 V_{10}^2 + \sum_{m=3}^{\infty} K_m V_{10}^m]}_{\text{response to } v_{10}} + \underbrace{[K_1 V_{rf} + K_2 V_{rf}^2 + \sum_{m=3}^{\infty} K_m V_{rf}^m]}_{\text{response to } v_{rf}} + \\
 & + \underbrace{[2K_2 V_{10} V_{rf} + 3K_3 V_{10}^2 V_{rf} + 3K_3 V_{10} V_{rf}^2 + \sum_{m=3}^{\infty} \sum_{n=1}^{m-1} K_m V_{10}^n V_{rf}^{m-n}]}_{\text{cross products}} \quad (4.21)
 \end{aligned}$$

It can be shown by trigonometrical identities that a term in V_{10}^m generates a frequency of mf_{10} and a term in V_{rf}^m generates a frequency of mf_{rf} . A cross term of $V_{10}^n V_{rf}^m$ will produce signals with a difference frequency $mf_{10} - nf_{rf}$ and with a sum frequency $mf_{10} + nf_{rf}$. In a mixer, only the cross term with frequency $f_{10} - f_{rf}$ is important. The other harmonics have to be eliminated, so that no term with difference frequency $mf_{10} - nf_{rf}$, with $m \neq 1 \wedge n \neq 1$ will be in the same frequency range as $f_{10} - f_{rf}$, or at least not at a significant power level.

4.2.1 Characteristics of mixers.

A. The conversion gain G_c

The conversion gain is defined as the ratio between the output IF power and the input RF power.

$$G_c = 10^{10} \log \frac{P_{if}}{P_{rf}} \quad (\text{dB}) \quad (4.22)$$

The conversion gain is always negative for a diode mixer and mostly positive for a transistor mixer. Losses occur because of:

- rejection of high–order intermodulation terms, this introduces a loss of at least –3dB, because the power that is in the summed frequency band is rejected, where this power should have the same value as the power in the difference frequency band,
- mismatching between the generators and the various inputs to the active component,
- the series resistance in diode mixers.

The value of G_c is closely related to the local oscillator amplitude and the type of mixer.

B. Voltage standing wave ratio.(see appendix A)

The Voltage standing wave ratio (VSWR) is a measure for the reflection of the incident wave of a microwave device. The VSWR at the input of a mixer is defined by:

$$\rho = \frac{1 + |\Gamma|}{1 - |\Gamma|} \quad (4.23)$$

where the reflection coefficient Γ is defined by:

$$\Gamma = \frac{Z_i - Z_c}{Z_i + Z_c} \quad (4.24)$$

Here Z_i is the input impedance of the mixer at a specified input frequency (RF, LO). Z_c is the characteristic impedance of the device, connected to the input port. The VSWR is strongly dependent on the LO amplitude which determines the operating point of the active component. The value of ρ is usually defined at the midpoint of its range of variation.

C. Isolation.

The isolation is defined as the insertion loss between two terminals of the mixer for a given RF, LO or IF frequency. Its value is given by the manufacturer, over a range of frequencies, as a function of the LO level, and sometimes as a function of the temperature. Usually, the LO input/RF input and LO input/IF output isolations are the only ones quoted. The RF input/IF output is only given if the RF level is such that there is a risk of some RF persisting at the IF input.

D. Mixer noise and noise temperature ratio.

In this part the noise temperature of a diode mixer is discussed. There are two types of mixers, the double sideband (DSB) mixer or the single sideband (SSB) mixer. The SSB mixer uses only one sideband where the DSB mixer uses both sidebands. For each sideband there is a transducer gain G_c , defined as the derivative of the output power of the mixer with respect to the input power at this sideband [16]. In case of an SSB mixer, a signal exists in one sideband only, so the SSB noise temperature only adds at one sideband. The

output noise temperature as given by Maas [16] is:

$$T_{\text{out}} = (T_i + T_{\text{ssb}})G_c + T_i G_c \quad (4.25)$$

Here T_i is the input noise temperature. Then the SSB noise temperature T_{ssb} is:

$$T_{\text{ssb}} = \frac{T_{\text{out}} - 2G_c T_i}{G_c} \quad (4.26)$$

T_d , the effective diode noise temperature can be defined with the next relation:

$$T_d(1 - 2G_c) = T_{\text{out}} - 2G_c T_i \quad (4.27)$$

T_{ssb} now relates to T_d as:

$$T_{\text{ssb}} = T_d(L_c - 2) \quad (4.28)$$

Here $L_c = 1/G_c$ is the mixer conversion loss.

In case of a DSB mixer, Two sidebands are viewed, and the output noise temperature T_{out} is:

$$T_{\text{out}} = (T_i + T_{\text{dsb}})G_c + (T_i + T_{\text{dsb}})G_c \quad (4.29)$$

Then the DSB noise temperature T_{dsb} is:

$$T_{\text{dsb}} = \frac{T_{\text{out}} - 2G_c T_i}{2G_c} \quad (4.30)$$

Using T_d and L_c :

$$T_{\text{dsb}} = T_d(L_c - 2)/2 \quad (4.31)$$

Usually, a noise temperature ratio N is defined [16]:

$$N = T_d/T_{\text{mix}} \quad (4.32)$$

Where T_{mix} is the physical temperature of the mixer. Then the expressions for T_{ssb} and T_{dsb} are:

$$T_{\text{ssb}} = NT_{\text{mix}}(L_c - 2) \quad (4.33)$$

$$T_{\text{dsb}} = NT_{\text{mix}}(L_c - 2)/2 \quad (4.34)$$

4.2.2 Diode mixers.

A typical non-linear element is a semiconductor diode. With diodes, the current-voltage curve is exponential (see also section 4.1) An exponential function can be written in a power series:

$$e^x = \sum_{n=0}^{\infty} \frac{x^n}{n!} = 1 + x + \frac{x^2}{2} + \frac{x^3}{6} + \dots \quad (4.35)$$

As follows from this equation, the higher harmonics are attenuated by $n!$ for the n -th harmonic. Figure 4.6 gives a basic scheme for a diode mixer. A voltage

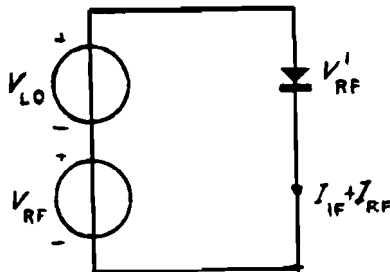


Figure 4.6: A basic scheme for a diode mixer.

$V = V_{10} + V_{\text{rf}}$ is applied to the diode, with $|V_{10}| \gg |V_{\text{rf}}|$. Because V_{rf} is small compared with V_{10} , the diode conductance G ($= dI/dV$) is modulated with V_{10} , so the conductance varies with $G = G_{10}$. V_{rf} produces a current I_{rf} ($I = I_{\text{rf}} + I_{\text{if}}$) through the diode with all harmonics of V_{rf} , which generates an output voltage V_{rf}' . G_{10} and V_{rf}' can be expressed in Fourier series:

$$G_{10} = \sum_{n=-\infty}^{\infty} g_n \exp(jn\omega_{10}t) \quad (4.36)$$

$$V_{rf}' = \sum_{m=-\infty}^{\infty} V_m \exp(jm\omega_{rf}t) \quad (4.37)$$

Now the IF current is the product of the diode conductance G_{10} and the diode voltage V_{rf}' :

$$I_{if} = \sum_{n=0}^{\infty} \sum_{m=0}^{\infty} g_n V_m \exp[j(\pm n\omega_{10} \pm m\omega_{rf})t] \quad (4.38)$$

It consists of all possible intermodulation products. In equation (4.38), g_n is proportional to $|V_{10}|^n/n!$ and V_m is proportional to $|V_{rf}|^m/m!$. This means:

$$g_n V_m = c_1 \frac{|V_{10}|^n |V_{rf}|^m}{n! m!} \quad (4.39)$$

With c_1 as a proportionality constant. The components with frequency $m\omega_{rf} \pm \omega_{10}$

($\omega_{rf} = 2\pi f_{rf}$, $\omega_{10} = 2\pi f_{10}$) will be much smaller than the components with frequency $f_{rf} \pm n f_{10}$, because $|V_{10}| \gg |V_{rf}|$. If we take $|V_{10}| = c_2 |V_{rf}|$, with c_2 another constant, greater than 1:

$$g_1 V_m = c_1 \frac{c_2 |V_{rf}| |V_{rf}|^m}{m!} \quad (4.40)$$

and:

$$g_n V_1 = c_1 \frac{(c_2)^n |V_{rf}|^n |V_{rf}|}{n!} \quad (4.41)$$

It is easy to see that, for $n=m>1$, $g_1 V_m$ is much smaller than $g_n V_1$, because $c_2 \gg 1$.

4.2.1 The mixer as used in the radiometer.

In a radiometer, the mixer is the main cause of receiver noise. In order to minimize the receiver noise, it is important to choose a mixer with a the lowest possible noise figure. A lower noise figure can also be achieved by using an RF amplifier at 30GHz before the mixer. There is only a financial problem to encounter. Such an RF amplifier costs very much. In the future, when RF amplifiers might be cheaper, it is very interesting to add this amplifier, or even to make a direct receiver, in which the mixer is removed from the

scheme. This would also remove the temperature dependency of the conversion gain.

4.3 The oscillator.

In order to get a signal to mix the RF signal with, a local oscillator is needed that produces a frequency of 29.9GHz. A microwave oscillator is a system of active and passive components that produces a periodic output signal, of which the amplitude is not related to an input signal other than the signal from the power supply. The frequency may be varied by an external control signal. The wave form may be purely sinusoidal or distorted, depending on the non-linear characteristics of the active element. In a radiometer, an oscillator can be used as a local oscillator, of which the output signal can be mixed with the input signal of the radiometer.

4.3.1 Characteristics of oscillators.

- A. The frequency at which it oscillates, f_o ,
- B. The range of frequency over which the oscillator can be varied by a given external control, the tuning range Δf ,
- C. The microwave power output, P_o ,
- D. The efficiency η . η is the ratio of the microwave power output to the DC power supply to the oscillator.
- E. The Quality factor or Q-factor. This is defined by the following expression, in which ϵ_a is the energy stored by the oscillator and ϵ_d the amount of energy dissipated per period:

$$Q = \frac{2 \pi \epsilon_a}{\epsilon_d} \quad (4.42)$$

- F. The stability S of the output signal. This is the ability of the oscillator to deliver a signal at a fixed frequency and amplitude whatever internal or external excitation.
- G. The spectral purity of the output. The output is affected by different types of noise, such as frequency-, phase- and amplitude-modulated noise, and harmonic distortion. Harmonic distortion is defined as the ratio of the sum of all the harmonics of the oscillation frequency to the amplitude of the fundamental:

$$\text{Harm. dist.} = \frac{\sum_{n=2}^{\infty} P(n f_o)}{P(f_o)} \quad (4.43)$$

H. The synchronization of the output signal. This is the ability of the oscillator to produce a signal with a frequency equal to that of the signal of another oscillator coupled to it.

4.3.2 An example: the negative resistance oscillator.

An oscillatory RLC circuit supplied with an input voltage V_i is taken and the output voltage V_o across the capacitor terminals is considered (figure 4.7). The transfer function of this circuit is:

$$T(s) = \frac{V_o(s)}{V_i(s)} = \frac{1}{1 + LCs^2 + RCs} \quad (4.44)$$

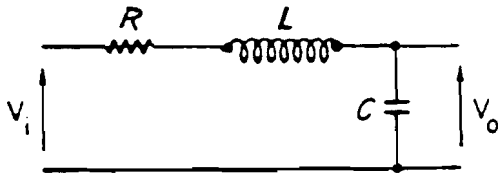


Figure 4.7: An RLC circuit.

Here $s (= j\omega)$ is the Laplace variable. Taking the standard form of this transfer function for a second-order circuit:

$$T(s) = \frac{1}{\frac{s^2}{\omega_n^2} + 2\alpha \frac{1}{\omega_n} s + 1} \quad (4.45)$$

where

$$\omega_n = \sqrt{\frac{1}{LC}} \quad (4.46)$$

$$\alpha = \frac{R}{2} \sqrt{\frac{C}{L}} \quad (4.47)$$

Take a step voltage for the input,

$$\begin{aligned} V_i(t) &= 0 \quad (t < 0) \\ V_i(t) &= E \quad (t \geq 0) \end{aligned} \quad (4.48)$$

The Laplace transform of the output voltage is now:

$$V_o(s) = T(s)V_i(s) = \frac{E}{s \left[1 + s \frac{2\alpha}{\omega_n} + \frac{s^2}{\omega_n^2} \right]} \quad (4.49)$$

Only when α is equal to zero, this system will oscillate. This means, from equation (4.21), that R has to be equal to zero to satisfy this condition. The oscillatory frequency would then be:

$$f_o = \frac{1}{2\pi} \omega_n = \frac{1}{2\pi \sqrt{LC}} \quad (4.50)$$

This can also be written as:

$$j\omega_n L = -\frac{1}{j\omega_n C} \quad (4.51)$$

This means that the system will oscillate under the following conditions:

sum of real parts of impedances = 0

sum of imaginary parts of impedances = 0

The frequency of the oscillator can be changed by changing the value of the capacitance. This can be done by replacing it by a variable capacitance diode or varactor. The tuning range will then be dependant on the range of the varactor. Because losses always exist in passive networks, which means that R can not be equal to zero in such a network, a negative resistance needs to be produced to compensate the losses. This can be done by using a two-terminal network, containing an active device.

4.3.2 The oscillator as used in the radiometer.

In a heterodyne total power radiometer, the oscillator operates as a local oscillator. For this purpose, the level of the oscillator signal should be quite stable, so the oscillator will not introduce any gain variations in the radiometer. In the measurement set-up of chapter 7, only the IF and video part of the radiometer is discussed. Therefore, no oscillator has been chosen to be used for the radiometer.

4.4 The amplifiers.

In order to amplify the signal to a sufficient level for the diode detector to operate in the square-law range, amplifiers are required. An amplifier is a two-port network at the input of which a signal power P_i is injected in order to extract a greater signal power P_o at the output. The main characteristic of an amplifier is the power gain, the ratio of P_o to P_i . An amplifier consists of one or more active components inserted into a passive circuit. First an active component has to be selected which suits the required performance the most. Next the passive circuit has to be constructed into which the active component is to be inserted.

4.4.1 Characteristics of amplifiers.

A. The voltage standing wave ratio (VSWR).

The microwave amplifier is considered as a linear two-port network defined by its S-parameters (see appendix A) at a frequency f in a system with characteristic impedance Z_c . The idealized structure of an amplifier is shown in figure 4.8.

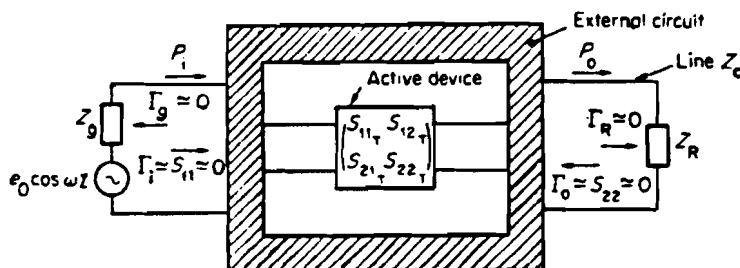


Figure 4.8: A model of an amplifier.

When the load across the terminals has a reflection coefficient of Γ_r (see appendix A), the

reflection coefficient measured across the input terminals is:

$$\Gamma_i = S_{11} + \frac{S_{12} S_{21} \Gamma_r}{1 - S_{22} \Gamma_r} \quad (4.52)$$

Then the VSWR at the input is defined by:

$$\rho_i = \frac{1 + |\Gamma_i|}{1 - |\Gamma_i|} \quad (4.53)$$

The same consideration can be done for the reflection coefficient Γ_o measured at the output of the network and the output VSWR:

$$\Gamma_o = S_{22} + \frac{S_{12} S_{21} \Gamma_g}{1 - S_{11} \Gamma_g} \quad (4.54)$$

$$\rho_o = \frac{1 + |\Gamma_o|}{1 - |\Gamma_o|} \quad (4.55)$$

Here Γ_g is the reflection coefficient of the generator connected across the input. To reach maximum power transfer from the line to the network, ρ_i should be as close as possible to unity. For maximum power transfer from the network to the output, ρ_o should be close to unity. It can be seen from these equations, that when the output and the input are correctly terminated ($\Gamma_r = \Gamma_g = 0$), which will be the best theoretical situation, then the following condition must be satisfied:

$$S_{11} = S_{22} = 0 \quad (4.56)$$

In practice, the active device(s) inside the network have a scattering matrix S_T such that:

- 1) S_{11T} and S_{22T} are different from zero;
- 2) S_{11T} and S_{22T} vary with frequency.

The design of an amplifier thus consists of finding a correcting network such that S_{11T} and S_{22T} are close to zero over the whole frequency range within which the amplifier is required to operate.

B. Power gain G , transducer gain G_T , available power gain G_A and insertion gain.

The gain of an amplifier is defined as the ratio of two microwave powers P_2 and P_1 :

$$G \triangleq 10^{10} \log \frac{P_2}{P_1} \text{ (dB) or } G \triangleq \frac{P_2}{P_1} \quad (4.57)$$

Depending on the way these powers are defined, at least six types of gain can be found. Here, four of them will be introduced, these are the most common types. The first one is the generalized version, the others are special types cases for special input or output terminations.

1) Power gain: the ratio of the output power P_o and the input power P_i . This can be expressed in terms of the incoming wave a and the outgoing wave b of the two-port network (see appendix A). Thus the power gain is:

$$G = \frac{P_o}{P_i} = \frac{|a_2|^2 - |b_2|^2}{|a_2|^2 + |b_2|^2} = \left| \frac{b_2}{a_1} \right|^2 \frac{|a_2/b_2|^2 - 1}{1 - |b_1/a_1|^2} \quad (4.58)$$

After replacing b_2/a_1 , a_2/b_2 and b_1/a_1 by their expressions in terms of Γ_g , Γ_r and the S-parameters (see appendix A):

$$G = |S_{21}|^2 \frac{1 - |\Gamma_r|^2}{|1 - S_{22}\Gamma_r|^2 (1 - |\Gamma_i|^2)} \quad (4.59)$$

Using equation (4.53), this shows when $\Gamma_r = 0$, G is given by:

$$G = \frac{|S_{21}|^2}{1 - |S_{11}|^2} \quad (4.60)$$

2) Transducer gain: If P_1 is equal to the maximum power available from the generator when the input is correctly terminated, then the transducer gain is found:

$$G_T = \frac{P_o}{P_a} = |S_{21}|^2 \frac{(1 - |\Gamma_r|^2)(1 - |\Gamma_g|^2)}{|1 - S_{22}\Gamma_r|^2 |1 - \Gamma_g\Gamma_i|^2} \quad (4.61)$$

3) Available power gain: This is a special value of G_T ; when the output is correctly terminated by a matched load, that is $\Gamma_r = \Gamma_o^*$, then the available power gain is given by:

$$G_A = |S_{21}|^2 \frac{1 - |\Gamma_g|^2}{|1 - S_{11}\Gamma_g|^2 (1 - |\Gamma_r|^2)} \quad (4.62)$$

4) Insertion gain: P_1 now represents the power P_{dir} which would be delivered to the load by the generator if these two elements were connected directly together:

$$G_T = \frac{P_o}{P_{dir}} = |S_{21}|^2 \frac{|1 - \Gamma_r\Gamma_g|^2}{|1 - S_{22}\Gamma_r|^2 |1 - \Gamma_g\Gamma_i|^2} \quad (4.63)$$

C. Amplifier stability.

It follows from the expressions for the transducer gain and the insertion gain, that these can reach infinity, theoretically, when $\Gamma_i\Gamma_g = 1$. This means that the circuit would start to oscillate. Furthermore, the amplifier must be able to operate for all values of Γ_g and Γ_r . Since $\Gamma_g \leq 1$, because Z_g is a passive impedance, it can be seen that this only occurs when $|\Gamma_i| > 1$. A coefficient K , the Rollet coefficient [12] can be found:

$$K = \frac{|\Delta|^2 + 1 - |S_{11}|^2 - |S_{22}|^2}{2|S_{12}S_{21}|} \quad (4.64)$$

Here $\Delta = S_{11}S_{22} - S_{12}S_{21}$. Now the coefficient $|\Gamma_i|$ will always remain less than 1 when K is greater than 1 and when the two quantities $|S_{11}|^2$ and $|S_{22}|^2$ are less than $1 - |S_{12}||S_{21}|$. Under these conditions the amplifier is said to be unconditionally stable. If they are not satisfied, oscillations can occur for certain values of Γ_g , which means that not every generator can be connected to the circuit. All these results are completely valid for Γ_r : an unconditionally stable amplifier can be connected to any load without any risk of oscillation.

When the amplifier is unconditionally stable, expression (4.61) will give the values of Γ_g and Γ_r , making the transducer gain a maximum [12]. These optimum values, inserted back into equation (4.61), yield a simple form of the gain called the maximum available gain, given by:

$$G_{A_{\max}} = \left| \frac{S_{11}}{S_{12}} \right| (K \pm \sqrt{K^2 - 1}) \quad (4.65)$$

where the negative sign is used if $1 + |S_{11}|^2 - |S_{22}|^2 - |\Delta|^2$ is positive and vice versa. This is maximum, but in practice, the available gain is generally lower than this.

D. Noise factor.

Any amplifier will generate noise which is superposed on any useful signal to be amplified. If the power of this noise is of the same order or greater than P_o , it becomes difficult to use the amplifier. In order to assess the ability of the amplifier to amplify small signals, a quantity known as the noise factor is used. The noise factor of an amplifier is defined as the total output power of the amplifier, divided by the power from the same amplifier without noise:

$$F = \frac{P_{o2} + P_{o1}}{P_{o1}} = 1 + \frac{P_{o2}}{P_{o1}} = 1 + \frac{T_e}{T_o} \quad (4.66)$$

where P_{o1} is the output noise power, theoretically found by amplifying the input noise power, and P_{o2} is the output power, due to amplifier noise. The amplifier becomes less noisy as P_{o2} becomes smaller compared with P_{o1} . T_e is the equivalent noise temperature of the amplifier. This means F becomes closer to unity, or as the noise figure defined by $F(\text{dB}) = 10 \log F$ becomes closer to zero.

It can be shown that the noise factor can be written as a function of the generator reflection coefficient:

$$F = F_{\min} + 4r_n \frac{|\Gamma_{go} - \Gamma_g|^2}{(1 - |\Gamma_g|^2) |1 + \Gamma_{go}|^2} \quad (4.67)$$

Here F_{\min} , r_n and $|\Gamma_{go}|$ are positive constants depending only on the characteristics of the internal noise sources of the amplifier at a given frequency. The noise factor is always greater than or equal to F_{\min} , which thus represents the minimum noise factor. To achieve this noise factor, the reflection coefficient of the generator should be equal to Γ_{go} .

4.4.2 The amplifiers as used in the radiometer.

As stated in chapter 2, amplifiers are needed in order to increase the IF power. These

amplifiers introduce noise and gain variations, when the physical temperatures of these amplifiers change. The amplifiers used in the radiometer that was subject to measurements in this project, are an A1 modular amplifier, manufactured by Watkins–Johnson, and a GPD201 low cost amplifier, manufactured by Avantek. specific properties of these amplifiers are [17,18]:

A1:

- Gain 16.0 dB
 - Minimum 15.0 dB (0 °C – +50 °C)
 - Minimum 14.5 dB (–54 °C – +85 °C)
- Noise figure 2.5 dB
 - Maximum 3.0 dB (0 °C – +50 °C)
 - Maximum 3.5 dB (–54 °C – +85 °C)
- VSWR 2.0

GPD201:

- Gain minimum: 30 dB (0 – 50 °C)
 - some typical gain values at different temperatures ($f = 100\text{MHz}$)
 - 34.6 dB (–25 °C)
 - 34.1 dB (+25 °C)
 - 33.0 dB (+85 °C)
- Noise figure (typical): 3.0 dB
 - some typical noise figures at different temperatures ($f = 100\text{MHz}$):
 - 2.6 dB (–25 °C)
 - 3.0 dB (+25 °C)
 - 3.6 dB (+85 °C)
- Input VSWR (typical): 1.22
 - some typical input VSWR's at different temperatures ($f = 100\text{ MHz}$)
 - 1.3 (–25 °C)
 - 1.2 (+25 °C)
 - 1.1 (+85 °C)

4.5 The video amplifier.

In order to amplify the low frequency output signal from the diode detector to a level of a few volts, it is necessary to use a video amplifier. A video amplifier is a two–port network

at the input of which a signal voltage V_i is applied in order to find a greater signal voltage at the output. The main characteristic of a video amplifier is the voltage gain, the ratio of V_o to V_i .

A video amplifier usually consists of an operational amplifier, used in a feedback loop.

4.5.1 Characteristics of video amplifiers.

Voltage gain.

A video amplifier is usually implemented as in figure 4.9. It can be shown that the ratio of the output voltage and the input voltage is the ratio of the feedback resistance, R_f and the input resistance R_i (see figure 4.9).

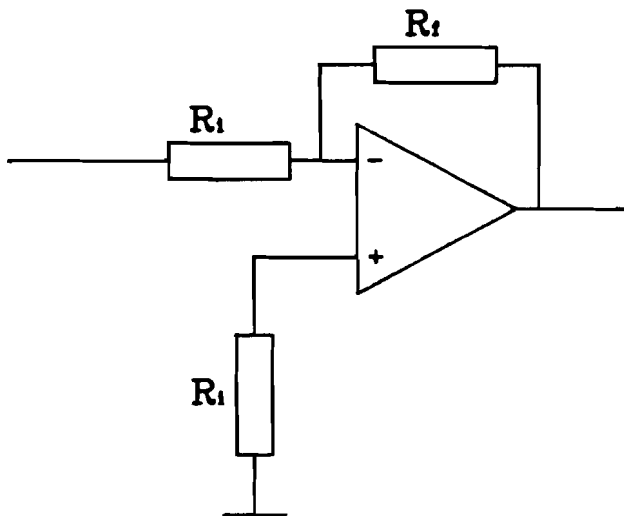


Figure 4.9: The scheme of a video amplifier.

$$G = \frac{R_f}{R_i} \quad (4.68)$$

As long as the open loop gain of the operational amplifier is very high compared to the gain as calculated from equation (4.68), the gain of the video amplifier is not really dependent on the operational amplifier characteristics.

Input offset voltage.

In general, the output voltage of an operational amplifier is not zero when the input voltage is zero. Then the output voltage is only zero when a certain bias voltage bias is

applied to the input terminals. This voltage is named the input offset voltage. The voltage can be compensated for in any regular operational amplifier. A remaining problem is, that this input offset voltage appears to drift with changing temperature. Specifications of operational amplifiers usually give the input offset voltage drift as a function of the temperature.

Input noise.

For an operational amplifier, also an input voltage noise spectral density is defined. This figure has the dimension of $\text{nV}/\sqrt{\text{Hz}}$, root mean square nano volts per square root Hertz.

4.5.4 The video amplifier as used in the radiometer.

In a radiometer, the video amplifier is used to amplify the signal, coming from the diode output. The actual scheme as it is used in the radiometer is shown in figure 4.10. The operational amplifier, used in this scheme, is an OPA 27 [19], manufactured by Burr–Brown. The capacitors in this scheme are basically used to cut off noise with a frequency of over 10 kHz. This to make sure nothing from the diode input will directly appear at the output without being demodulated. For the frequency at which this operates, the influence of the capacitor can be neglected. The feedback resistance is $3.3\text{M}\Omega$ and the input resistance is $4.7\text{k}\Omega$ [13]. This results in a gain G:

$$G = \frac{3.3 \times 10^6}{4.7 \times 10^3} = 700 \quad (4.69)$$

The input offset voltage is compensated. Only a small offset voltage will remain at room temperature. A more important aspect is the input voltage drift, which has a typical value of $0.2\mu\text{V}/\text{K}$ and a maximum value of $0.6\mu\text{V}/\text{K}$. Multiplied with the gain, this causes a change of the output voltage of $0.42\text{mV}/\text{K}$.

The maximum input noise, generated by the video amplifier, is only $3.8\text{nV}/\sqrt{\text{Hz}}$. At a bandwidth of 10 kHz, this is would be 380nV root mean square noise.

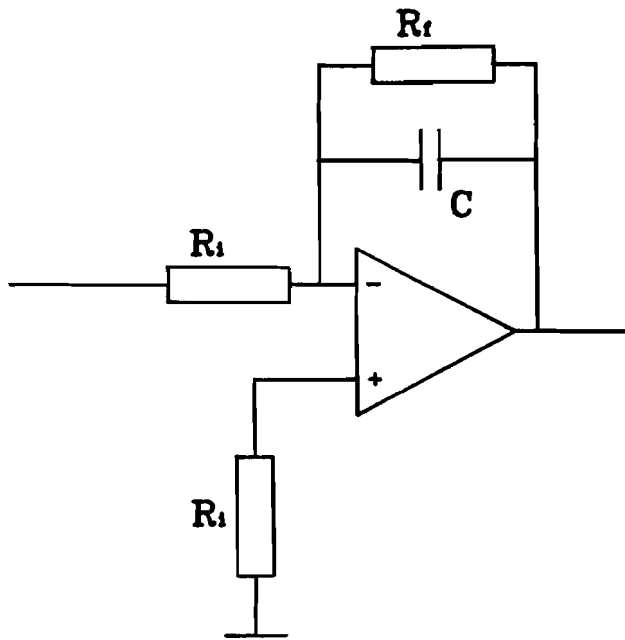


Figure 4.10: The video amplifier as used in the radiometer.

5. TEMPERATURE DEPENDENCE OF THE RADIOMETER PARAMETERS.

In this chapter the overall and local parameters of the radiometer are discussed, such as gain and the receiver noise temperature. These are necessary to find the radiometer sensitivity (chapter 3). To find these parameters, the different parts of the radiometer must be defined. Then an expression for the overall receiver noise temperature and the overall gain can be found. These parameters are dependent on the local temperatures of the different components. It is also of chief importance to achieve a theoretical model for the effects of local temperature changes, after which measurements can be made to prove this theory.

5.1 A mathematical model for a total power radiometer.

In order to achieve a good mathematical model for the whole radiometer, a transfer function TF_i , a noise input N_i , a noisy signal input S_i and an output signal O_i can be assigned to each part.(Figure 5.1).

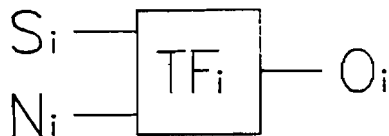


Figure 5.1: Local parameters of a radiometer part.

These parameters are related to each other as:

$$O_i = TF_i(S_i + N_i) \quad (5.1)$$

Here the dimensions of O_i , S_i and N_i are either Volts or Watts, depending on the device. The dimension of the transfer function TF_i is either Volts/Watt for the square-law device while the transfer functions of the other devices have no dimensions. Now the radiometer can be seen as a number of these devices, put in cascade (figure

5.2).

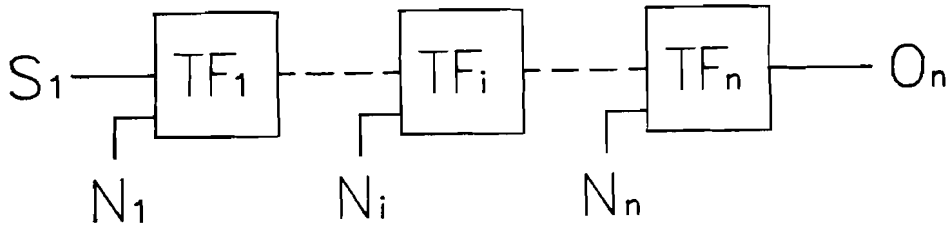


Figure 5.2: The total power radiometer as a cascade of n functional parts.

Every output signal of a device becomes the input signal for the next device. If we take the number of devices to be n, it is found that:

$$O_{10} = S_1 \prod_{i=1}^n (TF_i) + \sum_{i=1}^n N_i \prod_{j=i}^n (TF_j) \tag{5.2}$$

The first term in this equation is the part of the output signal, due to the radiometer input signal. The second term is the noise contribution of the radiometer. To use overall parameters of the radiometer the local variables should be converted to overall parameters.

5.2 The radiometer on a block diagram level.

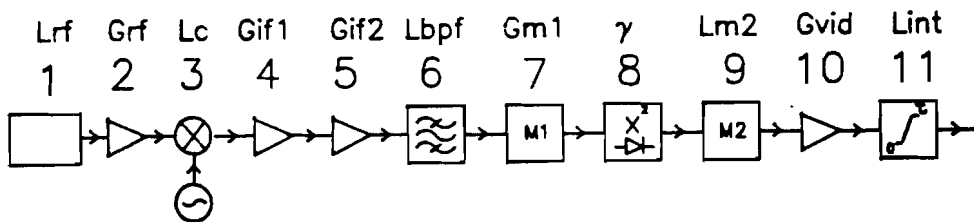


Figure 5.3: The extended radiometer block diagram.

Describing the characteristics of a total power radiometer, the system is split into 10 parts, with each of them their own parameters. The parameters as they are found in the radiometer of figure 5.3 are stated in table 5.1

Table 5.1

i	name	TF _i	N _i	bandwidth
1	RF waveguide	1/l _{rf}	kBT _{rf} (l _{rf} -1)	B
2	RF amplifier	g _{rf}	kBT _{grf} (F _{rf} -1)	
3	DSB Mixer	1/l _c	kBNT _{mix} (l _c -2)/2	
	SSB Mixer	1/l _c	kBNT _{mix} (l _c -2)	
4	IF amplifier	g _{if}	kBT _{if} (F _{if} -1)	
5	Bandpass filter	1/l _{bpf}	kBT _{bpf} (l _{bpf} -1)	
6	Diode input match	g _{mi}	kBT _{mi} (F _{mi} -1)	
7	Diode detector	γ		
8	Diode output match	1/l _{mo}		
9	Video amplifier	g _{vid}		
10	Integrator	1/l _{int}		1/τ

Every part also has a different reflection coefficient Γ_{xx} , an equivalent noise temperature T_{xx}^{eq} and a physical temperature T_{xx} . For every part, these parameters have their own subscript, here represented by xx. Note that every transfer function is multiplied with $(1-\Gamma_{xx})$ to include the reflection losses. The transfer functions of device 8, 9 and 10 are voltage gains, the transfer functions of device 1 to 6 are power gains, the transfer function of device 7 is Volts/Watt.

5.3 The receiver noise temperature.

As stated in chapter 2, the noise contribution of the radiometer is expressed in the receiver noise temperature T_{rec} . In this way, all the noise contributions of all the parts are summed and seen as one noise contribution at the radiometer input. This can be

expressed as in the following equation:

$$O_{10} = (S_1 + N_{\text{rec}}) \prod_{i=1}^{10} (TF_i) \quad (5.3)$$

Using 5.1 and 5.2, the receiver noise will be:

$$N_{\text{rec}} = \left[\sum_{i=1}^{10} N_i \prod_{j=i}^{10} (TF_j) \right] / \left[\prod_{i=1}^{10} (TF_i) \right] \quad (5.4)$$

This can be reduced to:

$$N_{\text{rec}} = \sum_{i=1}^{10} N_i \prod_{j=i}^{i-1} (TF_j)^{-1} \quad (5.5)$$

Knowing the receiver noise is expressed in the receiver noise temperature:

$$N_{\text{rec}} = k B T_{\text{rec}} \quad (5.6)$$

Now it is easy to derive from equations (5.5) and (5.6):

$$T_{\text{rec}} = \left[\sum_{i=1}^{10} N_i \prod_{j=i}^{i-1} (TF_j)^{-1} \right] / kB \quad (5.7)$$

5.4 The overall gain.

The other important overall parameter is the overall gain G , defined by (paragraph 2.1):

$$V_{\text{out}} = ckBG(T_a + T_{\text{rec}}) \quad (5.8)$$

Using $O_{10} = V_{out}$ and $S_1 = P_a = kBT_a$, where P_a is the available noise power and T_a the available noise temperature. Equation (5.3) changes to the following equation:

$$V_{out} = k B (T_a + T_{rec}) \prod_{i=1}^{10} (TF_i) \quad (5.9)$$

Substituting the values from table 5.1 in equation (5.9), it is found that:

$$ckBG = kB \frac{g_{v i d}}{l_{i n t l m o}} \gamma \frac{g_{r f} g_{i f} g_{m i}}{l_{r f} l_c l_{b p f}} \quad (5.10)$$

Note that all power gain factors and the voltage sensitivity should be multiplied by a factor $(1-\Gamma_{xx})$, where the subscript xx must be substituted by the subscript, belonging to the particular device with this reflection factor. The power loss factors should be divided by this factor. In fact, these reflection coefficients are dependent on the characteristic impedance of the device before the device with this reflection factor and on the input impedance of the device. These are dependent on the impedances of the components, which can be temperature dependent. Of course, the power gain factors and power loss factors themselves are dependent on these impedances and are more or less temperature dependent, just like the voltage sensitivity of the detector (see chapter 4). The power supply varies with temperature and it can also vary with time by other random causes. All these causes can affect the parameters of the radiometer. The variations of the power supply are assumed to be negligible.

5.5 The effect of a temperature change.

When changing the temperature of the radiometer, most parameters of the radiometer will change, with a certain relation to this temperature. To find the effect of temperature changes, the derivative of the output voltage as given in equation (5.2) to the block temperature can be taken. In equation (5.2) O_{10} is substituted by V_{out} and S_1 is substituted by kBT_a . It is assumed that the block temperature of the whole radiometer is T and that $T_a = T$:

$$\begin{aligned} \frac{d V_{out}}{dT} = kB \prod_{i=1}^n (TF_i) \frac{dT_a}{dT} + kB T_a \frac{d}{dT} \left[\prod_{i=1}^n (TF_i) \right] + \\ \sum_{i=1}^n \frac{d}{dT} \left[N_i \prod_{j=i}^n (TF_j) \right] \end{aligned} \quad (5.11)$$

According to the chain rule, it is found that:

$$\begin{aligned} \frac{d V_{out}}{dT} = kB \prod_{i=1}^n (TF_i) + kB T_a \sum_{k=1}^n \left[\left[\prod_{\substack{i=1 \\ i \neq k}}^n (TF_i) \right] \frac{dTF_k}{dT} \right] + \\ + \sum_{i=1}^n \left[\left[\prod_{j=i}^n (TF_j) \right] \frac{dN_i}{dT} + N_i \sum_{k=i}^n \left[\left[\prod_{\substack{j=i \\ j \neq k}}^n (TF_j) \right] \frac{dTF_k}{dT} \right] \right] \end{aligned} \quad (5.12)$$

This formula holds for a global change in the block temperature. In case of a local temperature change, for which only the temperature of one component changes without changing another temperature, the transfer of component k , TF_k , and the noise it generates, N_k , are only dependent on the temperature T_k of this component k . In formulas:

$$\frac{dTF_i}{dT_k} = 0, \text{ for } i \neq k; \quad \frac{dN_i}{dT_k} = 0, \text{ for } i \neq k \quad (5.13)$$

So, the derivative of V_{out} with respect to T_k can be found from (5.12), using (5.13).

$$\begin{aligned} \frac{dV_{out}}{dT_k} = kB T_a \prod_{\substack{i=1 \\ i \neq k}}^n (TF_i) \frac{dTF_k}{dT_k} + \\ + \left[\prod_{j=1}^n (TF_j) \right] \frac{dN_k}{dT_k} + \sum_{i=k}^n \left[N_i \left[\prod_{\substack{j=i \\ j \neq k}}^n (TF_j) \right] \frac{dTF_k}{dT_k} \right] \end{aligned} \quad (5.14)$$

When the load temperature is changed without affecting the other local temperatures:

$$\frac{dV_{out}}{dT_a} = \prod_{i=1}^n (TF_i) \frac{dP_a}{dT_a} = kB \prod_{i=1}^n (TF_i) \quad (5.15)$$

It is quite easy to see that the sum of all derivatives of V_{out} to T_k (5.14) and the derivative of V_{out} to T_a (5.15) is equal to the derivative of V_{out} to T (5.12). This only makes sense in a mathematical formula if the derivatives of the local temperatures are partial derivatives:

$$\frac{dV_{out}}{dT} = \frac{\partial V_{out}}{\partial T_a} + \sum_{k=1}^n \frac{\partial V_{out}}{\partial T_k} \quad (5.16)$$

From equation (5.16) it follows that the overall output voltage change can be found by adding the contributions of every component in the radiometer.

Now it is necessary to find the main causes of gain variations and noise. First the parts where $\frac{\partial TF_k}{\partial T_k}$ is non-significant can be excluded from the calculations:

- RF waveguide
- bandpass filter
- integrator
- diode output match

For the bandpass filter, the integrator and the diode output match, $\frac{\partial N_k}{\partial T_k}$ is also non-significant.

6 WRITING PROGRAMS FOR SIMULATION AND CORRECTION OF THE RADIOMETER OUTPUT.

In order to simulate and correct the variations in the radiometer output signal, programs had to be written. These programs are written in pascal. For simulating the radiometer performance, it proved very useful to consider every single component of the radiometer as a functional block. Translated into program language, each radiometer part is represented as a procedure with different parameters, possibly dependent on the physical temperature, an input signal and an output signal. The radiometer would consist of 11 functional parts, because the IF amplifier is built up from two IF amplifiers. Each of them is represented by a procedure.

To calculate the change in the 11 transfers, as a function of the temperature, the procedure Tempdependence was written. This procedure uses as input values the different physical temperatures, transfer functions at $T=T_0$ and the temperature dependence of each functional part. The output of this procedure are the transfers of the functional parts at the specified physical temperatures.

A main procedure was written that integrates the 11 procedures and therefore calculates the output voltage for a given available noise temperature at the input of the radiometer, and also for given transfer functions (gains, losses) of the radiometer parts. It also calculates the equivalent noise temperatures of the RF and IF radiometer parts. This procedure is named Radiometer. For the system as discussed in chapter 7, the RF part is omitted, which means that the gain of each RF part is 0dB and the noise figure is also 0 dB.

Then a function was written to calculate the overall receiver noise temperature. It calculates this from the different transfer functions and equivalent noise temperatures of the RF and IF parts.

These two procedures and the function calculate the output voltage of a radiometer, given by the parameters from the file PARAM.DAT (the data from this file is used by both procedures and the function), with any specified overall or local physical temperature. Using these procedures, several programs were written.

6.1 The procedure Tempdependence (flowchart fig. 6.1)

Tempdependence exist of 11 subprocedures. Each of them calculate the in transfer of a radiometer part for the physical temperature that is given. For the detector, this procedure is named Voltsensvar (voltage sensitivity variation), for the components at the IF and RF

parts, where the signals have the dimension of power, this procedure is named Gainvar, for the components at the video part the procedure is named Voltgainvar. Voltsensvar calculates the value of the voltage sensitivity for the given physical temperature. For this, equation (4.16) is used.

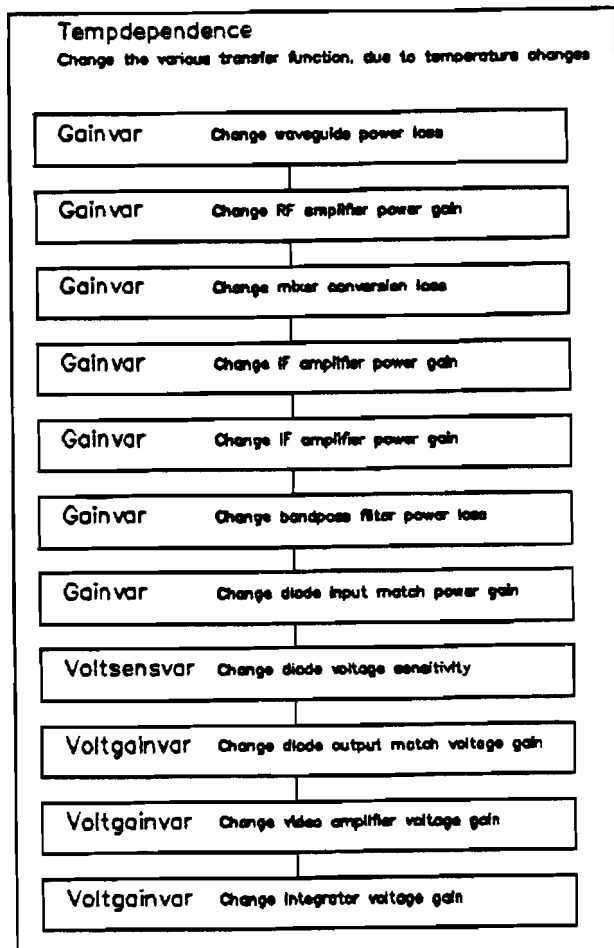


Figure 6.1 The flowchart of the procedure Tempdependence.

The procedure Gainvar goes through a somewhat simpler procedure. This procedure takes the difference between the temperature $T = 298\text{K}$ and the actual physical temperature of the component. Then it multiplies this difference with the value $td[i]$ where i is the number of the radiometer part. $td[i]$ is entered in PARAM.DAT and this is the temperature dependence of this part. This value is expressed in dB/K. The formula for this is:

$$GdB(T_{ph}) = GdB(T_0) + td[i] \cdot (T_{ph} - T_0)$$

This, of course is an approximation, but usually this is how the gain variations are given in the specifications of a component. By measuring and therefore calibrating, it should be possible to extract the real temperature dependence of the different components.

6.2 The procedure Radiometer (flowchart fig 6.2a)

The procedure Radiometer again exists of 11 subprocedures, each of which manages the calculation of the

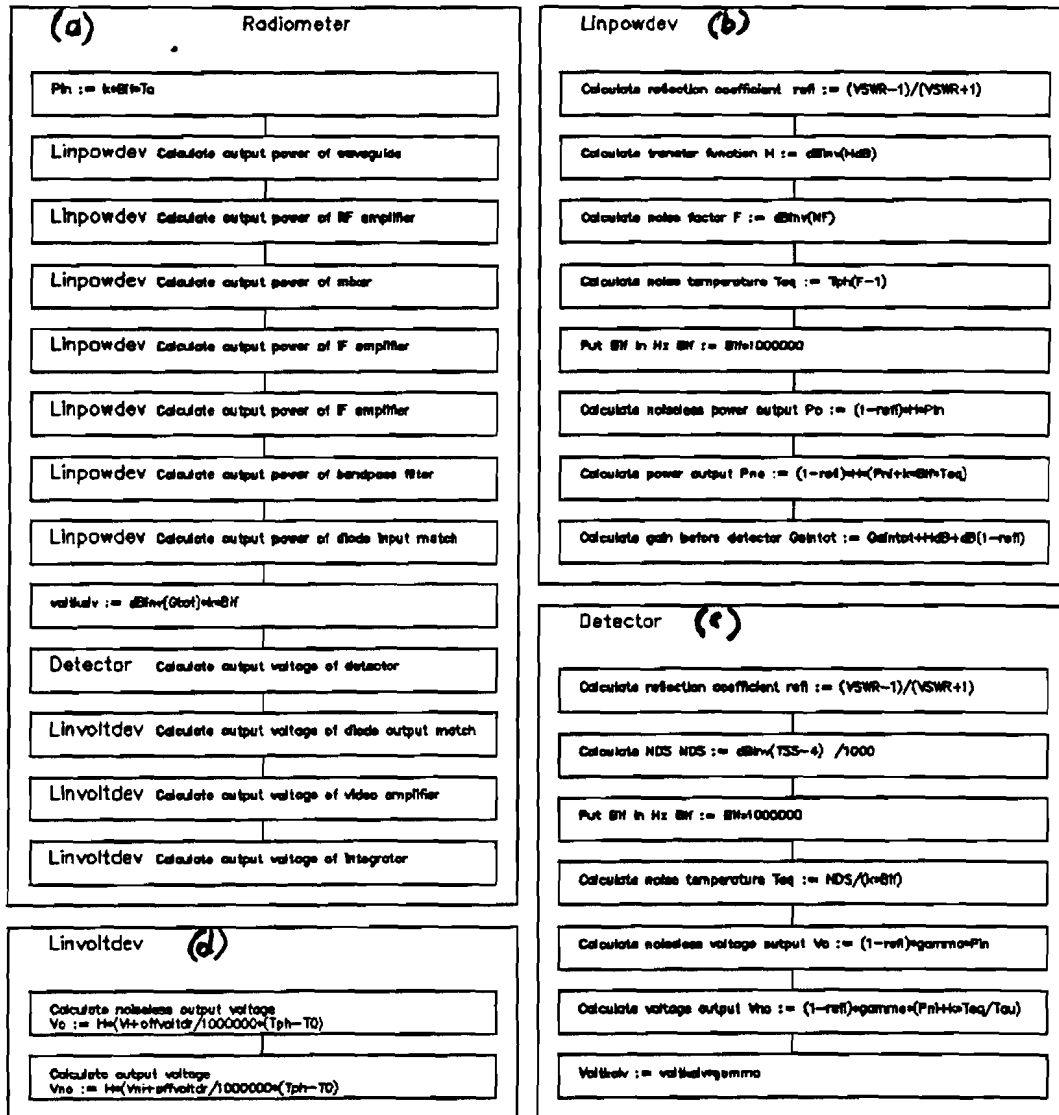


Figure 6.2 The flowcharts of the procedures (a) Radiometer, (b) Linpowdev, (c) Detector and (d) Linvoltdev.

output signal, when no receiver noise exists and the calculation of the output signal when this does exist. These procedures are mainly the same and are split into 4 different types: the procedures that manage the devices with a power input and power output signal (Linpowdev, flowchart fig. 6.2b), the procedure that handles the detector (Detector, flowchart fig. 6.2c), the procedures that handle the devices that have a voltage input signal and a voltage output signal (Linvoltdev, flowchart fig. 6.2d) and the procedures that

handle the IF amplifiers, that have a different way to calculate the equivalent noise temperature (IFamplifier, flowchart similar to Linpowdev).

Linpowdev first calculates the reflected power refl:

$$\text{refl} := (\text{VSWR}-1)/\text{VSWR}+1)$$

then it gets the gain value H:

$$H := \text{dBinv}(\text{HdB})$$

then it gets the noise factor F:

$$F := \text{dBinv}(\text{NFigure})$$

Then it calculates the equivalent noise temperature Teq:

$$\text{Teq} := \text{Tph} \times (F-1)$$

Then it calculates the output power without noise Po:

$$P_o := (1-\text{refl}) \times H \times P_{in}$$

and the output power with receiver noise Pno:

$$P_{no} := (1-\text{refl}) \times H \times (P_{ni} + k \times B_{if} \times \text{Teq})$$

Here VSWR is the voltage standing wave ratio, Tph is the physical temperature, Pin is the input power without noise and Pni is the input power with receiver noise.

IFamplifier runs the same lines as linpowdev, with the exception that the noise factor is calculated by:

$$F = \text{dBinv}(\text{NFigure} + 0.02(\text{Tph} - T_0))$$

and the equivalent noise temperature by:

$$\text{Teq} = 290 \times (F-1)$$

The calculation of the noise factor is based on the fact, that the noise figure increases 1dB at a range of 50K

Detector first calculates the reflected power,

then it calculates the output voltage without noise:

$$V_o := (1-\text{refl}) \times \text{gamma} \times P_{in}$$

and the output voltage with receiver noise:

$$V_{no} := (1-\text{refl}) \times \text{gamma} \times (P_{ni} + k \times \text{Teq} / \text{Tau})$$

where Tau is the time constant of the integrator.

Linvoltdev first calculates the output voltage without noise:

$$V_o := H \times (V_i + \text{offvolt} / 1000000 \times (\text{Tph} - T_0))$$

then it calculates the output voltage with receiver noise:

$$V_{no} := H*(V_{ni} + \text{offvoldr}/1000000*(T_{ph} - T_0))$$

Here offvoldr is the offset voltage drift of the device, expressed in microVolts

6.3 The function Rectemp.

The function Rectemp calculates the receiver noise temperature from the equivalent noise temperatures and the transfer functions of the RF and IF radiometer parts. To achieve this it uses the following expressions:

```
rectemp := Teq[7] + Teq[8]/Gain[4]
rectemp := Teq[6] + rectemp*Loss[3]
rectemp := Teq[5] + rectemp/Gain[3]
rectemp := Teq[4] + rectemp/Gain[2]
rectemp := Teq[3] + rectemp*Loss[2]
rectemp := Teq[2] + rectemp/Gain[1]
rectemp := Teq[1] + rectemp*Loss[1]
```

6.4 The programs.

First a program named TEMPVAR (flowchart fig 6.3) was written to calculate the receiver noise temperature and the output voltage of the radiometer as a function of the physical receiver temperature.

These can be displayed with another program named PICTURE. The program TEMPVAR asks for the range of temperature for which the radiometer output needs to be calculated and also the number of devices and which devices need to be varied with temperature. Another program named VOUT was made to make a printout of the radiometer parameters, as they are entered in the file PARAM.DAT. Also, it gives the output powers/voltages of each part at a specified physical temperature.

Also, a program named CORRECT was written. This reads the temperatures from a file, made by CHARTCNV (discussed later in this section), together with the output voltage from the radiometer of the file. It calculates the output voltage, due to receiver noise at the input temperatures. This voltage is subtracted from the real output voltage. The difference voltage is then divided by the overall voltage sensitivity, the IF bandwidth and Boltzmann's constant.

$$T_a = (V_{out} - V_{out-calc}) / (G_{tot} * B_{if} * k)$$

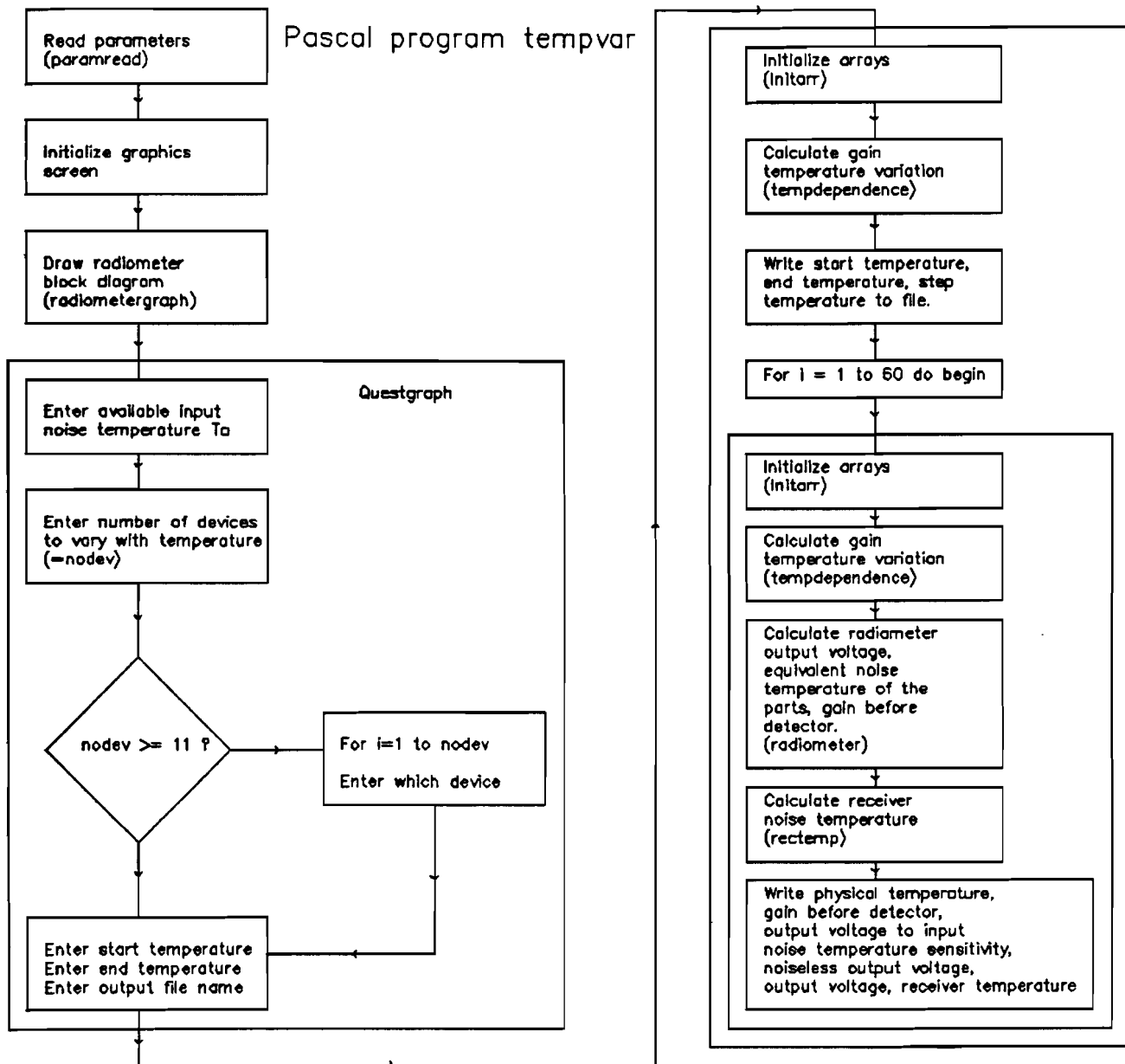
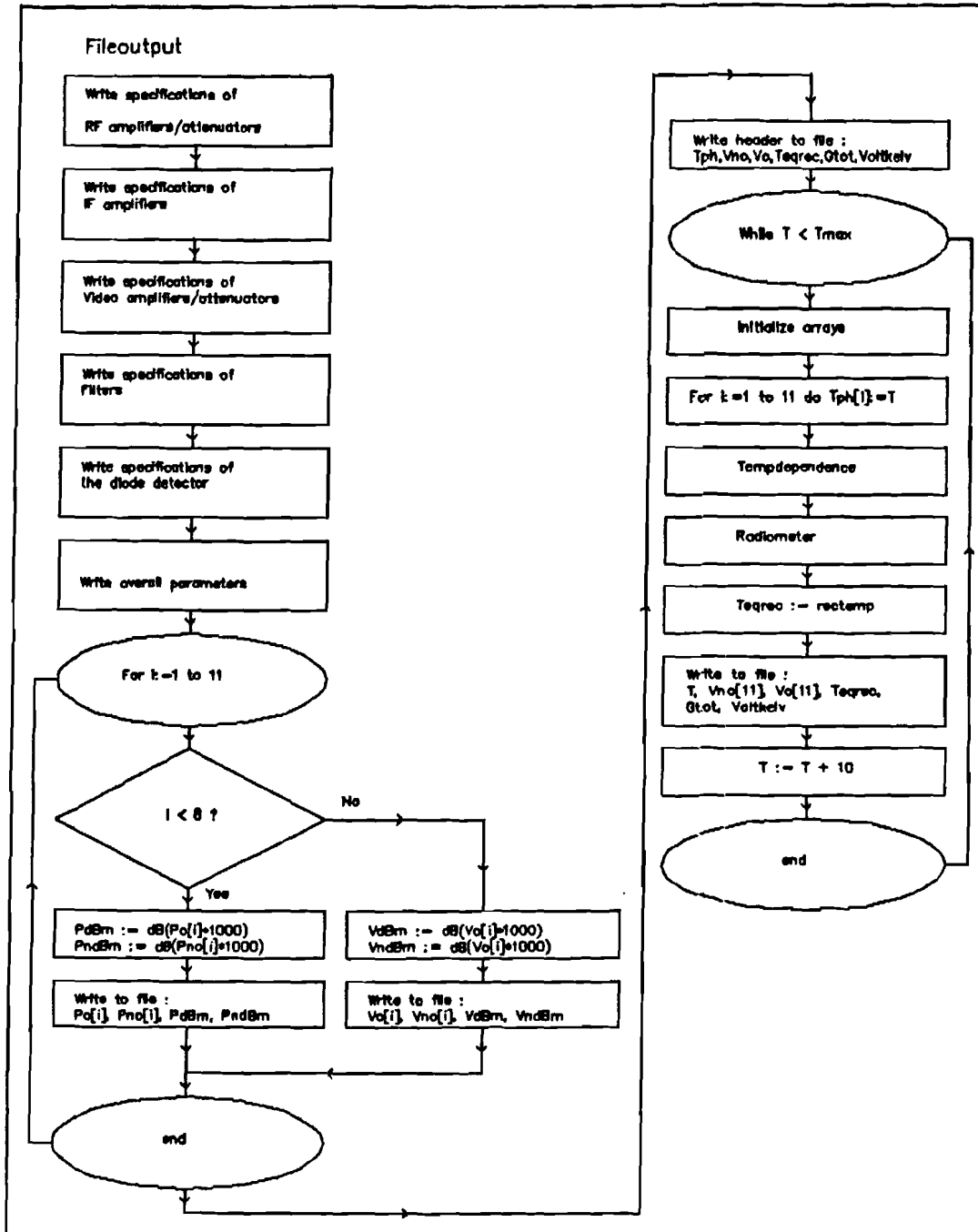


Figure 6.3: The flowchart of the computer program TEMPVAR.

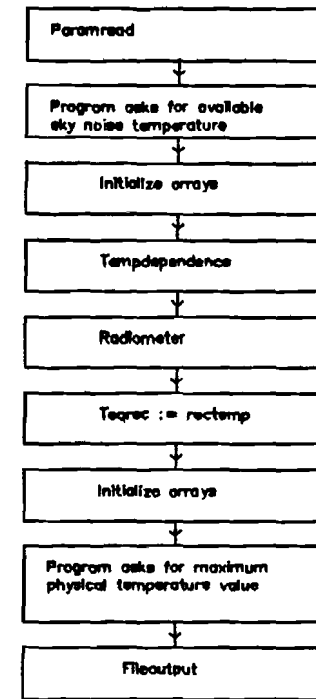
In order to be able to process the data as it is written to disk by the chart recorder, a program CHARTCNV is written. This program gets the temperatures and output voltages, cuts off the insignificant 0's at the end. The sequence in which they are put in a line is: Tcop, Tif1, Tif2, Tm1, Tdiode, Tvid, Vout, Tamb. These variables stand for:

- Tcop: the block temperature
- Tif1: the temperature of the A1 amplifier
- Tif2: the temperature of the GPD201 amplifier
- Tm1: the temperature of the input match (BF 494 transistor)

Fig 6.4 The flowchart of the computer program VOUT.



Pascal program Vout



Tdiode: the diode temperature
Tvid: the temperature of the video amplifier
Vout: the output voltage
Tamb: the air temperature

In order to process the data from a hot/cold load measurement, a program PROCDAT is written, this program asks for two filenames, the file of the cold load measurements and the file for the hot load measurement. The program gets the temperature values and output voltages of one file and interpolates the temperatures and output voltages from the other file. The interpolation is done by the procedure interpol. The interpolation is made by straight linear interpolation. The program now calculates the values of ckBG and Trec, as stated in chapter 2.

7 MEASUREMENTS.

7.1. The measurement setup.

As stated before, the parameters of the radiometer are affected by temperature variations. The temperature dependence of these parameters has to be known to correct the parameter variations due to temperature variations. Measurements are needed, to find the temperature dependence of the radiometer parameters. These measurements should lead to well defined temperature characteristics. In this chapter the measurement setup and the way to achieve the points stated above will be discussed.

7.1.1. The radiometer.

The measurement will be performed on a total power radiometer. The IF part and the video part of this radiometer are fit inside a messing block as it can be seen in figure 7.1. Originally, this circuit was designed to be a spare unit for a Dicke radiometer. Using it as a total power radiometer simply means, that the signal is taken directly from the integrator. Now the actual circuit is found in the upper compartments of the messing block. In the lower compartments, the voltage sources are seated. Looking at figure 7.1, the following IF and video parts of the total power radiometer can be seen (see also appendix E):

- an IF amplifier (A1 Watkins–Johnson),
- a second IF amplifier (GPD 201, Avantek),
- a triple stage Cauer bandpass 10–110MHz filter (three compartments),
- an input matching circuit for the diode detector, being an IF amplifier, implemented with a transistor (BF 494),
- a detector diode (HSC8 3486 Hewlett–Packard), situated in a partition between two compartments,
- a load resistor (output match) for the diode detector,
- a video amplifier OPA27 Burr–Brown,

As stated before, this is only the IF and video part of the radiometer. The RF part is found outside the messing block. This is a balanced diode mixer with a 30GHz Gunn local oscillator input. The RF noise source is provided by a 50 Ω , 30 GHz load. The connection between the mixer and the IF part is made by a coaxial cable, connected with SMA connectors.

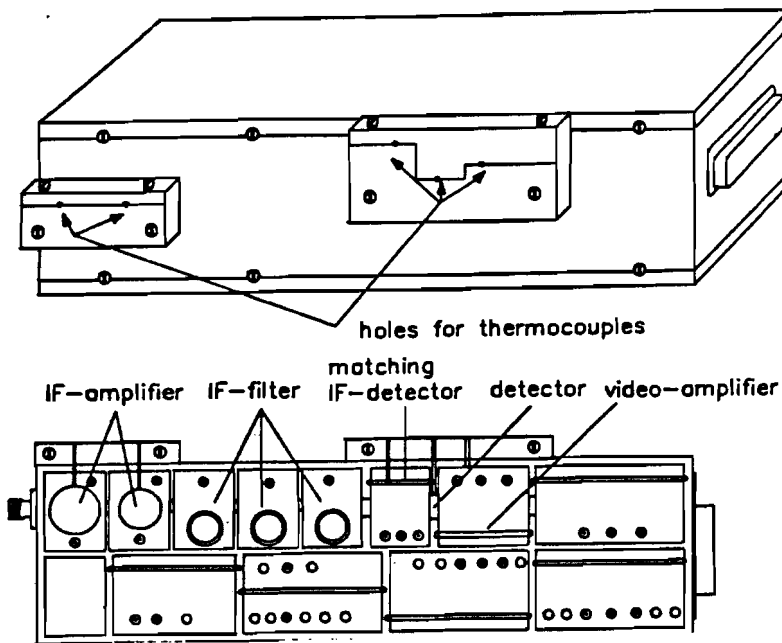


Figure 7.1: The IF and video part of the radiometer.

In the ideal situation, the temperature of every single component should be measured. To reduce the complexity of the measurement setup, priorities have to be made. In general the active components will generate more heat than the passive components. Also, the active components are affected more by temperature variations. Therefore it is useful to measure the temperature of the active components. These active components are:

- the mixer diode(s)
- IF amplifier I
- IF amplifier II
- diode match (IF amplifier III)
- detector diode
- video amplifier

The temperature of the other components will be assumed to be equal to the messing block temperature. This temperature is measured at the same side as the IF input side of the messing block.

7.1.2 Using the chart recorder.

To collect the local temperatures and the output voltage of the radiometer, a chart recorder is used. The chart recorder is a Siemens Multireg C1730. It contains a voltage to temperature conversion table for 8 thermocouple types. The chart recorder sends only 4 decimal digits through the RS232c interface. When the thermocouples have a range of

under 1000°C , which is the case for the following thermocouples, then the resolution is 0.1°C .

- 1 – type E thermocouples, NickelChromium–Constantan (NiCr–CuNi)
- 2 – type T thermocouples, Copper–Constantan (Cu–CuNi)
- 3 – type J thermocouples, Iron–Constantan (Fe–CuNi)

The data from the interface is registered by an XT 8086 computer, using the program Simesp, provided with the chart recorder. With this program, the chart recorder can be controlled remotely, which makes the chart recorder much easier to set up for a measurement.

The following channels were used (see also figure 7.2):

- Channel #1: Output Voltage
- Channel #3: Temperature of the A1 amplifier
- Channel #4: Temperature of the GPD201 amplifier
- Channel #5: Temperature of the diode input match
- Channel #6: Temperature of the diode detector
- Channel #7: Temperature of the video amplifier
- Channel #8: Temperature of the messing block
- Channel #9: Ambient temperature

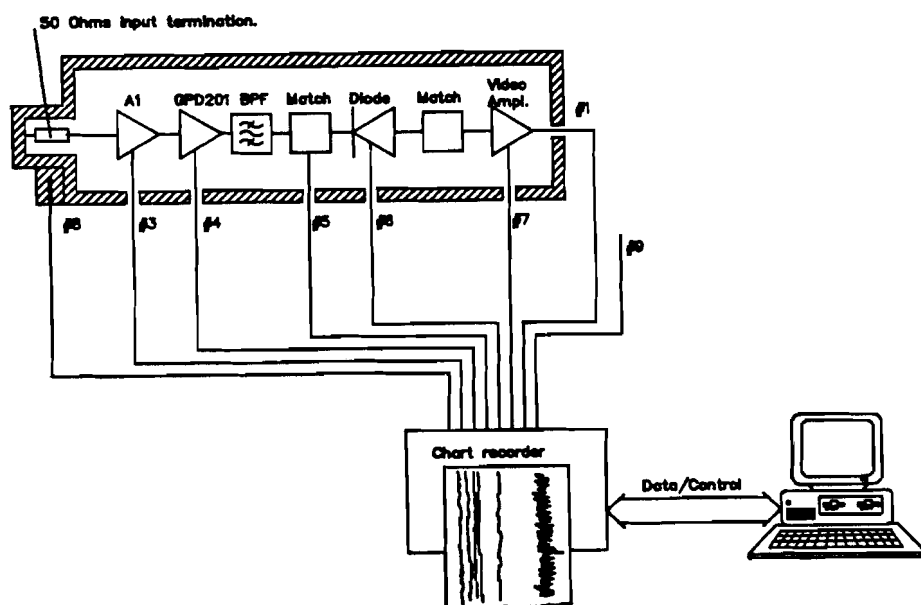


Figure 7.2: The scheme of the measurement setup with the chart recorder

The chart recorder has an option to set the scales for the chart. In case of temperature measurements, the temperature range displayed on the chart was 5°C , at a chart width of 25 cm. For this chart recorder, it already shows the discretization of the analog to digital converter inside the machine. On the chart, the discretization was 0.05°C . As mentioned before the discretization of the data sent to disk was 0.1°C . During the measurements, the C1730 chartrecorder broke down, due to ink problems. During the repair of this chart recorder, a spare chart recorder was used, supplied by the agent who sold the machine before. This chart recorder was a Siemens Multireg C1732. This chart recorder had a higher accuracy. Discretization of the data, sent to disk was 0.01°C , discretization of the data on the chart was not visible in this range. Unfortunately, special software was needed for this version, which could not be supplied for this short period. The local measurements with the video amplifier and the A1 IF amplifier were done with this chart recorder. These measurements were processed by reading the data from the chart paper.

7.1.3 Using a temperature stabilized environment.

For the temperature stabilized environment, a unit, manufactured by Statham was used. This unit can generate a very stable temperature, anywhere between -50°C and $+150^{\circ}\text{C}$. The unit is controlled by a thermostat. The temperature at which the unit stabilizes is tuned with a button. It indicates the temperature at which the unit stabilizes with an error of $\pm 1^{\circ}\text{C}$.

Because the unit is equipped with a constantly running motor, to keep the air circulating and it also switches many times (multiple times per second), one must be aware of the fact that the unit can generate some noise that can affect the radiometer performance. This noise was not detected while performing the measurements.

7.1.4 Temperature sensors.

In order to perform the measurements as discussed in paragraph 7.1, temperature sensors are needed. It is very difficult to measure the real temperature of the active device to be measured. Of course, every component is fit inside a package. This means it is impossible to put the temperature sensors directly at the active region of the device. Usually, there will be a temperature gradient from the active region to the outside boundaries of the package. To reduce heat conduction problems as much as possible, the sensors are put directly to the device package with heat conducting paste. The paste is used to make sure that the sensor has the same temperature as the device package. To get as close as possible

to the devices, holes will have to be drilled in the messing block.

To reduce interference by outside noise sources or internal interference between the components, these holes have to be as small as possible. The smallest temperature sensors available here were thermocouples with a radius of 1.2 mm (coating included). The output signals of the thermocouples will be processed by the recorder. (par. 7.1.2)

Because of the specified types in paragraph 7.1.2 only Iron–Constantan thermocouple wire was available at the university, this thermocouple type was chosen to use for the temperature measurements.

7.1.5 Calibrating the thermocouples.

The voltages coming from the thermocouples are converted to temperatures by the chart recorder. The chart recorder uses an internal correction for the cold junction. This to calibrate the thermocouples for degrees Celcius [21]. Because the voltage–temperature characteristics of the thermocouples can be different from the characteristics stored in the chart recorder, the thermocouples have to be calibrated as a system together with the chart recorder. The way to do this, is to put the sensors in a very well defined temperature stabilized environment and read the values coming from the thermocouple/chart recorder system. Now a curve can be drawn through these points in order to get a calibration characteristic. The temperature stabilized environment can be made in different ways. One way is to use the melting point of a certain pure material. This is used for the calibration at 0°C. The sensors are put into a test–tube, containing silicon oil. This test–tube is put into a thermos–flask, filled with melting ice (figure 7.3). The silicon oil is used as an insulation for the thermocouples. When the thermocouples would be put directly into the ice, the thermocouples would have been in short–circuit. To calibrate the sensors at other

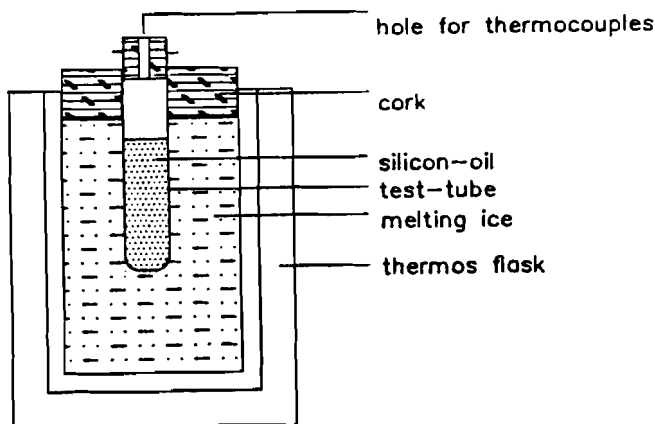


Figure 7.3 The setup for calibrating the thermocouples in melting ice.

temperatures, a different setup is made (figure 7.4). Sensors are put inside a copper block and this setup is put inside a temperature stabilized environment. The block is used to suppress fast temperature changes. In order to make a good heat conduction connection, the thermocouples were thermally connected to the copper block by heat conducting paste. The temperature of the block was measured by a thermometer, with an accuracy of 0.1°C , that was thermally connected with the copper block. The air temperature in this unit was set to -5°C , 10°C , 20°C and 30°C . Every new temperature took at least an hour to stabilize. The temperature output from the chart recorder was registered and the indicated temperature versus real temperature characteristics are given in appendix C.

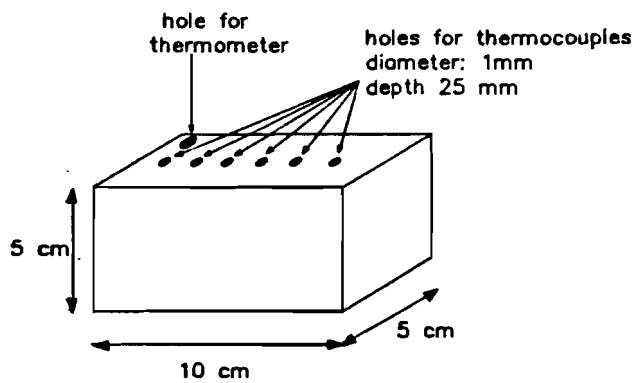


Figure 7.4: The setup for calibrating the thermocouples at other temperatures than 0°C .

7.1.6 Local heating/cooling.

In order to find the influence of local temperature variations, the active components should be heated or cooled. This to find the temperature dependence of several local parameters, such as gain and noise figure. The effects of local variations will be measured to find the relation between small local temperature changes and the change in the output voltage. This is of chief importance, because then it can be decided if some components have 'higher' priority in temperature measurements and corrections. several ways to change the local temperature were considered. At the start, it seemed to be quite logical to put temperature heating or cooling devices right at the components. The advantage of this method is, that the local temperature could be well-defined. A great disadvantage is, however, that these devices should be very small again, because the input and output terminals of the devices should not be touched. This requires the dimension of such devices

to be less than 2 mm. For such temperature control, heating IC's are available. These are about 4mm large and will not fit right on to the devices. Keeping a distance will highly disturb the heat conduction to these devices. Therefore this option is hypothetical for this radiometer. It would only be possible to change the mixer diode temperature. For cooling off the devices, heat pumps are available, known as Peltier elements. Again these elements are too large to be fit at the devices. Also, there is a problem in sinking the heat. The heat that would be pumped from the device to somewhere else should be left somewhere else in the circuit, which makes it very difficult not to affect the temperature of the other devices in the circuit. Another option to change the temperature of the devices, is to blow hot or cold air at the device package. This could be done with a small capillary tube, of which one end comes to the device and the other end is connected with a compressor. Such a capillary tube can have a diameter of 2mm. This capillary tube could be guided through melting ice or through other cold matter first, to cool the devices. Then the capillary tube could be heated by hot water to blow hot air at the devices. Especially for the first IF amplifiers, this is a very elegant method. The temperature is measured at the other end of the package, so the thermocouples will still measure the real package temperature. Only, to get a significant temperature change, the device should be cooled or heated quite intensively, which might affect the messing block temperature. For the devices that are not closely attached to the messing block, another problem rises. In this case the sensors might be cooled or heated directly. This means that the temperature indicated by the sensors might not be the same as the device package temperature. The advantage is here, that these devices do not sink their heat directly to the messing block, so significant temperature changes will be easier to achieve.

Local cooling by air.

As stated before, the components can be cooled by guiding cold air through a capillary tube and putting the end of the capillary tube close to the device package. This tub should be guided through melting ice to cool off the air within the tube. Since the air contains some water vapour, this vapour can condense. This means water could come out of the capillary tube. To extract the vapour from the air, the air is guided through a tube, containing silica gel. After this procedure, the air coming out of the tube is heated again by heat exchange between the tube and the air outside the tube. This means that the tube should be insulated to keep the heat out of the tube. After this whole procedure, the air coming out of the tube is 14 degrees Celsius, if the air coming in it is 24 degrees. For measurements where cooling this much is not sufficient, specifically the IF amplifiers, that are connected

to the messing block thermally, the ice could be mixed with salt. Then the ice can be cooled down to -20 degrees Celsius, which causes to drop the temperature of the air a few more degrees.

Local heating by air.

The capillary tube does not exchange enough heat from the hot water to the air within. Making the part of the tube within water longer just would not work, because the pressure and the air velocity drops very fast inside such a tube. Therefore it was decided, to use a larger tube, with an inner diameter of 6mm and an outer diameter of 8mm. In such a tube there is less heat exchange between the air and the tube per unit of volume, because the surface that exchanges heat with the air is relatively smaller. Instead of a 50 cm capillary tube, a tube was taken of 2 meters length, to provide good heat exchange. After this tube, still a small capillary tube is fit to it, to blow the hot air specifically at the radiometer component concerned. This capillary tube appeared to exchange too much heat with the air inside the cooling unit, so the air inside the tube was cooled off too fast, before it even came to the radiometer. Now the tube had to be insulated carefully. This could be done with glassfiber thread. In order to hold this together and to get a low convection loss (heat loss by air circulation), a terminal fit was used. These are usually utilised for insulating terminals electrically, but for this purpose it was used to hold the insulating glassfiber rope together.

7.2 Results.

The following paragraphs will show the results as they were retrieved from the measurements performed.

7.2.1 Overall temperature changes.

In order to find the gain to temperature characteristics of the IF/video unit of figure 7.1, this unit was placed inside the temperature stabilized environment (par.7.1.5). The input signal is the thermal noise of a 50 Ohms load. The load is thermally connected to the messing block and is assumed to have the same temperature as this block. The output signals from the set-up are registered by the chart recorder (par. 7.1.4), that also passes this data on to the disk of a personal computer. To initiate the measurements, the ambient temperature was set to 15 degrees Celcius. This first session was considered to be finished

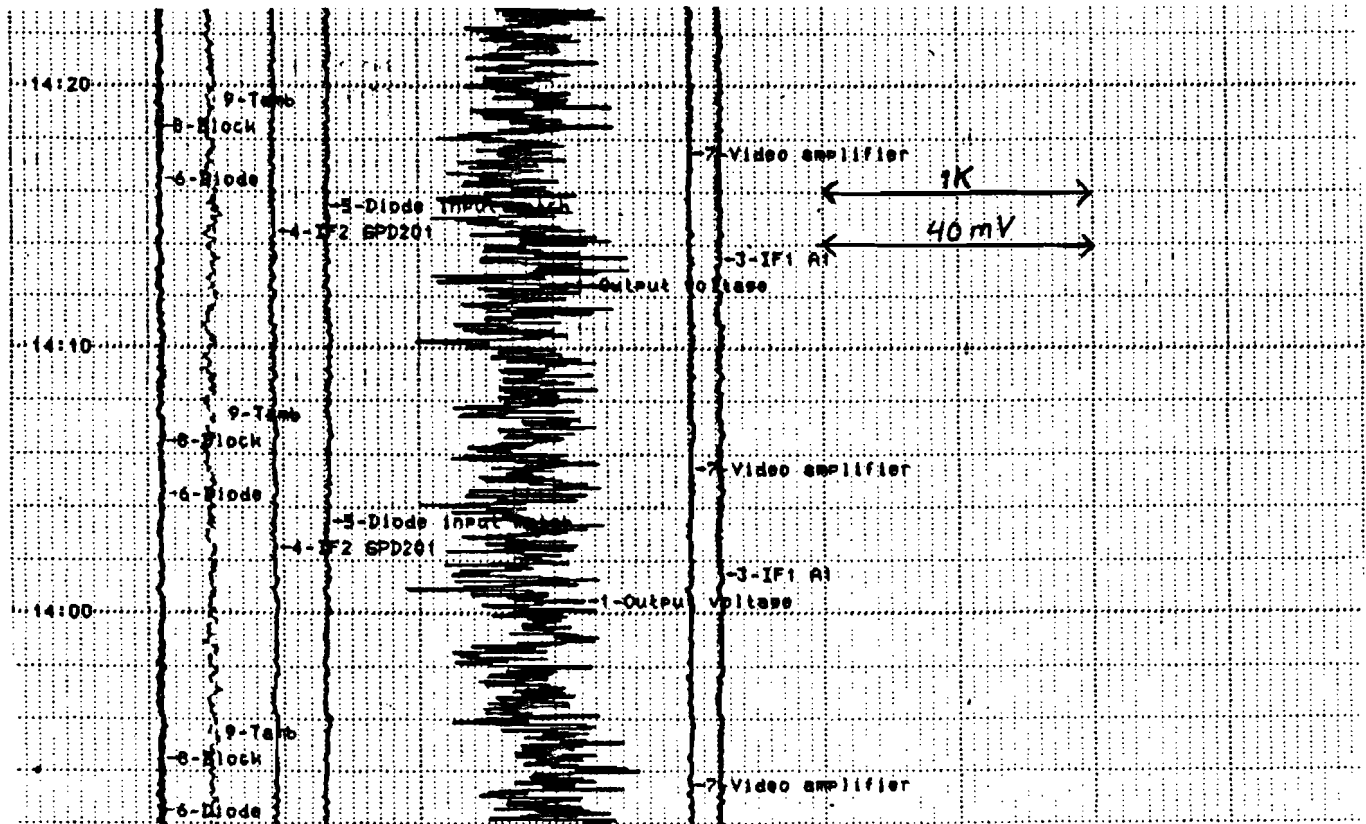


Figure 7.5: A chart of a stabilized measurement.

when all local temperatures were stable. As an example, part of a chart with stabilized measurements is shown in figure 7.5. For each next session, the ambient temperature was decreased with about 1 degree Celcius. The net time for such a session was about 1 hour. The ambient temperature was decreased 26 times until this temperature reached -10 degrees Celcius. This measurement session is named the downward measurements from now on. This resulted in the measurements as depicted in figure 7.6. To test any hysteresis effects, the ambient temperature was varied from -10 to 25 degrees Celcius, with a larger step size. From now on, these measurements are named the upward measurements. The results from these measurements are also depicted in figure 7.6. The stabilized system appears to suffer little or no influence from hysteresis. The differences between the downward and the upward measurements at a certain block temperature are always less than the random variations in the output signal as shown in figure 7.5.

Changing the overall ambient temperature it was found that the output voltage came close to a second order polynomial function of the block temperature. A fit with the downward measurements was made with the standard software Slidewrite. The measurement data from this measurement and the fit are shown in figure 7.6. The polynomial fit follows the equation:

$$V_{\text{out}} = -2.78466 \times 10^{-3} T^2 + 1.59199 T + 220.721 \quad (7.1)$$

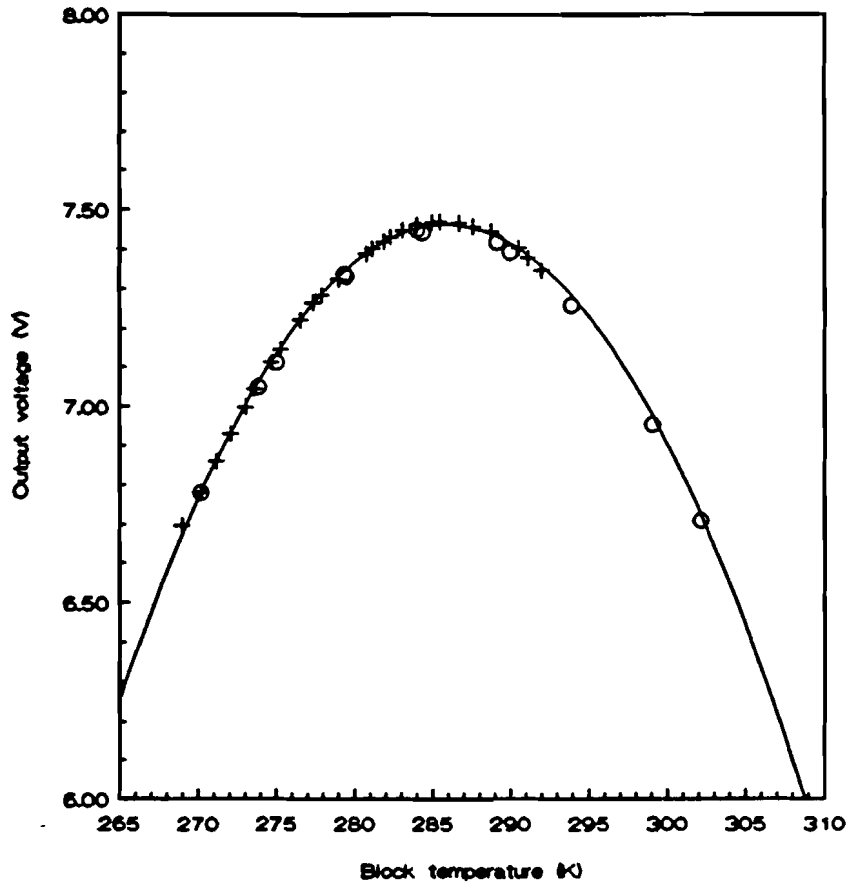


Figure 7.6: The output voltage as a function of the block temperature, for stabilized temperatures

+: $T_{\text{ambient}} = 15^{\circ}\text{C} \rightarrow -10^{\circ}\text{C}$, $\Delta T_{\text{ambient}} \approx -1^{\circ}\text{C}$.

o: $T_{\text{ambient}} = -10^{\circ}\text{C} \rightarrow 25^{\circ}\text{C}$, $\Delta T_{\text{ambient}} \approx 5^{\circ}\text{C}$

7.2.2. Local temperature changes.

In order to find the component that has the largest temperature dependence, the different components should be varied with temperature independently. A measurement set-up was made as described in paragraph 7.1.6 was used to do this.

Video amplifier

The video amplifier was the first component to be measured, because the temperature of this component could be varied easily without affecting the other local temperatures. This because the video amplifier is not connected to the messing block thermally, so it does not instantly sink its heat to the messing block. The measurements were done at 6 ambient temperatures, and at each of them the stabilized condition was measured and later the video amplifier temperature was changed as described in paragraph 7.1. The stabilized value of the output voltage at each temperature was higher than the stabilized voltage at the overall temperature measurement. These values as a function of the block temperature are plot in figure 7.7, together with the function of equation (7.1) and the function:

$$V_{\text{out}} = -2.45162 \times 10^{-3} T^2 + 1.40253 T - 192.986 \quad (7.2)$$

It is rather strange that the output voltages seems to differ at the same block temperature, but by setting up the measurements for the video amplifier dependency, several conditions with respect to the radiometer were changed. First of all, holes were drilled in the top of the messing block. This had to be done in order to blow hot or cold air to the radiometer. Second, in order to reduce the heat transfer from the video amplifier to the messing block or vice versa, the sides of the compartment in which the video amplifier is situated are insulated with teflon. This results in other stabilized local temperatures at the same block temperature. For the stabilized overall measurements the differences between the local temperatures and the block temperature appear to be constant over the whole ambient temperature range considered. The same holds for the local temperatures with the stabilized video amplifier temperature measurements. The differences are put into table 7.1.

The difference in output voltage at one block temperature, due to a video amplifier temperature change of 2.5 K is hardly larger than the random variations in the output voltage as found from figure 7.5.

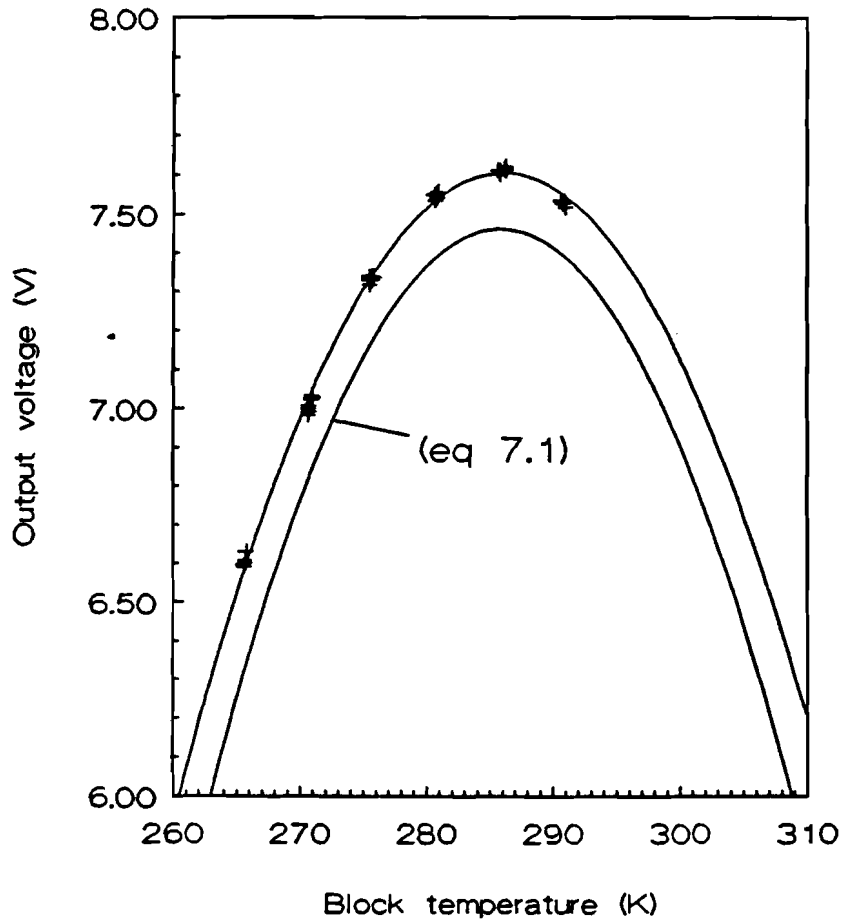


Figure 7.7: The output voltage as a function of the block temperature, for temperature changes in the video amplifier.

Table 7.1: The local temperature differences.

Measurement	$T_{a1} - T_{block}$	$T_{201} - T_{block}$	$T_{m1} - T_{block}$	$T_{diod} - T_{block}$	$T_{vid} - T_{block}$	V_{out}
Overall	0.30K	0.50K	-0.11K	0.22K	5.76K	
Vid. Ampl.	0.19K	0.42K	0.30K	-0.32K	6.97K	
Difference	-0.11K	-0.08K	0.41K	-0.54K	1.21K	0.192V

7.3 Measuring the IF/video unit after its repair.

During the measurements, the unit failed because of a broken terminal of the GPD201 amplifier. After a new one was inserted into the unit, the unit still failed. It appeared that

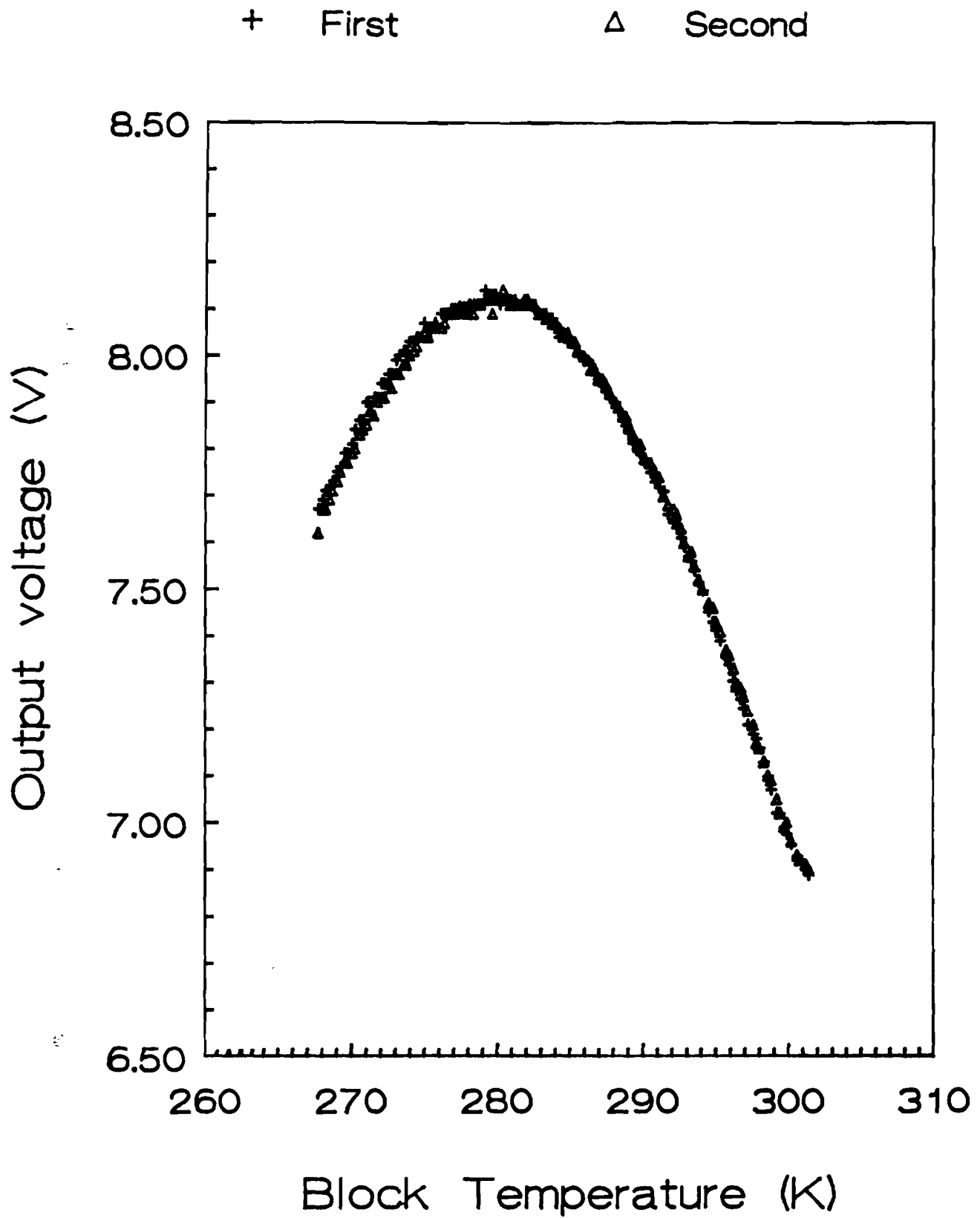


Figure 7.8: Reproducibility of a sweep measurement with a varying load temperature

the diode was broken, too. Because of a shortage of time, the measurements were all chosen to be sweep measurements. Such a sweep measurement can be performed in about 2 hours. Comparing this to the time needed for stabilized measurements, at least 26 hours, this could result in a considerable time gain. In this case, the accuracy of such measurements must be tested to verify if sweep measurements can replace stabilized measurements.

7.3.1 Reproducibility of sweep measurements.

At the start, a measurement is performed where the load was changing with the block temperature. To test the reproducibility of such a measurement, the same setup was repeated a few days later. Both measurements were done for the ambient temperature changing from $+25^{\circ}\text{C}$ to -10°C . These measurements resulted in the figure 7.8. From this figure, it is hard to tell, whether the differences are relevant. Calculating these differences, it appears that they are mostly in the range of 30mV, which is the actual random variation of the output voltage (see also figure 7.5) at a fixed block temperature. So, the differences are negligible. An important conclusion that can be taken, regarding the results of the measurements of the system with the first diode and those with the second diode, is that the maximum of the output voltage is at a higher level for the system with the second diode, namely about 8.2 V (figure 7.8), while it was about 7.7 V (figure 7.7). This means that every radiometer system with a different detector diode (same type) should be measured in order to find its temperature dependence. This makes new measurements hardly comparable to the previous ones.

7.3.2 Conversion factor and receiver noise temperature.

Important overall parameters that have to be determined are the conversion factor $ckBG$ and the receiver noise temperature T_{rec} . These can be calculated from two measurements, one with a 'hot' load, chosen to be melting ice, resulting in $T_a = 273$ K. The other with a 'cold' load, chosen to be vapourizing liquid nitrogen (N_2), leading to $T_a = 77$ K. Two equations can be formed:

$$V_{out\ ice}(T) = ckBG(T) \times (T_{rec}(T) + 273) \quad (7.3)$$

$$V_{out\ N_2}(T) = ckBG(T) \times (T_{rec}(T) + 77) \quad (7.4)$$

From these equations, the conversion factor $ckBG$ and the receiver noise temperature are found:

$$ckBG(T) = \frac{V_{out\ ice}(T) - V_{outN_2}(T)}{273 - 77} \quad (7.5)$$

$$T_{rec}(T) = \frac{V_{out\ ice}(T) \times 77 - V_{outN_2}(T) \times 273}{V_{outN_2} - V_{out\ ice}} \quad (7.6)$$

These equations only hold if the output voltage is a linear function of the system noise temperature, which means that $ckBG$ is constant for both input signals.

The values from the chartrecorder were stored on disk and converted to a 'workable' format with the pascal program CHARTCNV. This program gets data from a chart file, adds 273.15 to the temperature values (conversion degrees Celcius to Kelvin) and adds the offset temperature for each thermocouple (see appendix C). Another pascal program, PROCDAT calculates the conversion factor $ckBG$ and the receiver noise temperature at every block temperature from the chart files of the sweep measurements with the load at 273 K and 77 K. The radiometer output voltages of the two measurements are displayed in figure 7.9. The results of the calculation for the conversion factor and the receiver noise temperature are plotted in figure 7.10 and 7.11, respectively. A problem arises when the receiver noise temperature is calculated using (7.6). As can be seen from figure 7.11, it seems that the receiver noise decreases for increasing physical temperature. In terms of noise figure, the noise figure would be approximately 2.5 dB at $T = 265$ K and approximately 1.8 dB for $T = 300$ K. However, the noise figure of a device always increases with increasing temperature. To clear up this strange finding, it was decided to perform a noise figure measurement on the A1 amplifier that is used in the IF/video unit. The measurement was done at 3 different block temperatures (see table 7.2). From these measurements it follows that the noise actually increases for increasing temperature.

Table 7.2: Results of noise figure measurements on A1 amplifier.

T_{a1} (K)	NF (dB)	Gain (dB)	T_{rec}
267	2.2	13.4	191
282	2.2	13.3	191
302	2.3	13.1	202

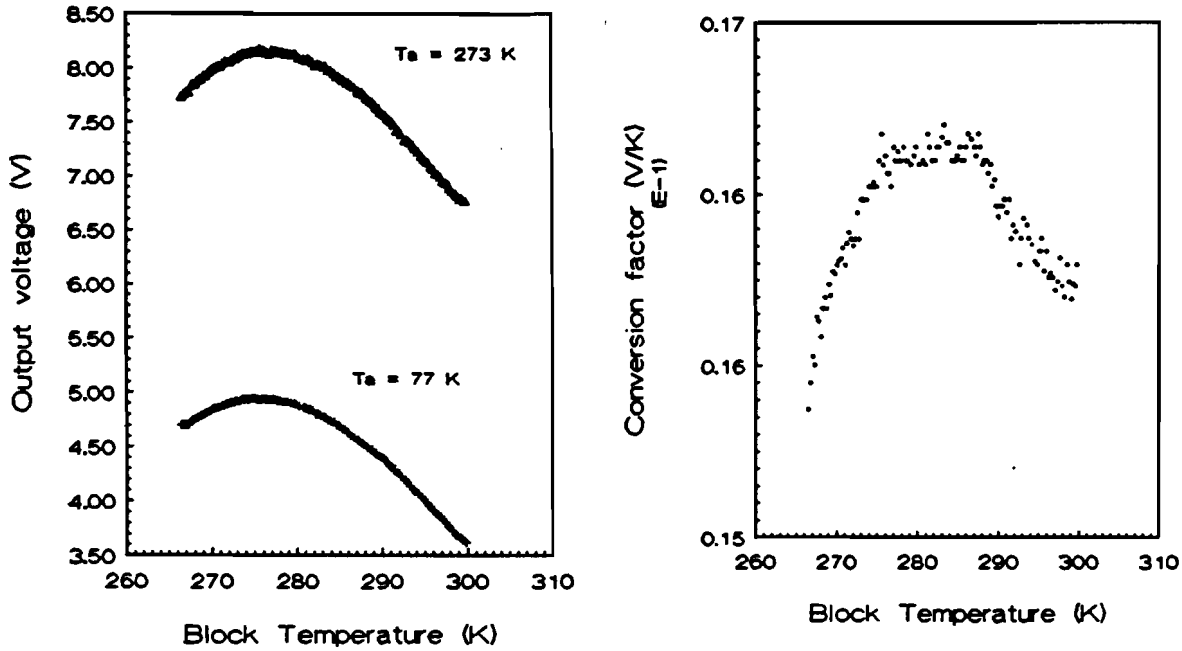


Fig 7.9: Output voltages of cold load and hot load measurements. Fig 7.10 Conversion factor, calculated from hot/cold load measurements.

As can be seen from (5.10), this conversion factor also includes the voltage sensitivity γ . As stated earlier, γ specifies the slope of the output voltage V_o , versus the input power P_i of the detector diode. Due to the fact that γ varies with temperature, an equal input power P_i will result in a different output voltage V_o [21]. This indicates that equation 7.3 should probably be changed to:

$$V_{out}(T) = ckBG(T) \times (T_{rec}(T) + T_a) + V_{off}(T) \quad (7.7)$$

Here V_{off} is a system offset voltage. In this expression, V_{off} can not be separated from $ckBG \times T_{rec}$, because only T_a can be changed independently from the other variables. So in fact, a part of the receiver noise as calculated from equation 7.6 actually comes from this

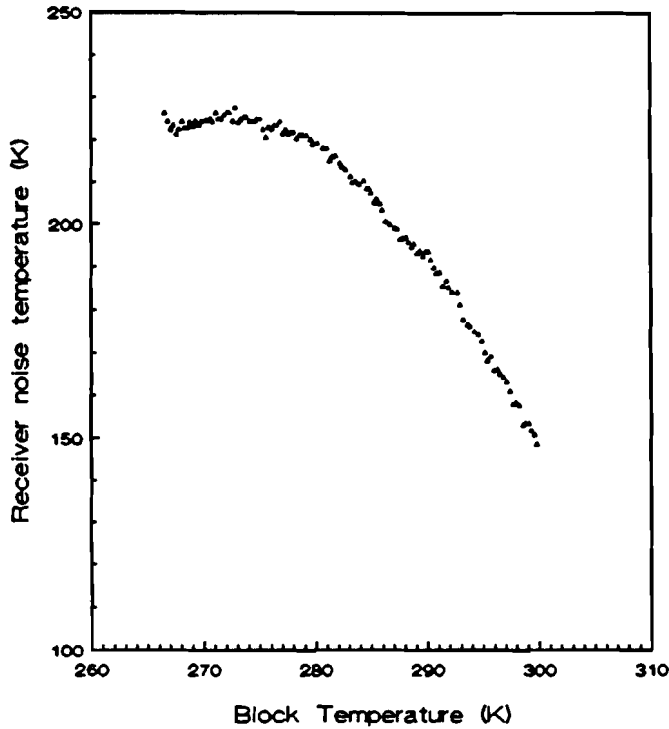


Fig 7.11: Receiver noise temperature, calculated from hot/cold load measurements.

offset voltage. This voltage is strongly dependent on the physical temperature. V_{off} must change at least -80mV/K in this range. This offset voltage can not come from the video amplifier. It can not come from an excess noise source in front of the detector, because the calculated receiver noise temperature is lower than the equivalent noise temperature of the first IF (A1) amplifier. By measuring the characteristics of the matching circuits, together with the diode and video amplifier, it was verified if such an offset voltage did originate from one of these system parts. Zero power was applied to the input match circuit, resulting in a nonzero output voltage, being the offset voltage. From these measurements, it was found that this offset is temperature dependent. This confirms that the offset voltage originates from the temperature dependence of the diode detector.

The errors in the calculated conversion factor and the receiver noise temperature, coming from discretization and random fluctuations of the signals from the temperature sensors and the output of the radiometer is calculated now. It can be seen from (7.5) that:

$$\frac{\Delta \text{ckBG}}{\text{ckBG}} = \frac{2 \Delta V_{\text{out}}}{V_{\text{out}_{N_2}}(T) - V_{\text{out}_{ice}}(T)} \quad (7.8)$$

The maximum error in the output voltage has three major causes:

Voltage discretization: the chart recorder uses an analog to digital converter to get the data. The output voltage can not be measured more accurate than 10 mV. With a lot of careful engineering and using very accurate temperature measurements, the resolution in the measured temperature could be brought down to $\Delta T_{\text{res}} = 0.1$ K. This should be multiplied by the maximum slope of the output voltage towards block temperature (found from figure 7.9), to find the error in the output voltage:

$$\Delta V_{\text{out},T} = \frac{\partial V_{\text{out}}}{\partial T} \times \Delta T_{\text{res}} = 0.06 \times 0.1 = 6 \text{ mV}$$

Furthermore, there is an uncertainty in the output voltage, due to the system sensitivity. This uncertainty equals $\text{ckBG} \times \Delta T = 0.016 \times 0.05 = 0.8 \text{ mV}$ (ckBG is found from figure 7.10). This all reviewed briefly:

1) error due to sensitivity: $\text{ckBG} \times \Delta T = 0.016 \times 0.05$	$\approx 1 \text{ mV}$
2) error due to voltage discretization:	$= 10 \text{ mV}$
3) error due to temperature resolution 0.06×0.1	$= 6 \text{ mV}$
Total error:	$= 17 \text{ mV}$

So, the relative error in the conversion factor is, according to (7.8), $2 \times 17 \text{ mV} / 3 \text{ V} = 11 \times 10^{-3}$ (the difference between the output voltage of the measurement with the load at 273 and the output voltage of the measurement with the load at 77K is approximately 3V). This results in a sensitivity of 5 K (from equation 3.16 follows taking $T_{\text{sys}} = 273 \text{ K} + 190 \text{ K}$, which includes the load temperature and the receiver noise from the first IF amplifier). Of the three causes for the output voltage error, the temperature resolution is the most difficult one to decrease. The discretization error can be improved by using an A/D converter with more bits, the sensitivity (without gain variations) can be decreased by increasing the integration time of the integrator. If only the error caused by the temperature resolution is taken into account, the error in the output voltage equals 6 mV. Then, the relative error in the conversion factor is $2 \times 6 \text{ mV} / 3 \text{ V} = 4 \times 10^{-3}$, corresponding to a sensitivity of 1.8 K. There is one option left to decrease this sensitivity. That is application of a limited temperature stabilisation around the maximum of the output voltage which occurs at a block

temperature of 278 K (5°C). If the temperature would be stabilized with a maximum temperature drift of 3K, the slope of V_{out} versus T , $\frac{\partial V_{out}}{\partial T}$, would be no more than 0.20 V/K (see figure 7.9), causing the error in V_{out} to be no more than 2mV. This would improve the best possible sensitivity to 0.6K.

The relative error in T_{rec} follows from (7.6):

$$\frac{\Delta T_{rec}}{T_{rec}} = \frac{350 \Delta V_{out}}{V_{out_{N_2}}(T) - V_{out_{ice}}(T)} \quad (7.9)$$

Using the values for ΔV_{out} and $V_{out_{N_2}}(T) - V_{out_{ice}}(T)$ as given before, it is found that the error in T_{rec} is:

—for all error causes, $\Delta V_{out} = 17\text{mV}$, $\frac{\Delta T_{rec}}{T_{rec}} = 2.0 \text{ K}$

—only the effect of temperature resolution: $\Delta V_{out} = 6\text{mV}$, $\frac{\Delta T_{rec}}{T_{rec}} = 0.7 \text{ K}$

—for limited physical temperature stabilization: $\Delta V_{out} = 2\text{mV}$, $\frac{\Delta T_{rec}}{T_{rec}} = 0.3 \text{ K}$

7.3.3 Hysteresis effects.

In order to check possible hysteresis of the system for sweep measurements, an extra measurement was made. The sweep measurement for the load at liquid nitrogen was performed in two directions: one (as described above), downward from +25°C to -10°C, the second was performed upward from -10°C to +25°C. The output voltages as a function of the block temperatures are displayed in figure 7.12. It is clear from this figure that:

- 1: The output voltage reaches its maximum at a higher block temperature for the upward sweep than for the downward sweep,
- 2: The maximum of the output voltage has a lower value for the upward sweep than for the downward sweep.

These differences can be explained by changes in the temperature gradients within the radiometer. Therefore a figure (7.13) was made, which shows the temperature differences of the local temperatures and the measuring block temperature. This figure shows a large discrepancy for the temperature differences between the upward sweep and the downward

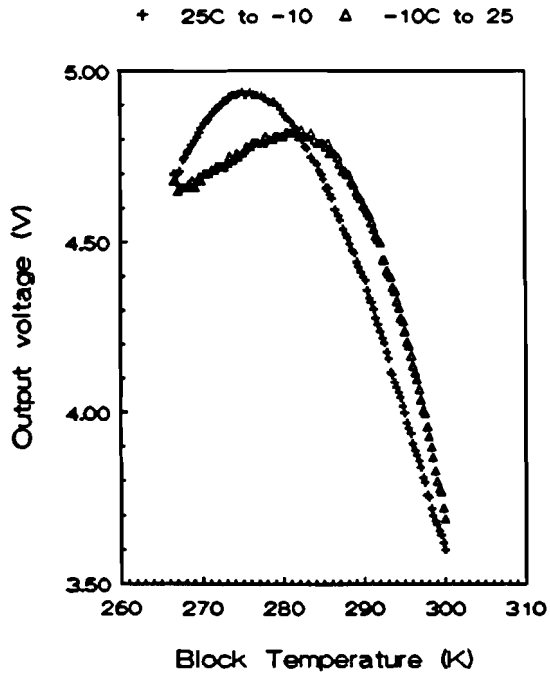


Fig 7.12: Sweep hysteresis measurements.

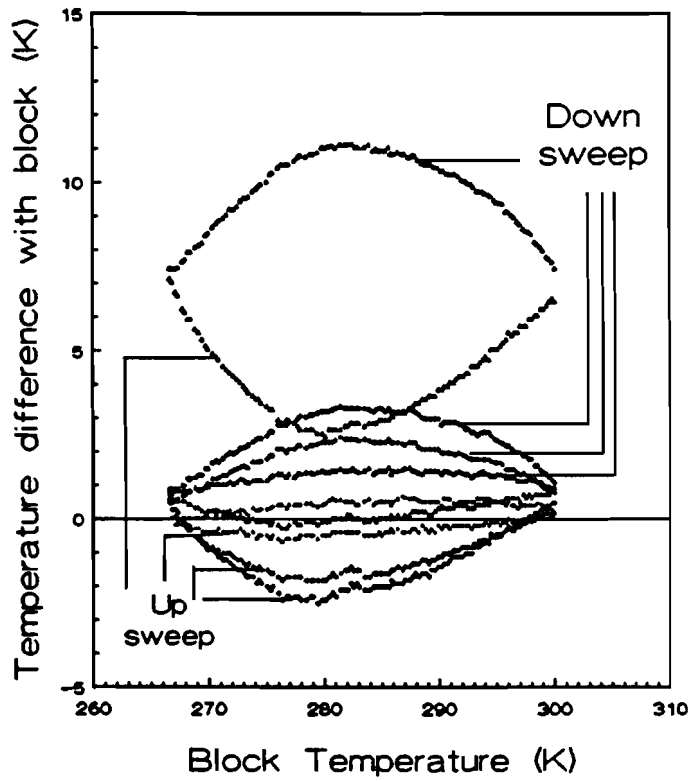


Fig 7.13: Temperature differences between the components and the messing block, in the radiometer, for sweep measurements

sweep. This causes the difference in output voltage of these measurements. For the stabilized overall measurements the differences between the local temperatures and the block temperature appear to be constant over the whole ambient temperature range considered. From this it can be concluded, that sweep measurement of 35°C (25°C to -10°C) will not match with data from stabilized measurements. So, sweep measurements can not be used to generate calibration curves necessary for software correction of temperature variations in a radiometer.

8. CONCLUSIONS AND RECOMMENDATIONS

In order to realize a sensitive radiometer, a very accurate temperature stabilization and reference to a known noise source is used in current radiometer systems. This results in complicated and consequently expensive radiometer designs, such as the Dicke switched and the noise injection radiometer. The gain of a radiometer varies with temperature, which causes the sensitivity of the radiometer to degrade. Therefore it was investigated whether the gain variations of a simple total power radiometer can be corrected by software.

In order to validate if software correction was possible a test set-up was designed. The first measurement performed with this test set-up was the reproducibility of the temperature dependence of the radiometer. It appeared that within a period of one week, the results were reproducible within the accuracy of the measurement set-up. Then two approaches of measuring the temperature dependence were verified, namely sweep measurements and the time consuming stabilized measurements. It appeared that sweep measurements do not supply reliable information on the temperature dependence in contrast to the stabilized measurements.

It was found, both theoretically and practically, that the diode causes the main parameter variations due to temperature fluctuations, and each individual diode causes another parameter variations. The temperature dependence of the video amplifier is almost negligible in this radiometer.

The accuracy of the measurement set-up is not sufficient, because the temperature measurements accuracy is fundamentally limited to an accuracy of 0.1 K, leading to a minimum sensitivity of 1.8 K. This is poorer than the sensitivity that is reached with current radiometers. This means that the very temperature dependent radiometer used, can not be corrected with the presently available experimental set-up.

It is recommended to implement software correction for a radiometer that is less temperature dependent. A lower temperature dependence can be achieved in different ways, e.g.:

- using a different (less temperature dependent) diode detector or
- application of limited external temperature stabilization of the radiometer

REFERENCES

- [1] Brussaard, G.
Radiometry: A useful prediction tool?
Louvain-la-Neuve (Belgium). Universite Catholique de Louvain 1985.
Doctoral Dissertation.
- [2] Skou, N.
Microwave radiometer systems: design and analysis.
Boston: Artech House, 1989
- [3] Evans, G. and McLeish, C.W.
RF Radiometer Handbook.
Dedham: Artech House, 1977
- [4] Dicke, R.H.
The measurement of thermal radiation of microwave frequencies.
Rev. Sci. Instr., vol.17, pp.268–275, July 1946.
- [5] Tiuri, M.E.
Radio Astronomy Receivers.
IEEE Trans. Ant. Prop. vol.12., pp.930–938, 1964
- [6] Ulaby, F.T., et al.
Microwave Remote Sensing, vol 2.
Boston: Artech House, 1982
- [7] Papoulis, A.,
Probability, random variables and stochastic processes,
Auckland: McGraw–Hill, 1980.
- [8] Anand, Y and Worsney, W.
Microwave Mixer and Detector Diodes.
HP–AN pp.183–194, may 1971.

- [9] The criterion for the Tangential Sensitivity measurement.
Application Note 956-1
Palo Alto: Hewlett-Packard, 1973.
- [10] Schottky barrier diode video detectors,
Application Note 923
Palo Alto: Hewlett-Packard, 1986.
- [11] Flicker noise in Schottky diodes
Application Note 956-3
Palo Alto: Hewlett-Packard, 1974.
- [12] Combes, P.F. et al.,
Microwave components, devices and active circuits.
Chichester: Wiley, 1987.
- [13] Thijssen, W.P.P.,
Ontwerp en bouw van een gedeelte van een
radiometer voor radio propagatie onderzoek.
Vocational training report,
Telecommunications division, Faculty of Electrical Engineering,
Eindhoven, University of Technology, 1986.
- [14] All Schottky diodes are zero bias detectors.
Application Note 988,
Palo Alto: Hewlett-Packard, 1982.
- [15] "Zero bias Schottky detector diodes.",
Hewlett-Packard diode and transistor designer's catalog. pp. 109-112
Palo Alto: Hewlett-Packard, 1982.
- [16] Maas, S.A.,
Microwave mixers,
Dedham: Artech house, 1986.

- [17] Watkins–Johnson
Thin film cascable amplifiers,
data sheets

- [18] "GPD series."
pp. 251–270, Modular and oscillator components data book,
Milpitas: Avantek, 1989.

- [19] "Ultra–low noise precision operational amplifiers."
pp. 2–27 to 2–30, Burr–Brown IC data book,
Tucson: Burr–Brown, 1989.

- [20] Harvey, A.F.,
"Radiometric Techniques"
pp. 773–783 Microwave engineering,
New York: Academic Press, 1963.

- [21] P.J.I. de Maagt,
Private communications, October 1990.

APPENDIX A.

A .1 S-PARAMETERS OF A TWO-PORT NETWORK

Consider a linear two-port network defined, for example, by its impedance matrix:

$$Z = \begin{pmatrix} Z_{11} & Z_{12} \\ Z_{21} & Z_{22} \end{pmatrix}$$

The directions of the root-mean-square (RMS) input and output voltages and currents are given by the usual conventions as in Figure 5.20:

$$\begin{pmatrix} V_1 \\ V_2 \end{pmatrix} = (Z) \begin{pmatrix} I_1 \\ I_2 \end{pmatrix} \quad (\text{A.1})$$

For each port, define what is called a reference impedance Z_1 for the input (port 1) and Z_2 for the output (port 2). The incident waves at ports 1 and 2 are then denoted by a_1 and a_2 and are given by:

$$a_1 = \frac{V_1 + Z_1 I_1}{2\sqrt{R_1}} \quad a_2 = \frac{V_2 + Z_2 I_2}{2\sqrt{R_2}} \quad (\text{A.2})$$

where R_1 and R_2 are the real parts of Z_1 and Z_2 respectively.

Similarly, the reflected waves b_1 and b_2 are given by:

$$b_1 = \frac{V_1 - Z_1^* I_1}{2\sqrt{R_1}} \quad b_2 = \frac{V_2 - Z_2^* I_2}{2\sqrt{R_2}} \quad (\text{A.3})$$

Note that the dimensions of each of these quantities are those of the square root of power.

The representation of Figure 5.20 then becomes equivalent to that of Figure 5.21.

Expressions (A.1), (A.2) and (A.3) show that a_1 , a_2 , b_1 and b_2 are not

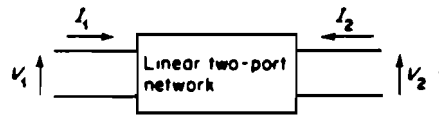


Figure 5.20

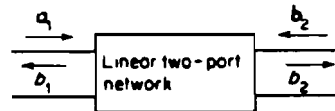


Figure 5.21

independent, so that we can write:

$$\begin{pmatrix} b_1 \\ b_2 \end{pmatrix} = \begin{pmatrix} S_{11} & S_{12} \\ S_{21} & S_{22} \end{pmatrix} \begin{pmatrix} a_1 \\ a_2 \end{pmatrix} \quad (\text{A.4})$$

where the matrix S is called the scattering matrix of the network. Its components are known as S -parameters and each of them has a special physical significance.

For example, if the output is terminated by a load Z_R equal to the reference impedance Z_2 , the output voltage V_2 would then be $-Z_2 I_2$, implying from equation (A.2) that a_2 is zero. We then have that $b_1 = S_{11} a_1$, i.e. that S_{11} is equal to the reflected wave divided by the incident wave at port 1. In practice, this is used to measure S_{11} by determining the incident and reflected powers

at the network input. In the same way, if the output is always terminated by Z_2 , the outgoing power at port 2 divided by the incident power at port 1 enables S_{12} , known as the transmittance, to be determined. Terminating the input by Z_1 would enable S_{22} and S_{12} to be determined in a similar way. The importance of the S -parameters lies in the fact that the concepts of current and voltage implicit in the parameters Z , Y , H , etc. are replaced by the concept of power which is more easily measured at microwave frequencies. There are, of course, transfer relationships enabling the conversion of S -parameters into any of the current or voltage parameters. More details of the properties of S -parameters will be found in Badoual (1984), Gentili (1984) and others.

A.2 EXAMPLE OF THE USE OF S -PARAMETERS IN THE MICROWAVE REGION

In practice, the impedance Z_1 and Z_2 in a two-port microwave network are not chosen at random but are both taken as equal to the characteristic impedance Z_c , assumed real, of the line into which the network is inserted ($Z_1 = Z_2 = Z_c$). This impedance is normally 75 ohms in the VHF-UHF region and 50 ohms in the microwave region. If the network load is an impedance Z_R ($V_2 = -Z_R I_2$), the quotient b_1/a_1 is, from equations (A.1), (A.2) and (A.3):

$$\frac{b_1}{a_1} = S_{11} + \frac{S_{21}S_{12}\Gamma_R}{1 - S_{22}\Gamma_R}$$

where $\Gamma_R = (z_R - 1)/(z_R + 1)$ is the reflection coefficient of Z_R ($z_R = Z_R/Z_c$).

Since b_1 and a_1 are the square roots of the incident and reflected powers at port 1, they are proportional to the incident and reflected voltages at the network input, and their quotient thus represents the reflection coefficient Γ_i of the input impedance Z_i ($z_i = Z_i/Z_c$) of the network. Hence:

$$\Gamma_i = \frac{z_i - 1}{z_i + 1} = \frac{b_1}{a_1} = S_{11} + \frac{S_{12}S_{21}\Gamma_R}{1 - S_{22}\Gamma_R} \quad (\text{A.5})$$

If Z_o is the output impedance of the network ($z_o = Z_o/Z_c$), its reflection coefficient Γ_o can be calculated in the same way:

$$\Gamma_o = \frac{z_o - 1}{z_o + 1} = S_{22} + \frac{S_{12}S_{21}\Gamma_g}{1 - S_{11}\Gamma_g} \quad (\text{A.6})$$

where $\Gamma_g = (z_g - 1)/(z_g + 1)$ is the reflection coefficient of the internal impedance Z_g of the generator connected to the network input ($z_g = Z_g/Z_c$).

From a knowledge of these S -parameters, it is thus possible to determine all the electrical properties of the two-port network concerned.

Comment: resultant power

It is known that the power absorbed at the input to the network is given by $P_i = \text{Re}(V_1 I_1^*)$. By calculating expressions for V_1 and I_1^* in terms of a_1 and b_1 from equations (A.1) and (A.2), and substituting the result in the expression for P_i , we have:

$$P_i = |a_1|^2 - |b_1|^2 \quad (\text{A.7})$$

The resultant power P_i absorbed is thus confirmed as the difference between the incident and reflected powers.

APPENDIX B: Multiple reflections

At the terminals of any microwave device, reflections of the incoming wave can occur (see also app. A). When looking at the situation between two consecutive devices as given in figure B.1, one can conclude that multiple reflections might be possible between the output terminals of device A and the input terminals device B. (See figure B.1). Since the microwave signals inside a radiometer are basically stochastic signals, the effect of multiple reflections can be calculated.

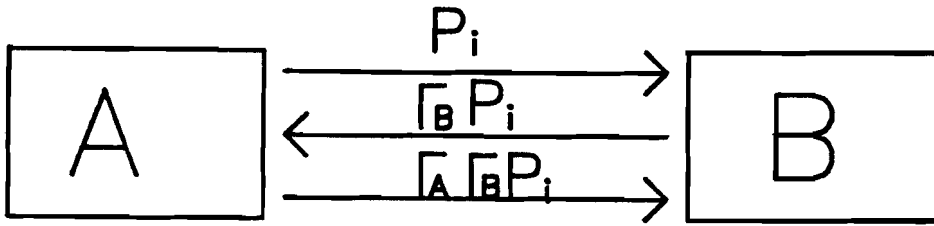


Figure B.1: Multiple reflections between two devices.

In figure B.1, Γ_A is the reflection coefficient of the output terminals of device A and Γ_B is the reflection coefficient of the input terminals of device B. The normal outgoing wave of device A is a stochastic microwave signal $x(t)$ with power P_x . A portion Γ_B of this signal returns to become the incoming wave for the terminals of device A. Again a portion Γ_A is reflected and will add to the incoming wave at the terminals of device B. This is also shown in figure B.2. Between the devices, the signal is also time delayed by a small time Δt . Now, deriving from picture, the equation for the wave $y(t)$, absorbed by device B is:

$$y(t) = (1 - \Gamma_B)x(t - \Delta t) + \Gamma_A \Gamma_B x(t - 3\Delta t) + \Gamma_A^2 \Gamma_B^2 x(t - 5\Delta t) + \dots \quad (\text{B.1})$$

If only the first reflection is included, the autocorrelation function of this signal is:

APPENDIX C.: The calibration curves of the thermocouples.

While calibrating the thermocouples, it appeared that the indicated temperature goes linearly with the real temperature, with a certain offset temperature. This offset is put in table C.1, together with the channels at which the thermocouples are used for the measurement setup.

Table C.1: The offset voltages of the thermocouples.

Thermocouple #	Channel #	Offset temp. (K)
1	9	-0.77
2	2{not used}	-0.93
3	3	-0.98
4	4	-1.02
5	5	-0.95
6	6	-0.84
7	7	-0.82
8	8	-0.87

The offset temperature T_{off} is defined by:

$$T_{\text{ind}} = T_{\text{real}} + T_{\text{off}} \quad (\text{C.1})$$

The curves are plotted in figure C.1 Obviously, at high temperatures ($T_{\text{real}} > 20^{\circ}\text{C}$), the indicated temperatures start to divert from the estimated line. One must be aware of the fact, that the real temperature is only indicated by a thermometer with an accuracy of 0.1°C . However, an extra digit is given for the offset temperature.

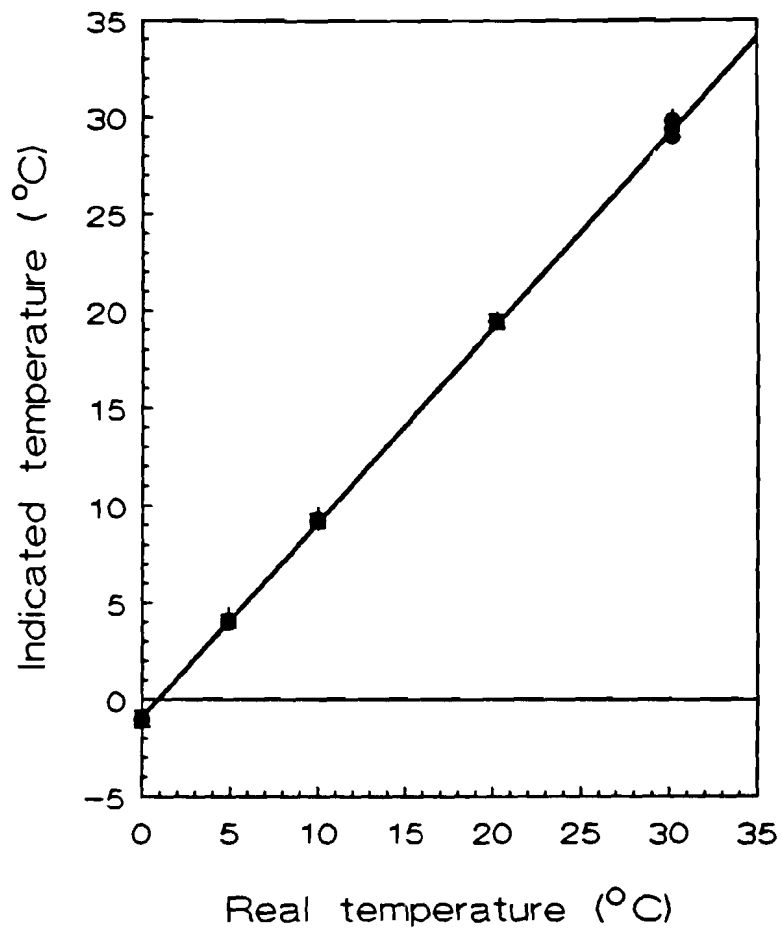


Figure C.1: The calibration curves of the thermocouples.

APPENDIX D: The program texts.

Unit Radunit;

Interface

Const

 k = 1.38E-23;

 T0 = 298;

Type

 Gainarray = array [1..5] of real;

 Noisearray = array [1..5] of real;

 Lossarray = array [1..5] of real;

 Comparray = array [1..11] of real;

 Powerarray = array [1..7] of real;

 Voltarray = array [8..11] of real;

 Cointarray = array [1..11] of integer;

{-----}

function dBinv(value :real):real;

{-----}

function dB(value :real):real;

{-----}

procedure Paramread(var Tph:comparray; var Bif, gamma298,

 TSS, Rv298, Rs298, Tau:real;

 var GaindB:gainarray;

 var LossdB:lossarray;

 var NFigure:noisearray;

 var Td, VSWR:comparray;

 var offvoltdr: real);

{-----}

procedure Initarr(LolddB:Lossarray;GolddB:Gainarray;

 var LdB:Lossarray;var GdB:Gainarray);

{-----}

procedure CalcBetacl(var Beta, cl:real; Rv298, Rs298, Rl,

 gamma298, freq, cap:real);

{-----}

function Rectemp(Teq:comparray; Gaindb:gainarray;

 Lossdb:lossarray; Bif, Rv, gamma,

```

    Tau :real):real;
{-----}
procedure Tempdependence(var LossdB :lossarray;
    var GaindB:gainarray;
    var gamma:real; Td, Tph:comparray;
    freq, cap, Rs298, Rl, c1,
    Beta:real);
{-----}
procedure Radiometer(Ta:real; Tph:comparray; gamma, TSS,
    Bif, Tau :real; Ldb :lossarray;
    GdB :gainarray; NF :noisearray;
    VSWR :comparray; offvoltdr:real; var Po,
    Pno :powerarray; var Vo, Vno :voltarray;
    var Gbefore, Voltkelv :real;
    var Teq :comparray);
{-----}
Implementation
{-----}
function dBinv(value :real):real;
{inverse deciBel function}
begin
    dBinv:=exp(value*ln(10)/10)
end;
{-----}
function dB(value :real):real;
{deciBel function}
begin
    dB:=10*ln(value)/ln(10)
end;
{-----}
procedure paramread(var Tph:comparray; var Bif, gamma298,
    TSS,Rv298,Rs298, Tau:real;
    var GaindB:gainarray;
    var LossdB:lossarray;
    var NFigure:noisearray; var Td,
    VSWR:comparray;

```

```

        var offvoltdr:real);
{read parameters from file param}
var i :integer;
    Tp :real;
    inv :text;

begin
    Assign(inv,'param.dat');reset(inv);
    Readln(inv, Tp);
    Readln(inv, Bif);
    Readln(inv, gamma298);
    Readln(inv, TSS);
    Readln(inv, Rv298);
    Readln(inv, Rs298);
    Readln(inv, Tau);
    For i := 1 To 5 Do Readln(inv, Gaindb[i]);
    For i := 1 To 5 Do Readln(inv, Lossdb[i]);
    For i := 1 To 5 Do Readln(inv, NFigure[i]);
    For i := 1 To 8 Do Begin
        Readln(inv, Td[i]);
        Readln(inv, VSWR[i]);
        Tph[i] := Tp
    End;
    For i := 9 To 11 Do Begin
        Readln(inv, Td[i]);
        Tph[i] := Tp
    End;
    Readln(inv, offvoltdr);
    Close(inv)
End;
{-----}
procedure Initarr(Lolddb:Lossarray;Golddb:Gainarray;
    var LdB:Lossarray;var GdB:Gainarray);
var i :integer;
Begin
    Ldb:=Lolddb;

```

```

    GdB:=Golddb;
End;
{-----}
procedure CalcBeta1(var Beta, c1:real; Rv298, Rs298, Rl,
                    gamma298, freq, cap:real);
Begin
    c1 := exp(5600/298) / (11350*298*(Rv298-Rs298));
    Beta := gamma298/Rv298*(1+(sqr(2*Pi*freq*cap)*
        Rs298*Rv298))*(Rl+Rv298)/Rl;
End;
{-----}
function Rectemp(Teq:comparray; Gaindb:gainarray;
                Lossdb:lossarray; Bif, Rv, gamma,
                Tau :real):real;
{calculate receiver noise temperature from the equivalent
noise temperature of the different components of the
radiometer}
var Teqrec                :real;
    Gain                  :gainarray;
    Loss                  :lossarray;
    i                    :integer;
Begin
    Bif := Bif*1000000;
    For i:= 1 To 3 Do Loss[i] := dBinv(Lossdb[i]);
    For i:= 1 To 4 Do Gain[i] := dBinv(Gaindb[i]);
    Teqrec := (Teq[8])/Gain[4];
    Teqrec := Loss[3]*(Teq[7]+Teqrec);
    Teqrec := (Teq[6]+Teqrec)/Gain[3];
    Teqrec := (Teq[5]+Teqrec)/Gain[2];
    Teqrec := Loss[2]*(Teq[4]+Teqrec);
    Teqrec := (Teq[3]+Teqrec)/Gain[1];
    Teqrec := Teq[1]+Loss[1]*(Teq[2]+Teqrec);
    rectemp:= Teqrec
End;
{-----}
procedure Gainvar(var H:real;Td,Tph:real);

```

```

Begin
  H := H + Td*(Tph-T0);
  if H < 0 then H := 0
End;
{-----}
procedure VoltGainvar(var H:real;Td,Tph:real);
var Hdb:real;
Begin
  HdB := dB(H);
  If Abs(td*(Tph-T0))>Abs(HdB) Then Begin
    Writeln('Warning: local gain changes to loss');
    HdB := 0          end
  Else HdB := HdB + Td*(Tph-T0);
  H := dBinv(Hdb)
End;
{-----}
procedure VoltSensVar(var gamma:real;Tph, freq, Cap, Rs298,
                    Rl, c1, Beta:real);
var Rs, Rv:real;
Begin
  Rs := Rs298*Tph/298;
  Rv := exp(5600/Tph)/(11350*c1*Tph)+Rs;
  gamma := (Rl/(Rl+Rv))*Beta*Rv/(1+sqr(2*Pi*freq*cap)
    *Rs*Rv);
End;
{-----}
procedure Tempdependence(var LossdB :lossarray;
                        var GaindB:gainarray;
                        var gamma:real; Td, Tph:comparray;
                        freq, Cap, Rs298, Rl, c1,
                        Beta :real);
begin
  Gainvar(LossdB[1],Td[1],Tph[1]);
  Gainvar(GaindB[1],Td[2],Tph[2]);
  Gainvar(LossdB[2],Td[3],Tph[3]);
  Gainvar(GaindB[2],Td[4],Tph[4]);

```

```

Gainvar(GaindB[3],Td[5],Tph[5]);
Gainvar(LossdB[3],Td[6],Tph[6]);
Gainvar(GaindB[4],Td[7],Tph[7]);
VoltSensVar(gamma, Tph[8], freq, Cap, Rs298, Rl, c1,
            beta);
VoltGainvar(GaindB[5],Td[10],Tph[10]);
VoltGainvar(LossdB[5],Td[11],Tph[11]);
end;
{-----}
procedure Linpowdev(Pin, Pni, Tph, Hdb, NFigure, Bif,
                  VSWR: real; var Po, Pno, Gainbef,
                  Teq:real);
{calculate output of a linear power device}
var H, F, Refl :real;
Begin
  Refl:= (VSWR-1)/(VSWR+1);
  H := dBinv(Hdb);
  F := dBinv(NFigure);
  Teq := Tph*(F-1);
  Bif := Bif*1000000;
  Po := (1-refl)*H*Pin;
  Pno := (1-refl)*H*(Pni+k*Bif*Teq);
  Gainbef := Gainbef+Hdb+dB(1-refl)
end;
{-----}
procedure IFAmplifier(Pin, Pni, Tph, Hdb, NFigure, Bif,
                    VSWR: real; var Po, Pno, Gainbef,
                    Teq:real);
{calculate output of IF amplifier}
var H, F, Refl :real;
Begin
  Refl:= (VSWR-1)/(VSWR+1);
  H := dBinv(Hdb);
  F := dBinv(NFigure+0.02*(Tph-T0));
  Teq := 290*(F-1);
  Bif := Bif*1000000;

```



```

    Po := (1-Refl)*H*Pin;
    Pno := (1-Refl)*H*(Pni+k*Bif*Teq);
    Gainbef := gainbef+Hdb+dB(1-Refl)
End;
{-----}
procedure Detector(Pin, Pni, Tph, gamma, TSS, Bif, Tau,
    VSWR:real; var Vo, Vno, voltkelv,
    Teq:real);
{calculate output of the detector}
var NDS, Refl : real;
Begin
    Refl:= (VSWR-1)/(VSWR+1);
    NDS := dBinv(TSS-4);
    NDS := NDS/1000;
    Bif := Bif*1000000;
    Teq := NDS/(k*Bif);
    Vo := (1-refl)*gamma*Pin;
    Vno := (1-refl)*gamma*(Pni+k*Teq/Tau);
    Voltkelv:= Voltkelv*gamma;
End;
{-----}
procedure Linvoltdev(Vi,Vni, Tph, H, offvoldr:real;
    var Vo, Vno, Voltkelv:real);
{calculate output of a linear voltage device}
Begin
    Vo := H*(Vi+offvoldr/1000000*(Tph-T0));
    Vno := H*(Vni+offvoldr/1000000*(Tph-T0));
    Voltkelv := H*Voltkelv
end;
{-----}
procedure Radiometer(Ta:real; Tph:comparray; gamma, TSS,
    Bif, Tau :real; Ldb :lossarray;
    GdB :gainarray; NF :noisearray;
    VSWR :comparray; offvoldr:real;
    var Po, Pno :powerarray;
    var Vo, Vno :voltarray; var Gbefore,

```

```

        Voltkelv :real; var Teq :comparray);
{calculate output of the radiometer}
var Pin :real;
begin
  Pin := k*Bif*1000000*Ta;
  Linpowdev( Pin, Pin, Tph[1], -Ldb[1], Ldb[1],
            Bif, VSWR[1], Po[1], Pno[1], Gbefore, Teq[1]);
  Linpowdev( Po[1], Pno[1], Tph[2], Gdb[1], NF[1], Bif,
            VSWR[2], Po[2], Pno[2], Gbefore, Teq[2]);
  Linpowdev( Po[2], Pno[2], Tph[3], -Ldb[2], NF[2], Bif,
            VSWR[3], Po[3], Pno[3], Gbefore, Teq[3]);
  IFamplifier( Po[3], Pno[3], Tph[4], Gdb[2], NF[3], Bif,
            VSWR[4], Po[4], Pno[4], Gbefore, Teq[4]);
  IFamplifier( Po[4], Pno[4], Tph[5], Gdb[3], NF[4], Bif,
            VSWR[5], Po[5], Pno[5], Gbefore, Teq[5]);
  Linpowdev( Po[5], Pno[5], Tph[6], -Ldb[3], Ldb[3], Bif,
            VSWR[6], Po[6], Pno[6], Gbefore, Teq[6]);
  Linpowdev( Po[6], Pno[6], Tph[7], Gdb[4], NF[5], Bif,
            VSWR[7], Po[7], Pno[7], Gbefore, Teq[7]);
  Voltkelv:=dBinv(Gbefore)*k*Bif*1000000;
  Detector( Po[7], Pno[7], Tph[8], gamma, TSS, Bif, Tau,
            VSWR[8], Vo[8], Vno[8], voltkelv, Teq[8]);
  Linvoltdev(Vo[8], Vno[8], Tph[9], 1, 0, Vo[9], Vno[9],
            voltkelv);
  Linvoltdev(Vo[9], Vno[9], Tph[10], Gdb[5], offvoldr,
            Vo[10], Vno[10], voltkelv);
  Linvoltdev(Vo[10], Vno[10], Tph[11], Ldb[5], 0,
            Vo[11], Vno[11], voltkelv);
End;
Begin
End.

```

```

program tempvar;
uses crt, graph, radunit;
var
  Ta, Tmin, Tmax, Tstep, offvoltdr, Voltkelv :real;
  gamma, Bif, Bint, Rv, tau, TSS, squarelawtop:real;
  gamma298, Rv298, Rs298, c1, Beta, Rl, freq :real;
  cap                                     :real;
  Nodev, Right, Bottom                   :integer;
  LdB                                     :lossarray;
  GdB                                     :gainarray;
  NF                                      :noisearray;
  Td, VSWR, Tph                           :comparray;
  Filenaam                               :string;
  inv, uit                                :text;
  Devnr                                   :cointarray;
{-----}
procedure ReadTextXY(x,y:integer;var instring:string);
{Reads text from the keyboard and displays it on the screen,
 at coordinates x, y}
var
  ch      : char;
begin
  instring := '';
  SetViewPort(x,y,x+80,y+8,ClipOff);
  While Ord(ch) <> 13 do
  begin
    ch := readkey;
    if Ord(ch) = 8 then
    begin
      delete(instring,length(instring),1);
      ClearViewPort;
      OutTextXY(0,0,instring)
    end
    else
    if Ord(ch) <> 13 then
    begin

```

```

    instring := instring + ch;
    OutTextXY(0,0,instring);
  end
end;
SetViewPort(0,0,Right,Bottom,ClipOn)
end;
{-----}
procedure Radiometergraph;
{Draws the scheme of the radiometer on the screen}
Var
  i          : integer;
Begin
  Arc(20, 30, 300, 60, 20); {antenna}
  Line(40, 30, 50, 30);
  OutTextXY(20,0,'Ta');
  OutTextXY(20,48,'0');
  Rectangle(50, 20, 90, 40); {Lrf}
  Line(90,30,100,30);
  OutTextXY(60,0,'Lrf');
  OutTextXY(70,48,'1');
  Line(100,40,100,20);    {Grf}
  Line(100,20,140,30);
  Line(140,30,100,40);
  Line(140,30,150,30);
  OutTextXY(110,0,'Grf');
  OutTextXY(120,48,'2');
  Circle(170,30,20);      {Mixer}
  Line(157,24,183,36);
  Line(157,36,183,24);
  Line(190,30,200,30);
  OutTextXY(160,0,'Mix');
  OutTextXY(170,48,'3');
  Line(200,40,200,20);    {Gif}
  Line(200,20,240,30);
  Line(240,30,200,40);
  Line(240,30,250,30);

```

```

OutTextXY(210,0,'Gif');
OutTextXY(220,48,'4');
Rectangle(250,20,290,40); {BPF}
Line(290,30,300,30);
OutTextXY(260,0,'BPF');
OutTextXY(270,48,'5');
MoveTo(260,35);
For i := 0 To 20 Do
  LineTo(260+i,35-Trunc(3*Sin(Pi*i/10)));
Line(270,37,270,33);
MoveTo(260,30);
For i := 0 To 20 Do
  LineTo(260+i,30-Trunc(3*Sin(Pi*i/10)));
MoveTo(260,25);
For i := 0 To 20 Do
  LineTo(260+i,25-Trunc(3*Sin(Pi*i/10)));
Line(270,27,270,23);
Rectangle(300,20,340,40); {Match I}
Line(340,30,360,30);
OutTextXY(310,0,'M1');
OutTextXY(320,48,'6');
Line(360,35,360,25); {Detector}
Line(360,25,380,30);
Line(380,30,360,35);
Line(380,35,380,25);
Rectangle(350,20,390,40);
Line(380,30,400,30);
OutTextXY(360,0,'Det');
OutTextXY(370,48,'7');
Rectangle(400,20,440,40); {Match II}
Line(440,30,450,30);
OutTextXY(410,0,'M2');
OutTextXY(420,48,'8');
Line(450,40,450,20); {Gvid}
Line(450,20,490,30);
Line(490,30,450,40);

```

```

Line(490,30,500,30);
OutTextXY(460,0,'Gvid');
OutTextXY(470,48,'9');
Rectangle(500,20,540,40); {Integrator}
OutTextXY(510,0,'Int');
OutTextXY(520,48,'10')
End;
{-----}
procedure QuestGraph(var Ta, Tmin, Tmax, Tstep:real;
  var Devnr:cointarray; var Filenaam:string;
  var Nodev:integer);
{Asks for the equivalent noise temperature of the input
signal, the number of devices that are varied with
temperature, the numbers of these devices, the temperature
range for which these should be varied and the output
file, to which the calculated values are written. This
file has an extension .LYN}
var code, i :integer;
instring:string;
Begin
  OutTextXY(10,64,'Give sky noise temperature ');
  ReadTextXY(500,64,instring);val(instring,Ta,code);
  OutTextXY(10,73,
'How many devices do you want to vary with temperature');
  ReadTextXY(500,73,instring);val(instring,Nodev,code);
  If Nodev >= 11 Then
    Begin For i := 1 to 11 do Devnr[i] := i; i:=1 End
  Else For i := 1 To Nodev Do
    Begin
      OutTextXY(10,73+9*i,'Which device (1-11) ');
      ReadTextXY(500,73+9*i,instring);
      val(instring,Devnr[i],code);
    End;
  OutTextXY(10,91+9*i,'From temperature ');
  ReadTextXY(500,91+9*i,instring);val(instring,Tmin,code);
  OutTextXY(10,100+9*i,'To temperature ');

```

```

ReadTextXY(500,100+9*i,instring);val(instring,Tmax,code);
OutTextXY(10,109+9*i,'Name of output file ');
ReadTextXY(500,109+9*i,filenaam);
Filenaam := Filenaam + '.lyn';
Tstep := (Tmax-Tmin)/60
end;
{-----}
procedure PickCoord(var Right, Bottom:integer);
{PickCoord checks the screendriver of the screen used. Then
it assigns values to the righthmost and the bottom coordinate}
var GraphDriver, GraphMode, ErrorCode :integer;
Begin
  GraphDriver := Detect;
  InitGraph(GraphDriver,GraphMode,'');
  ErrorCode := GraphResult;
  If GraphDriver = 1 Then
    Begin Right := 639; Bottom := 199 End
  Else
    If GraphDriver = 7 Then
      Begin Right := 719; Bottom := 347 End
    Else
      If GraphDriver = 3 Then
        Begin Right := 639; Bottom := 347 End;
End;
{-----}
procedure Tempvarout(Filenaam:string; Tph:comparray; Bif,
  gamma298, TSS, Tau:real;
  GolddB:gainarray; Lolddb:lossarray;
  NFigure:noisearray; Td, VSWR:comparray;
  offvoltdr, Ta, Tmin, Tmax, Tstep:real;
  Devnr:cointarray; Nodev:integer; freq,
  cap, Rv298, Rs298, Rl, Beta, c1 :real);
{Tempvarout takes care of the calculations for 60 values
within the range specified earlier. It calculates the
system noise temperature, the gain before the detector,
the voltage sensitivity of the detector, the output voltage

```

without receiver noise and the output voltage with receiver noise and puts this in the output file as specified earlier.}

```

var LdB :lossarray;
    GdB :gainarray;
    Po, Pno:powerarray;
    Vo, Vno:voltarray;
    T, Gbefore, Teqrec :real;
    Teq :comparray;
    i, j :integer;
begin
  Initarr(Lolddb,GolddB,LdB,GdB);
  Assign(uit,Filenaam);Rewrite(uit);
  Calcbetac1(Beta,c1,Rv298,Rs298,Rl,gamma298,freq,cap);
  Writeln(uit,Tmin:6:1,Tmax:8:1,Tstep:6:1);
  T := Tmin;
  For j := 1 to 60 Do
  Begin
    For i := 1 To Nodev Do Tph[Devnr[i]] := T;
    Gbefore := 0;
    Initarr(Lolddb, GolddB, LdB, GdB);
    Tempdependence(LdB, GdB, gamma, Td, Tph, freq, cap,
      Rs298,Rl,c1,Beta);
    Radiometer(T, Tph, gamma, TSS, Bif, Tau, Ldb, GdB, NF,
      VSWR, offvoltdr, Po, Pno, Vo, Vno, Gbefore,
      Voltkelv, Teq);
    Teqrec := Rectemp(Teq, Gdb, Ldb, Bif, Rv, gamma, Tau);
    Writeln(uit,T,Gbefore,gamma,' ',Vo[11],' ',Vno[11],
      Teqrec+T);
    T := T + Tstep
  End;
  Close(uit)
end;
{-----}
Begin {Main program}
  Paramread(Tph, Bif, gamma298, TSS, Rv298, Rs298, Tau,

```



```
Gdb, Ldb, NF, Td, VSWR, offvoltdr);  
Rl := Ldb[4]; freq:=1e8; cap := 0.3E-12;  
PickCoord(Right, Bottom);  
Radiometergraph;  
QuestGraph(Ta, Tmin, Tmax, Tstep, devnr, filenaam,  
            nodev);  
Tempvarout(Filenaam, Tph, Bif, gamma298, TSS, Tau, GdB,  
            LdB, NF, Td, VSWR, offvoltdr, Ta, Tmin, Tmax,  
            Tstep, Devnr, Nodev, freq, cap, Rv298, Rs298,  
            Rl, Beta, c1);  
CloseGraph  
end.
```

```

program vout;
uses crt, radunit;
var
  Teqrec, Gbefore, Ta, gamma298, Tmax      :real;
  offvoltdr, freq, cap, gamma, Bif, Bint  :real;
  Rv298, Rs298, tau, TSS, voltkelv, Rl     :real;
  Beta, c1, Rv, Tmin                       :real;
  i                                         :integer;
  LdB, Lolddb                              :lossarray;
  GdB, Golddb                              :gainarray;
  NF                                         :noisearray;
  Teq, td, VSWR, Tph                       :comparray;
  Po, Pno                                   :powerarray;
  Vo, Vno                                   :voltarray;
  inv, uit                                  :text;
{-----}
procedure uitvoer(Tmax, Tmin, Ta, Bif, gamma, TSS, Rv,
  Rs298, Tau, Gbefore, voltkelv,
  Teqrec :real; GdB :gainarray;
  LdB :lossarray; NF :noisearray; Tph,td,
  teq, VSWR :comparray; offvoltdr:real;
  Po, Pno :powerarray; Vo, Vno :voltarray);
{write output to file vout.jpg}
Var Pdbm, Vdbm, Pndbm, Vndbm, T :real;

begin
  assign(uit,'vout.jpg');rewrite(uit);
  writeln(uit,'RF AMPLIFIERS/ATTENUATORS');
  writeln(uit,'Naam          Gain Noise Fig. ',
    'VSWR Temp.Dep. Teq');
  writeln(uit,'          (dB) (dB) ',
    '          (dB/K) (K) (%)');
  writeln(uit,'Wave Guide      ',-Ldb[1]:9:1,
    Ldb[1]:9:1,VSWR[1]:6:1,Td[1]:9:3,
    Teq[1]:9:1);
  writeln(uit,'RF Amplifier    ',Gdb[1]:9:1,NF[1]:9:1,

```

```

        VSWR[2]:6:1,Td[2]:9:3,Teq[2]:9:1);
writeln(uit,'Mixer          ',-Ldb[2]:9:1,NF[2]:9:1,
        VSWR[3]:6:1,Td[3]:9:3,Teq[3]:9:1);
writeln(uit,'IF AMPLIFIERS');
writeln(uit,'IF Amplifier 1  ',Gdb[2]:9:1,NF[3]:9:1,
        VSWR[4]:6:1,Td[4]:9:3,Teq[4]:9:1);
writeln(uit,'IF Amplifier 2  ',Gdb[3]:9:1,NF[4]:9:1,
        VSWR[5]:6:1,Td[5]:9:3,Teq[5]:9:1);
writeln(uit,'Match Circuit I ',Gdb[4]:9:1,NF[5]:9:1,
        VSWR[7]:6:1,Td[7]:9:3,Teq[7]:9:1);
writeln(uit,'VIDEO AMPLIFIER');
writeln(uit,'          Gain Temp.dep  ',
        'Off.volt.dr.');
```

```

writeln(uit,'          (dB/K)  ',
        ' uV/K');
```

```

writeln(uit,'Video Amplifier ',Gdb[5]:9:1,Td[10]:9:3
        ,offvolt:10:2);
writeln(uit);
writeln(uit,'FILTERS');
writeln(uit,'Naam          Gain Noise Fig. ',
        'VSWR Temp.Dep. Teq Bandwidth/Tau');
```

```

writeln(uit,'          (dB) (dB)  ',
        ' (dB/K) (K)');
```

```

writeln(uit,'Band Pass Filter ',-Ldb[3]:9:1,
        Ldb[3]:9:1,VSWR[6]:6:1,Td[6]:9:3,
        Teq[6]:9:1,Bif:6:1, ' MHz');
```

```

writeln(uit,'Integrator      ',Ldb[5]:9:1,Ldb[5]:9:1,
        ' None',Td[11]:9:3,' None',tau:6:2,
        ' s ');
writeln(uit);
writeln(uit,'DETECTOR');
```

```

writeln(uit,' gamma (298 K)      : ',gamma:9:1,
        ' V/W');
```

```

writeln(uit,' Rv (298 K)      : ',Rv:9:1,' Ohms');
```

```

writeln(uit,' TSS          : ',TSS:9:1,' dBm');
```

```

writeln(uit,' Rs (298 K)      : ',Rs298:9:1,
```

```

        ' dBm');
writeln(uit, ' VSWR           : ', VSWR[8]:9:1);
writeln(uit, ' Teq           : ', Teq[8]:9:1,
        ' K');
writeln(uit, ' Load resistance(MII): ', Ldb[4]:9:3);
writeln(uit);
writeln(uit, 'OVERALL PARAMETERS');
writeln(uit, ' Physical temperature : ', Tph[1]:9:0
        , ' K');
writeln(uit, ' Antenna temperature : ', Ta:9:0
        , ' K');
writeln(uit, ' Receiver temperature : ', Teqrec:9:1,
        ' K');
writeln(uit, ' Total gain           : ', Gbefore:9:1
        , ' dBV/W');
writeln(uit, ' Voltage temperature sens.: ',
voltage*1000:9:1, ' mV/K');
writeln(uit);
writeln(uit, 'Out':7, 'Po':9, 'Pno':9, 'PdBm':11,
        'PndBm':11);
for i:= 1 to 11 do begin
    if i < 8 then begin
        Pdbm := dB(Po[i]*1000);
        Pndbm := dB(Pno[i]*1000);
        writeln(uit, 'Pout['',i,'] :', Po[i]:9, ' ', Pno[i]:9
            , ' ', Pdbm:6:1,
            ' dBm ', Pndbm:6:1, ' dBm ') end
        else begin
            Vdbm := dB(abs(Vo[i]*1000));
            Vndbm := dB(abs(Vno[i]*1000));
            writeln(uit, 'Vout['',i,'] :', Vo[i]:9, ' ', Vno[i]:9,
                ' ', Vdbm:6:1, ' dBm ', Vndbm:6:1,
                ' dBm ')
        end;
    end;
end;
writeln(uit);

```

```

writeln(uit,' Tph  Vno', Vo Teqrec ',
        'Gtot Voltkelv');
If Tmin > Tmax Then Begin T := Tmax; Tmax := Tmin End
        Else T := Tmin;
while T < Tmax do begin
Gbefore:=0;
Initarr(Lolddb,Golddb,LdB,GdB);
For i:= 1 to 11 do Tph[i] := T;
Tempdependence(LdB, GdB, gamma, td, Tph, freq, cap,
                Rs298, Rl, c1, Beta);
radiometer(Ta, Tph, gamma, TSS, Bif, Tau, Ldb, GdB,
            NF, VSWR, offvoltdr, Po, Pno, Vo, Vno,
            Gbefore, voltkelv, Teq);
Teqrec := rectemp(Teq, Gdb, Ldb, Bif, Rv, gamma, Tau);
writeln(uit,T:6:1,' ',Vno[11]:9,' ',Vo[11]:9,' ',
        Teqrec:6:1,' ',Gbefore:6:1,' ',
        voltkelv*1000:6:1);
T:=T+10 end;
close(uit)
end;
{-----}
begin
paramread(Tph, Bif, gamma298, TSS, Rv298, Rs298, Tau,
           Golddb, Lolddb, NF, Td, VSWR, offvoltdr);
Rl := Lolddb[4]; freq := 1e8; cap := 0.3e-12;
CalcBetacl(Beta, c1, Rv298, Rs298, Rl, gamma298, freq,
           cap);
clrscr;
write('Give sky noise temperature ');readln(Ta);
Gbefore := 0;
Initarr(Lolddb,Golddb,LdB,GdB);
Tempdependence(LdB, GdB, gamma, Td, Tph, freq, cap,
                Rs298, Rl, c1, Beta);
radiometer(Ta, Tph, gamma, TSS, Bif, Tau, Ldb, GdB,
            NF, VSWR, offvoltdr, Po, Pno, Vo, Vno,
            Gbefore, voltkelv, Teq);

```

```
Teqrec := rectemp(Teq, Gdb, Ldb, Bif, Rv, gamma, Tau);
Initarr(Lolddb,GolddB,LdB,GdB);
write('Give min temperature range ');readln(Tmin);
write('Give max temperature range ');readln(Tmax);
uitvoer(Tmax, Tmin, Ta, Bif, gamma, TSS, Rv, Rs298,
        Tau, Gbefore, voltkelv, Teqrec, GdB, LdB, NF,
        Tph, td, teq, VSWR, offvoltdr, Po, Pno, Vo,
        Vno)
end.
```

```

Program Chart_Conversion;

uses crt;

Var Tcop, Tif1, Tif2, TM1, Tdiode, Tvid, Vout :real;
    Time, Date, Tamb, Tstep, Told          :real;
    i                                       :integer;
    outp,inp                               :text;
    SoFilename, Temp, DeFilename           :string;

Begin
  ClrScr;
  Writeln('CHART RECORDER DATA FILE CONVERSION');
  Writeln;
  Writeln('This program reads data from a file, written');
  Writeln('by the Siemens C1730 chartrecorder, specified');
  Writeln('by chart filename with the extension .PRN');
  Writeln('It writes the data in an ASCII format to a');
  Writeln('file specified by destination data file and');
  Writeln('gets the extension .DAT, so it can be read');
  Writeln('by standard software like Slidewrite. The');
  Writeln('program assumes that the channels are:');
  Writeln('    #1: Output voltage');
  Writeln('    #2: Not measured');
  Writeln('    #3: Temperature of A1 amplifier');
  Writeln('    #4: Temperature of GPD201 amplifier');
  Writeln('    #5: Temperature of diode input match');
  Writeln('    #6: Temperature of diode detector');
  Writeln('    #7: Temperature of video amplifier');
  Writeln('    #8: Temperature of messing block');
  Writeln('    #9: Temperature of air');
  Writeln('Enter NO extensions !!!');
  Write('Enter chart filename ');readln(SoFilename);
  Write('Enter destination data file ');readln(DeFilename);
  Write('Enter temperature step ');readln(Tstep);
  Temp := SoFilename + '.prn';

```

```
Assign(inp, Temp);
Reset(inp);
Temp := DeFilename + '.dat';
Assign(outp, Temp);
Rewrite(outp);
i:=0;Readln(inp); Told := 0;
Repeat begin
  Readln(inp, Time, Date, Vout, Tif1, Tif2, TM1, Tdiode,
    Tvid, Tcop, Tamb);
  Tif1 := Tif1 + 273.15 +0.98;
  Tif2 := Tif2 + 273.15 +1;
  Tm1 := Tm1 + 273.15 +0.95;
  Tdiode := Tdiode + 273.15 +0.84;
  Tvid := Tvid + 273.15 +0.82;
  Tcop := Tcop + 273.15 +0.87;
  Tamb := Tamb + 273.15 +0.77;
  If Abs(Told-Tcop) > Abs(Tstep) Then Begin
    Writeln(outp, Tcop:7:2, Tif1:7:2, Tif2:7:2, TM1:7:2,
      Tdiode:7:2, Tvid:7:2, Vout:7:3, Tamb:7:2);
    Told := Tcop End;
  i:=i+1;
End
Until Eof(inp);
Close(inp);
Close(outp)
End.
```



```

Program Process_Data;
Type Pointarray = array[1..500,1..2] Of real;

Var Tcop, Tif1, Tif2, TM1, Tdiode, Tvid, Vout :real;
  Voff, Tsys, Curve, CnvFac, Vcold, Tamb :real;
  outp,inp :text;
  Maxpoint :integer;
  Filename1,Filename2,Filename3 :string;
  Temp1, Temp2, Temp3 :string;
  Points :Pointarray;
{Process_Data gets a data file, created by Chartcnv and
calculates the series resistance (Rs), the video resistance
(Rv), the voltage sensitivity (Gamma) of the diode, the
system noise temperature Tsys and the radiometer
sensitivity (Sens) from the data in this file and puts the
values in a file that has the same name, but instead of an
extension .DAT it gets an extension .CNV}
{-----}
procedure Readpoints(Filename:string;var points:pointarray;
  var maxpoint:integer);
var inv:text; Pointsrev:pointarray; i:integer;
begin
  assign(inv,Filename);
  reset(inv);Maxpoint :=0;
  Repeat
  Begin
  Maxpoint := Maxpoint + 1;
  Readln(inv,Pointsrev[Maxpoint,1],Tif1,Tif2, TM1,Tdiode,
    Tvid,Pointsrev[Maxpoint,2])
  End
  Until Eof(inv);
  For i := 1 to Maxpoint do
  Begin
  Points[i,1] :=Pointsrev[Maxpoint+1-i,1];
  Points[i,2] :=Pointsrev[Maxpoint+1-i,2]
  End;

```

```

    close(inv)
end;
{-----}
Procedure interpol(points: pointarray; maxpoint :integer;
                  xvalue :real;
                  var yvalue: real);
var i, j : integer;
begin
    if xvalue <= Points[1,1] then j := 1;
    for i:= 1 to maxpoint do
        if xvalue > Points[i,1] then j := i+1;
    if j=1 then
        yvalue := Points[2,2]+(Points[2,1]-xvalue)*
            Points[1,2]-Points[2,2))/(Points[2,1]-Points[1,1])
    else
    if j<=maxpoint then
        yvalue := Points[j,2]+(Points[j,1]-xvalue)*
            Points[j-1,2]-Points[j,2])/
            (Points[j,1]-Points[j-1,1])
    else
        yvalue := Points[maxpoint,2]+
            (Points[maxpoint,1]-xvalue)*
            (Points[maxpoint-1,2]-Points[maxpoint,2])/
            (Points[maxpoint,1]-Points[maxpoint-1,1]);
    end;
}-----}
Begin
    Write('Enter hot filename ');readln(Filename1);
    Write('Enter cold filename ');readln(Filename2);
    Write('Enter output filename ');readln(Filename3);
    Temp1 := Filename1 + '.dat';
    Temp2 := Filename2 + '.dat';
    Temp3 := Filename3 + '.dat';
    Assign(inp, temp1);
    Reset(inp);
    Assign(outp, Temp3);

```

```
Rewrite(outp);
Readpoints(temp2,points,maxpoint);
Repeat
  Begin
    Readln(inp,Tcop,Tif1,Tif2,TM1,Tdiode,Tvid,Vout,Tamb);
    Interpol(Points,Maxpoint,Tcop,Vcold);
    CnvFac := (Vout-Vcold)/(273.15-77);
    Tsys := Vout/CnvFac;
    Voff := (Tsys-476)*CnvFac;
    Writeln(outp, Tcop:7:2,' ',Vout, Tsys, CnvFac, ' ',
            Voff,' ',Vcold,' ',Tamb)
  End
Until eof(inp);
Close(inp);
Close(outp)
End.
```

```

program parinput;
uses Crt;
type
  stringtype = string[6];
  naam       = string[30];
  gainarray  = _array [1..5] of real;
  lossarray  = array [1..5] of real;
  noisearray = array [1..5] of real;
  comparray  = array [1..11] of real;
{-----}
var
  Tph, Bif, gamma298, TSS, Rv298, Rs298, Tau : real;
  offvoldr                                     : real;
  Gaindb                                       : gainarray;
  Lossdb                                       : lossarray;
  NFigure                                      : noisearray;
  td, VSWR, deltagain                          : comparray;
  janee                                       : char;
  inv, uit                                     : text;
{-----}
procedure Readvalue(var value:real);
var
  ch      : char;
  x, y ,code : integer;
  instring : string;
begin
  instring := '';
  x:= wherex; y:= wherey;
  While Ord(ch) <> 13 do begin
    ch := readkey;
    if Ord(ch) = 8 then
      begin
        delete(instring,length(instring),1);
        gotoxy(x,y);
        write(instring, ' ')
      end
    end
end

```

```

else if Ord(ch) <> 13 then
  begin
    instring := instring + ch;
    gotoxy(x,y);
    write(instring)
  end
end;
if length(instring) <> 0 then
  val(instring,value,code);
  writeln
end;
{-----}
procedure amplifierinp(amplifier: naam; var gaindb,
  noisefigure, tempdep, VSWR:real);
begin
  clrscr;
  writeln(amplifier);writeln;
  writeln('Gain (dB) ');
  writeln('Noise figure (dB) ');
  writeln('Temperature dependence (dB/K) ');
  writeln('VSWR');
  window(45,3,52,8);
  writeln(gaindb:6:1);
  writeln(noisefigure:6:1);
  writeln(tempdep:6:4);
  writeln(VSWR:6:1);
  window(54,3,61,7);textbackground(blue);clrscr;
  gotoxy(1,1);
  readvalue(gaindb);
  readvalue(noisefigure);
  readvalue(tempdep);
  readvalue(VSWR);
  window(1,1,80,25);textbackground(black)
end;
{-----}
procedure vidampinp(var gaindb, tempdep, offvoltdr:real);

```

```

begin
  clrscr;
  writeln('Video amplifier');writeln;
  writeln('Gain ');
  writeln('Temperature dependence (dB/K) ');
  writeln('Offset voltage drift (uV/C)');
  window(45,3,52,9);
  writeln(gaindb:6:1);
  writeln(tempdep:6:4);
  writeln(offvoltdr:6:1);
  window(54,3,61,8);textbackground(blue);clrscr;
  gotoxy(1,1);
  readvalue(gaindb);
  readvalue(tempdep);
  readvalue(offvoltdr);
  window(1,1,80,25);textbackground(black)
end;
{-----}
procedure lossinp(loss:naam;var lossdb, tempdep, VSWR:real);
begin
  clrscr;
  writeln(loss);writeln;
  writeln('Loss (dB) ');
  writeln('Temperature dependence (dB/K) ');
  writeln('VSWR');
  window(45,3,52,7);
  writeln(lossdb:6:1);
  writeln(tempdep:6:4);
  writeln(VSWR:6:1);
  window(54,3,61,6);
  textbackground(blue);
  clrscr;
  gotoxy(1,1);
  readvalue(lossdb);
  readvalue(tempdep);
  readvalue(VSWR);

```

```

    window(1,1,80,25);
    textbackground(black)
end;
{-----}
procedure matchIinp(var Rload, tempdep:real);
begin
    clrscr;
    writeln('DIODE OUTPUT MATCH');writeln;
    writeln('Load resistance ');
    writeln('Temperature dependence (dB/K) ');
    window(45,3,52,7);
    writeln(Rload:6:1);
    writeln(tempdep:6:4);
    window(54,3,61,6);
    textbackground(blue);
    clrscr;
    gotoxy(1,1);
    readvalue(Rload);
    readvalue(tempdep);
    window(1,1,80,25);
    textbackground(black)
end;
{-----}
procedure mixerinp(var lossdb, noisefigure, tempdep,
                  VSWR:real);
begin
    clrscr;
    writeln('MIXER');writeln;
    writeln('Loss (dB) ');
    writeln('Noise figure (dB) ');
    writeln('Temperature dependence (dB/K) ');
    writeln('VSWR');
    window(45,3,52,8);
    writeln(lossdb:6:1);
    writeln(noisefigure:6:1);
    writeln(tempdep:6:4);

```

```

writeln(VSWR:6:1);
window(54,3,61,7);
textbackground(blue);
clrscr;
readvalue(lossdb);
readvalue(noisefigure);
readvalue(tempdep);
readvalue(VSWR);
window(1,1,80,25);
textbackground(black)
end;
{-----}
procedure detectorinp(var gamma298, TSS, Rv298, Rs298,
                      tempdep, VSWR:real);
begin
  clrscr;
  writeln('DETECTOR');writeln;
  writeln('Gamma (298 K) (V/W) ');
  writeln('TSS (dBm) ');
  writeln('Rv (298K) (Ohms) ');
  writeln('Rs (298K) (Ohms) ');
  writeln('Temperature dependence (dB/K) ');
  writeln('VSWR');
  window(45,3,52,10);
  writeln(gamma298:6:1);
  writeln(TSS:6:1);
  writeln(Rv298:6:1);
  writeln(Rs298:6:1);
  writeln(tempdep:6:4);
  writeln(VSWR:6:1);
  window(54,3,61,9);
  TextBackground(blue);
  clrscr;
  readvalue(gamma298);
  readvalue(TSS);
  readvalue(Rv298);

```



```

    readvalue(Rs298);
    readvalue(tempdep);
    readvalue(VSWR);
    window(1,1,80,25);
    TextBackground(black)
end;
{-----}
procedure filterinp(var bandwidth, lossdb, tempdep,
                   VSWR:real);

begin
    clrscr;
    writeln('IF FILTER');writeln;
    writeln('Bandwidth (MHz) ');
    writeln('Loss (dB) ');
    writeln('Temperature dependence (dB/K) ');
    writeln('VSWR');
    window(45,3,52,8);
    writeln(bandwidth:6:1);
    writeln(lossdb:6:1);
    writeln(tempdep:6:4);
    writeln(VSWR:6:1);
    window(54,3,61,7);
    Textbackground(blue);
    clrscr;
    readvalue(bandwidth);
    readvalue(lossdb);
    readvalue(tempdep);
    readvalue(VSWR);
    window(1,1,80,25);
    Textbackground(black)
end;
{-----}
procedure integratorinp(var Tau, lossdb, tempdep:real);
begin
    clrscr;

```

```

writeln('INTEGRATOR');writeln;
writeln('Tau (s) ');
writeln('Gain ');
writeln('Temperature dependence (dB/K) ');
window(45,3,52,8);
writeln(Tau:6:1);
writeln(lossdb:6:1);
writeln(tempdep:6:4);
window(54,3,61,7);
Textbackground(blue);
clrscr;
readvalue(Tau);
readvalue(lossdb);
readvalue(tempdep);
window(1,1,80,25);
Textbackground(blue)
end;
{-----}
procedure tempinp(var Tph:real);
begin
  clrscr;
  writeln('Physical temperature :');
  window(45,1,52,3);
  writeln(Tph:6:1);
  window(54,1,61,1);
  Textbackground(blue);
  clrscr;
  readvalue(Tph);
  window(1,1,80,25);
  textbackground(black)
end;
{-----}
procedure paramwrite(Tph, Bif, gamma, TSS, Rv, squarelawtop,
  Tau :real; gaindb:gainarray;
  lossdb:lossarray; NF :noisearray; td,
  deltagain, VSWR :comparray;

```

```

        offvoltdr:real);
var i : integer;
begin
    assign(uit,'param.dat');rewrite(uit);
    writeln(uit, Tph);
    writeln(uit, Bif);
    writeln(uit, gamma298);
    writeln(uit, TSS);
    writeln(uit, Rv298);
    writeln(uit, Rs298);
    writeln(uit, Tau);
    for i:= 1 to 5 do writeln(uit, gaindb[i]);
    for i:= 1 to 5 do writeln(uit, lossdb[i]);
    for i:= 1 to 5 do writeln(uit, NF[i]);
    for i:= 1 to 8 do begin
        writeln(uit, td[i]);
        writeln(uit, VSWR[i])
    end;
    for i:= 9 to 11 do writeln(uit, td[i]);
    writeln(uit, offvoltdr);
    close(uit)
end;
{-----}
procedure paramread(var Tph, Bif, gamma, TSS, Rv, Rs298,
                    Tau :real; var Gaindb:gainarray;
                    var Lossdb:lossarray;
                    var NF :noisearray; var td, deltagain,
                    VSWR: comparray;
                    var offvoltdr :real);
var i: integer;
begin
    assign(inv,'param.dat');reset(inv);
    readln(inv, Tph);
    readln(inv, Bif);
    readln(inv, gamma298);
    readln(inv, TSS);

```

```

readln(inv, Rv298);
readln(inv, Rs298);
readln(inv, Tau);
for i := 1 to 5 do readln(inv, gaindb[i]);
for i := 1 to 5 do readln(inv, lossdb[i]);
for i := 1 to 5 do readln(inv, NF[i]);
for i := 1 to 8 do begin
    readln(inv, td[i]);
    readln(inv, VSWR[i]);
end;
for i := 9 to 11 do readln(inv, td[i]);
readln(inv, offvoldr);
close(inv)
end;
{-----}
begin
    clrscr;
    writeln('INPUT RADIOMETER PARAMETERS');writeln;
    write('Oude gegevens inladen ? ');readln(janee);
    if janee = 'j' then
        paramread(Tph, Bif, gamma298, TSS, Rv298, Rs298,
            Tau, gaindb, lossdb, Nfigure, td,
            deltagain, VSWR, offvoldr);
    tempinp(Tph);
    lossinp('WAVE GUIDE',Lossdb[1],td[1],VSWR[1]);
    amplifierinp('RF AMPLIFIER',Gaindb[1],NFigure[1],td[2],
        VSWR[2]);
    mixerinp(lossdb[2],NFigure[2],td[3],VSWR[3]);
    amplifierinp('IF AMPLIFIER 1',Gaindb[2],NFigure[3],
        td[4],VSWR[4]);
    amplifierinp('IF AMPLIFIER 2',Gaindb[3],NFigure[4],
        td[5],VSWR[5]);
    filterinp(Bif,Lossdb[3],td[6],VSWR[6]);
    amplifierinp('MATCHING CIRCUIT I',Gaindb[4],NFigure[5],
        td[7],VSWR[7]);
    detectorinp(gamma298,TSS,Rv298,Rs298,td[8],VSWR[8]);

```

```
matchIinp(Lossdb[4],td[9]);  
vidampinp(Gaindb[5],td[10],offvoltdr);  
integratorinp(Tau,Lossdb[5],td[11]);  
paramwrite(Tph, Bif, gamma298, TSS, Rv298, Rs298, Tau,  
           Gaindb, Lossdb, Nfigure, td, deltagain,  
           VSWR, offvoltdr)  
end.
```

APPENDIX E: Specifications of the semiconductor components in the IF/video unit.

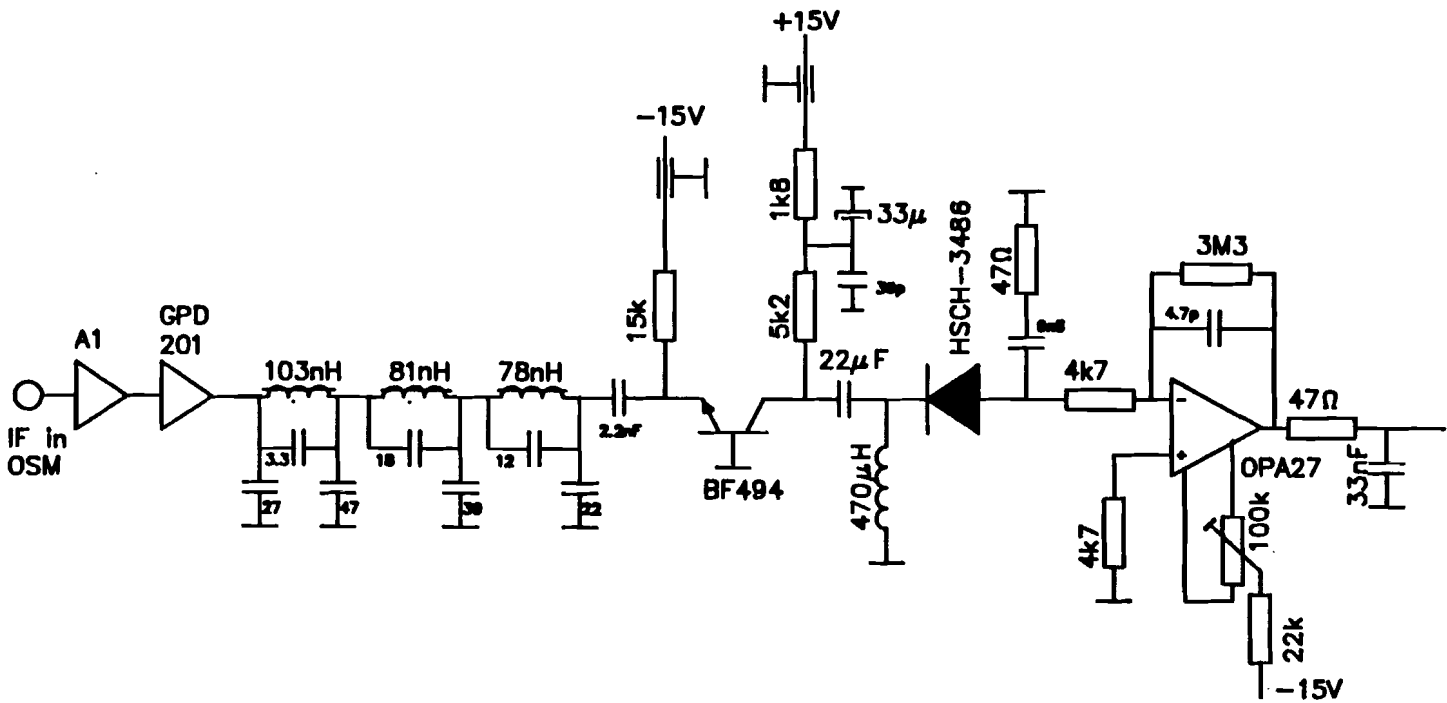


Fig E.1: The scheme of the IF/video unit.

Appendix E.1: The data sheets of the A1 amplifier.

Watkins-Johnson Company has committed its extensive thin-film technology to the development of a complete line of cascadable amplifiers that offer the system designer maximum flexibility in performance options.

These TO-8 modules were designed to bring the repeatability, stability and economy of thin-film processing to a broad range of RF amplifier applications. Each amplifier can be thought of as a quantized gain block which the designer can employ in a systems approach to amplifier design.

Since these units are unconditionally stable, exceptionally flat and provide a good 50 ohm interface, they may be easily cascaded in a 50 ohm microstrip circuit without loss of gain, power output or bandwidth. Thus, the designer may select an appropriate low noise module for his first stage followed by as many gain blocks as required for his design. Cascaded power output will be determined by the final stage, whose output will be unchanged, provided sufficient drive is available.

Each of these thin-film, cascadable amplifiers is a complete amplifier in itself, including stable DC biasing circuitry and independent power supply

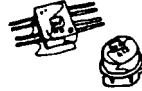
decoupling. A choice of hermetic packages is provided between the four-pin TO-8, or the eight-pin flatpack.

Intended to cover a maximum number of applications, these amplifiers offer noise figure as low as 1.7 dB for narrow band applications, frequency coverage as broad as 5 to 2000 MHz, and power output in excess of +20 dBm. Most of these units are designed for a positive 15 volt supply voltage, while some may accept 24 volts or a range as wide as 8 to 20 volts. Overall, these universal modules can be characterized by stable and repeatable performance over a very broad range of frequencies, temperature and supply voltages.

The construction of the Watkins-Johnson amplifier series involves the highest levels of thin-film technology. The thin-film metalization is performed by using a high vacuum RF sputtering system for both resistor and conductor metalizations. All conductor traces are gold metalization. The thin-film resistors are formed from tantalum nitride and are passivated at high temperature to yield excellent long-term stability. The resistor composition is such that there is less than 150 ppm/°C of change in resistor value

Thin Film Cascadable Amplifiers

Typical (25°C) Performance



Model	Frequency	Gain	Noise Figure	Output Power
A1	1-500 MHz	16.0 dB	2.5 dB	-1 dBm
A3 & A4	5-500 MHz	15.5 dB	3.5 dB	-1 dBm
A5 & A6	5-500 MHz	14.7 dB	4.5 dB	+9 dBm
A7 & A8	5-500 MHz	14.7 dB	5.5 dB	+14 dBm
A9	5-500 MHz	11.0 dB	8.0 dB	+22 dBm
A11	1-1000 MHz	14.7 dB	3.6 dB	-2 dBm
A11-1	1-1000 MHz	14.7 dB	3.2 dB	-2 dBm
A13	1-1000 MHz	14.7 dB	4.3 dB	-2 dBm
A15	1-1000 MHz	14.5 dB	5.5 dB	+8.5 dBm
A17	5-1000 MHz	12.0 dB	7.0 dB	+15 dBm
A19	5-1000 MHz	7.0 dB	10.0 dB	+21 dBm
A25	1-1600 MHz	10.0 dB	6.0 dB	+9 dBm
A71	1-200 MHz	16.5 dB	1.7 dB	+2.5 dBm
A63	1-1000 MHz	16.0 dB	4.0 dB	+3.0 dBm

over the full operating temperature range.

Thin-film circuitry offers very precise control of resistor and circuit patterns. Thin-film inductors, etched on the substrate, yield a high degree of repeatability from unit to unit. This is particularly important when repeatable VSWR, gain, and phase characteristics are required.

All RF transistors are bonded to the substrate using a specially developed gold-silicon eutectic die-attach process. This eliminates the need for scrubbing the thin-film gold and results in superior adhesion and more uniform contact which, in turn, gives better reliability and heat transfer.

The Watkins-Johnson cascaded amplifier provides the system designer with a reliable, low-cost, ultra-miniature approach to his circuit design and allows him to concentrate on the complexities of the system without worrying about the intricacies of the RF transistor amplifier design.

Several accessory components which further enhance the versatility of this approach are the TO-8 packaged passive limiters and gain control modules. A combination of up to four TO-8 modules may be integrated in a W-J metal housing with SMA connec-

tors. Other complementary signal processing components available from Watkins-Johnson include high quality mixers, hybrids, and transformers which may be integrated with the amplifier series into a number of useful subassemblies.



Signal Processing Units



Thin Film Attenuator

Model	Frequency Range	Insertion Loss		Attenuator		VSWR Max	Control		Bias	
		Typ	Max	Typ	Min		V	I (mA)	V	I (mA)
G1	~ 5-1000 MHz	2.0 dB	2.5 dB	25 dB	20 dB	2.0:1	0-15	0-5	15	10
	5-2000 MHz	2.8 dB	3.3 dB	19 dB	15 dB	2.3:1	0-15	0-5	15	10

The WJ-G1 is designed to be used wherever control is needed over gain or output power. Cascades of fixed gain amplifiers such as the WJ-A3, A5, A7 and A9 can be precisely controlled so that arrays of amplifiers can be matched, or a single cascade can be given a precise gain. With the

addition of a detector and driver circuit the WJ-G1 can make a fixed gain amplifier or cascade into an automatic gain control amplifier. This AGC function is enhanced by the inherent linearity of attenuation vs. control voltage of the G1 which minimizes changes in loop gain.

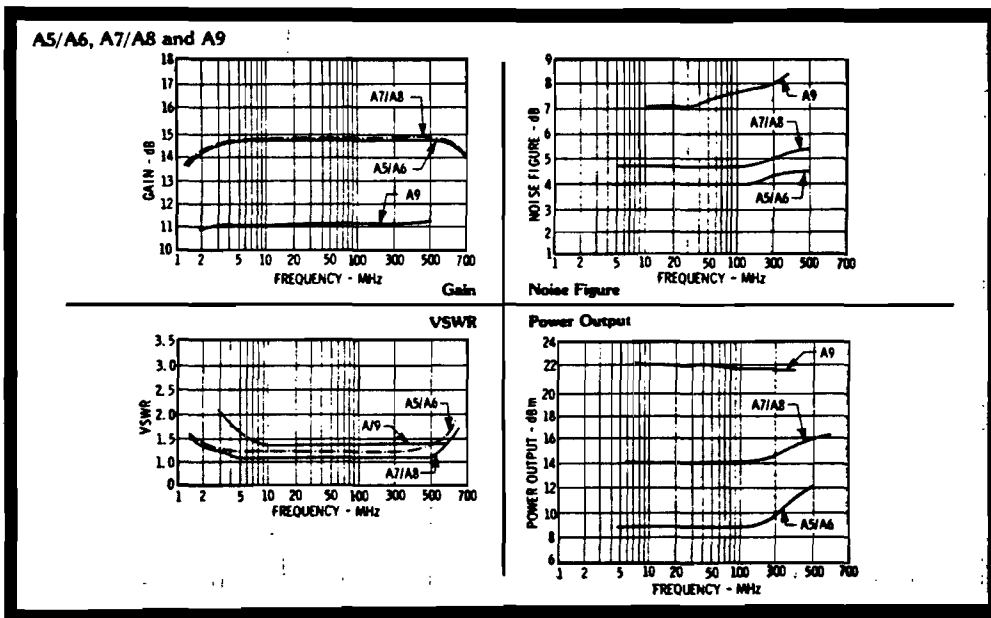
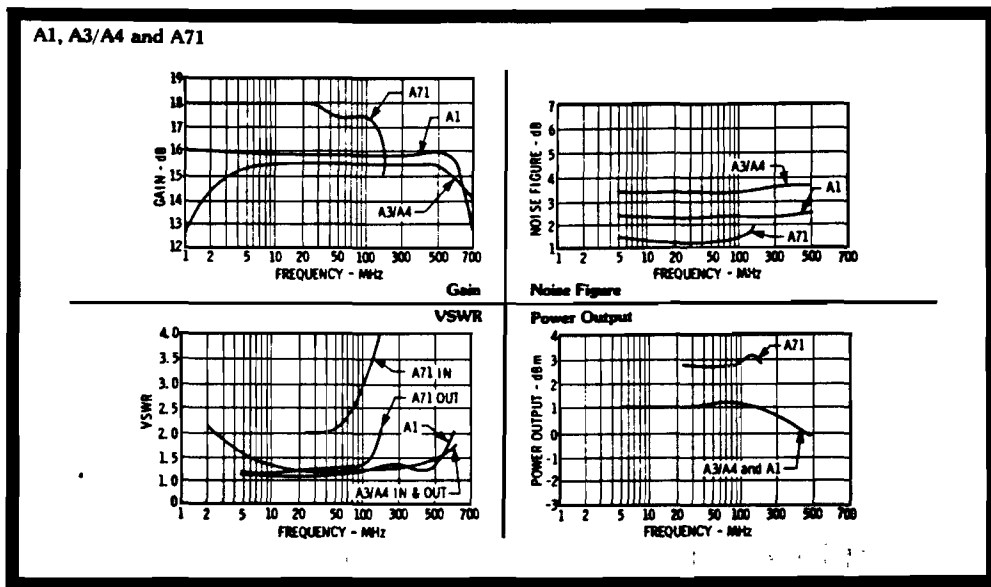
Thin Film Limiter

Model	Frequency Range	Insertion Loss		Limiting Level (Max)			VSWR Max	Control Voltage
		Typ	Max	20V	15V	10V		
L1	50-1500 MHz	2.0 dB	3.0 dB	+2	0	-2 dBm	2.2:1	10 to 24 V

The WJ-L1 limiter module is designed for low level VHF-UHF signal processing applications. Typical applications are limiting signal amplitude (reduction in dynamic range)

to maintain proper operation of signal processing components and to remove any amplitude variations prior to a FM discriminator.

TYPICAL PERFORMANCE AT 25°C



Guaranteed Specifications

0° to 50°C

(Specifications subject to change without notice)

Model	Frequency	Small Signal Gain (Min)	Gain Flatness (Max)	Noise Figure (Max)	VSWR In and Out (Max)	Power Output @ 1 dB Gain Compression (Min)	Intercept Point (Typ)	DC Voltage (Nominal)	DC Current (Typ)
A1	5-500 MHz	15.0 dB	±1.0 dB	3.0 dB	2.0:1	-2 dBm	+11 dBm	15V	9 mA
A3 & A4	5-500 MHz	14.0 dB	±.7 dB	4.0 dB	1.7:1	-2 dBm	+11 dBm	15V	9 mA
A5 & A6	5-500 MHz	14.0 dB	±.7 dB	5.5 dB	2.0:1	+7 dBm	+22 dBm	15V	25 mA
A7 & A8	5-500 MHz	14.0 dB	±.7 dB	6.5 dB	2.0:1	+13 dBm	+26 dBm	24V	43 mA
A9	5-500 MHz	10.0 dB	±1.0 dB	10.0 dB	2.0:1	+20 dBm	+36 dBm	24V	110 mA
A11	5-1000 MHz	14.0 dB	±1.0 dB	4.0 dB	2.0:1	-3 dBm	+10 dBm	15V	9 mA
A11-1	5-1000 MHz	14.0 dB	±1.0 dB	3.5 dB	2.0:1	-3 dBm	+10 dBm	15V	9 mA
A13	5-1000 MHz	14.0 dB	±1.0 dB	5.0 dB	2.0:1	-3 dBm	+10 dBm	15V	9 mA
A63	5-1000 MHz	15.0 dB	±1.0 dB	5.0 dB	2.0:1	+2 dBm	+15 dBm	15V	14 mA
A15	5-1000 MHz	14.0 dB	±1.0 dB	6.5 dB	2.0:1	+7 dBm	+21 dBm	15V	24 mA
A17	10-1000 MHz	10.0 dB	±1.0 dB	8.0 dB	2.0:1	+14 dBm	+30 dBm	15V	44 mA
A19	10-1000 MHz	6.0 dB	±1.0 dB	12.0 dB	2.2:1	+20 dBm	+34 dBm	15V	100 mA
A25	5-1500 MHz	9.0 dB	±.6 dB	7.5 dB	2.0:1	+7 dBm	+21 dBm	15V	24 mA
A71	5-170 MHz	14.0 dB	—	1.7 dB (5-100 MHz) 2.5 dB (5-170 MHz)	4.5:1 (In) 2.5:1 (Out)	+1 dBm	+15 dBm	15V	11 mA

-54°C to +85°C

(Specifications subject to change without notice)

Model	Frequency	Small Signal Gain (Min)	Gain Flatness (Max)	Noise Figure (Max)	VSWR In and Out (Max)	Power Output at 1 dB Gain Compression (Min)	Intercept Point (Typ)	DC Voltage (Nominal)	DC Current (Typ)
A1	5-500 MHz	14.5 dB	±1.0 dB	3.5 dB	2.0:1	-3 dBm	+11 dBm	15V	9 mA
A3 & A4	5-500 MHz	13.5 dB	±1.0 dB	4.5 dB	2.0:1	-3 dBm	+11 dBm	15V	9 mA
A5 & A6	5-500 MHz	13.5 dB	±1.0 dB	6.5 dB	2.0:1	+7 dBm	+22 dBm	15V	25 mA
A7 & A8*	5-500 MHz	13.5 dB	±1.0 dB	6.5 dB	2.0:1	+12.5 dBm	+26 dBm	24V	43 mA
A9*	5-500 MHz	9.5 dB	±1.0 dB	10.5 dB	2.0:1	+20 dBm	+36 dBm	24V	110 mA
A11	5-1000 MHz	13.5 dB	±1.2 dB	4.5 dB	2.0:1	-4 dBm	+10 dBm	15V	9 mA
A11-1	5-1000 MHz	13.5 dB	±1.2 dB	4.0 dB	2.0:1	-4 dBm	+10 dBm	15V	9 mA
A13	5-1000 MHz	13.5 dB	±1.2 dB	5.5 dB	2.0:1	-4 dBm	+10 dBm	15V	9 mA
A63	5-1000 MHz	14.5 dB	±1.0 dB	5.5 dB	2.2:1	+2 dBm	+15 dBm	15V	14 mA
A15	5-1000 MHz	13.0 dB	±1.2 dB	7.0 dB	2.0:1	+6 dBm	+21 dBm	15V	24 mA
A17	10-1000 MHz	10.0 dB	±1.2 dB	8.5 dB	2.0:1	+13 dBm	+30 dBm	15V	44 mA
A19	10-1000 MHz	5.5 dB	±1.2 dB	12.5 dB	2.2:1	+19 dBm	+34 dBm	15V	100 mA
A25	5-1500 MHz	8.0 dB	±1.0 dB	8.0 dB	2.2:1	+6 dBm	+21 dBm	15V	24 mA
A71	5-170 MHz	14.0 dB	—	1.7 dB (5-100 MHz) 2.5 dB (5-170 MHz)	4.5:1 (In) 2.5:1 (Out)	+1 dBm	+15 dBm	15V	11 mA

* 21°C Maximum Temperature at 24 Volts

MOUNTING INSTRUCTIONS

To achieve maximum cascaded gain, gain flatness and to realize the inherent stability provided in each unit, it is very important to assure good RF grounding between the case and the ground plane. The case should make intimate contact with ground prior to soldering pins. For greater assurance in making ground contact a conductive epoxy preform, such as Ablefilm ECF535 available from Ablestick Laboratories, can be utilized quite satisfactorily as shown in Fig. 1. A second method is to use a TO-8 accessories kit No. 251050-001 supplied by Watkins-Johnson as shown in Fig. 2. This method is particularly advantageous when higher power TO-8 amplifiers such as the WJ-A7 and WJ-A9 are used and where maximum heat transfer is needed.

Since the A9 dissipates approximately 2.5 watts at 24 volts, its bottom case surface should be attached to a heat sink. Mounting with good thermal contact on a metal plate or copper ground plane which is heat sunk within 1 inch of the unit is also adequate.

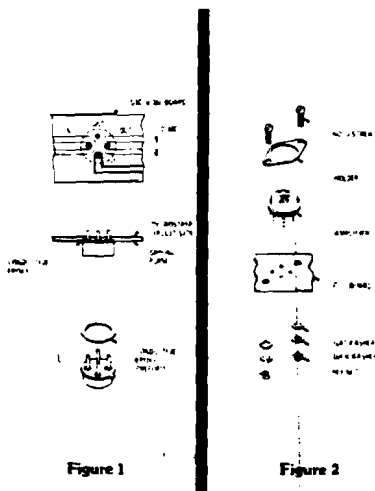
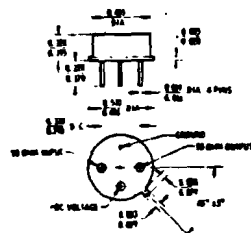


Figure 1

Figure 2

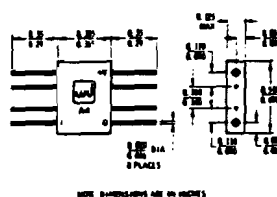
Outline Drawings

TO-8 Package Amplifiers and limiter



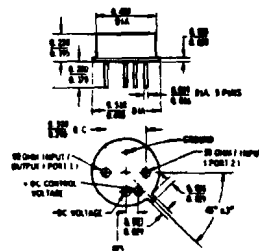
Weight: 2 grams

Flatpack Package for the W-J A4, A6 and A8.



Weight: 2 grams

Package for the Attenuator G1.



Weight: 2 grams

Environmental

W-J thin film cascaded amplifiers are designed to meet the following tests per MIL-STD-202E:

Exposure	Method	Test Condition	Exposure	Method	Test Condition
Thermal Shock	107D	B	Humidity	106D	
Altitude	105C	G	Terminal Strength	211A	C
H.F. Vibration	204C	D	Resistance to Soldering Heat	210A	B
Mechanical Shock	213B	C	Solderability	208C	
Random Vibration (15 minutes per axis)	214	H F			

They are also designed to meet the environmental requirements of MIL-E-16400F, Class 1, and MIL-E-5400L, Class 2.

Appendix E.2: The data sheets of the GPD201 amplifier.

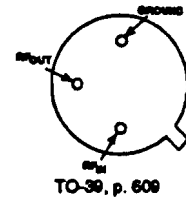
Selection
Guide

GPD Series

PRODUCT DESCRIPTION

The GPD and GPM amplifiers, available in TO-12 (4-pin) and TO-39 (3-pin) packages, are designed for applications which require the highest performance-to-cost ratio or where size is an important factor. Some versions are equipped with internal coupling and bypass capacitors, however the "60" Series

uses external coupling and bypass capacitors. This gives the user freedom to set the low frequency roll-off as needed. The GPM modules contain Si MMICs, while the GPD modules are discrete hybrid devices. These amplifiers are excellent for IF amplification purposes such as mixer postamps.



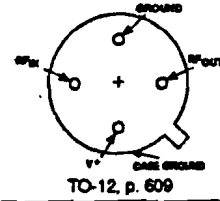
GPD SERIES LOW COST AMPLIFIERS, TO-39 PACKAGE*

Guaranteed Specifications at 0° to 50°C Case Temperature

Model	Frequency Response (MHz)	Gain over 0° to 50°C	Gain ² over -55° to +85°C	Noise Figure (dB)	Power Output at 1 dB Gain Compression (dBm)	Gain Flatness (±dB)	3rd-Order Intercept Point (dBm)	Input Power (±1% Reg.)	
		(dB)	(dB)					Voltage (VDC)	Current (mA)
	Minimum	Minimum	Minimum	Typical	Typical	Typical	Typical	Typical	Typical
GPD-110	0.1-400	—	12	4.0	-2.0	1.0	+12	2.5	10
GPD-120	0.1-400	—	13	5.5	+8.0	1.0	+24	5.5	25
GPD-130	0.1-400	—	12	7.0	+17.0	1.0	+27	6.0	60
GPD-310	0.1-1000	8	7	5.0	-1.0	1.0	+11	2.3	10
GPD-320	0.1-1000	8	7	5.0	+8.0	1.0	+18	3.0	25
GPD-330	0.1-1000	7	6	6.5	+16.0	1.0	+26	4.5	60
GPD-311	0.1-1000	12	11	4.5	+3.0	1.0	+15	2.7	15
GPD-321	0.1-1000	12	11	4.7	+8.0	1.0	+20	3.5	25
GPD-331	0.1-1000	10	9	6.0	+16.0	1.0	+28	5.5	60
GPD-410	0.1-1500	12	11	4.2	+2.5	1.0	+15	2.5	15
GPD-420	0.1-1500	11	10	4.7	+8.0	1.0	+20	2.6	25
GPD-430	0.1-1500	10	9	6.3	+16.0	1.0	+28	5.0	60

- NOTES: 1. Three external capacitors (input, output coupling and RF bypass) are required to establish low frequency roll-off. An external bias resistor, with a value determined by the available bias voltage ($R_b = [V_{cc} - V_D] / I_D$, where R_b is the value of the bias resistor (Ohms), V_{cc} is the available source voltage, V_D is the required device bias voltage (per specification) and I_D is the device current (per specification)), is also required.
2. Military temperature conditions: -55° to +85°C

GPD Series Selection Guide



GPD SERIES LOW COST AMPLIFIERS, TO-12 PACKAGE
 Guaranteed Specifications at 0° to 50°C Case Temperature

Model	Frequency Response (MHz)	Gain (dB)	Gain ² (dB)	Noise Figure (dB)	Power Output for 1 dB Gain Compression (dBm)	Gain Flatness (±dB)	3rd-Order Intercept Point (dBm)	Input Power (±1% Reg.) Voltage (VDC)	Current (mA)	Page Number
	Minimum	Minimum	Minimum	Typical	Typical	Typical	Typical	Typical		
GPD-201	5-200	30	26	3.0	+5	1.0	+13	+15	30	254
GPD-202	5-200	25	23	5.5	+11	1.0	+18	+15	60	254
GPM-552	5-500	33	32	4.5	0	0.2	+14	+15	34	264
GPM-1052	5-1000	20	20	7.0	+8	0.3	+20	+15	60	268
GPD-251	5-200	25	23	4.0	+1	1.0	+10	+5	30	256
GPD-252	5-200	15	14	4.0	0	1.0	+12	+5	11	257
GPD-401/-461 ¹	5-200	13	12	4.0	-2	1.0	+9	+15	10	258
GPD-411	5-400	12	11	3.0	-6	1.0	+4	+15	7	263
GPD-402/-462 ¹	5-400	13	12	8.0	+8	1.0	+18	+15	24	259
GPD-403/-463 ¹	5-400	9	8	7.5	+16	1.0	+25	+24	65	260
GPD-404/-464 ¹	5-400	9	8	7.5	+17	1.0	+26	+15	70	261
GPD-405	10-400	13	12	5.0	+24	1.0	+36	+15	90	262
GPD-1001/-1061 ¹	5-1000	12	11	6.0	0	1.0	+12	+15	15	265
GPD-1002/-1062 ¹	5-1000	12	11	7.0	+6	1.0	+16	+15	27	266
GPD-1003/-1063 ¹	5-1000	10	9	7.0	+14	1.0	+25	+15	65	267

NOTES: 1. The 60 Series is the same as the standard series except that three external capacitors are required to establish low frequency roll-off.
 2. Military temperature conditions: -55° to +85°C

MAXIMUM RATINGS AND THERMAL CHARACTERISTICS TABLE

Model	Maximum Ratings					Thermal Characteristics ¹				
	DC Voltage (Volts)	Continuous RF Input Power (dBm)	Operating Case Temperature (°C)	Storage Temperature (°C)	"R" Series Burn-in Temperature (°C)	θ_{JC} (°C/W)	Active Transistor Power Dissipation (mW)	Junction Temperature Above Case Temperature (°C)	MTBF MIL-HDBK-217E, A_{LTP} @ 80°C (hrs)	Weight (Grams)
GPD-201	+17	+13	-55 to +125	-62 to +150	+125	105	33	3	1,878,671	1.5
GPD-202	+17	+13	-55 to +125	-62 to +150	+125	105	117	12	1,821,478	1.5
GPD-251	+12	+13	-55 to +125	-62 to +150	+125	105/105	23/43	25	1,878,323	1.5
GPD-252	+12	+13	-55 to +125	-62 to +150	+125	105	20	2	2,000,740	1.5
GPD-401/461	+17	+13	-55 to +125	-62 to +150	+125	90	14	2	2,045,316 (401) 2,388,527 (461)	1.5
GPD-402/462	+17	+13	-55 to +125	-62 to +150	+125	90	82	7	2,325,901 (402) 2,640,323 (462)	1.5
GPD-403/463	+25	+13	-55 to +125	-62 to +150	+125	85	275	23	3,058,127 (403) 3,802,215 (463)	1.5
GPD-404/464	+17	+13	-55 to +115	-62 to +150	+115	85	330	28	2,435,672 (404) 2,512,908 (464)	1.5
GPD-405	+17	+13	-55 to +100	-62 to +150	+100	55	750	-41	1,607,022	1.5
GPD-411	+17	+13	-55 to +125	-62 to +150	+125	105 ²	24 ²	3 ²	1,808,303	1.5
GPM-552	+17	+17	-55 to +100	-62 to +100	+100	135/135	85/85	12/12	-	1.5
GPD-1001/-1061	+17	+13	-55 to +125	-62 to +150	+125	105	37	-4	1,839,228 (1001) 1,910,387 (1061)	1.5
GPD-1002/-1062	+17	+13	-55 to +125	-62 to +150	+125	105	81.6	-9	1,839,228 (1002) 1,882,476 (1062)	1.5
GPD-1003/-1063	+17	+13	-55 to +125	-62 to +150	+125	75	185	14	889,341 (1003) 2,101,101 (1063)	1.5
GPM-1052	+17	+17	-65 to +71	-62 to +71	+71	130/130	125/175	16/23	-	1.5

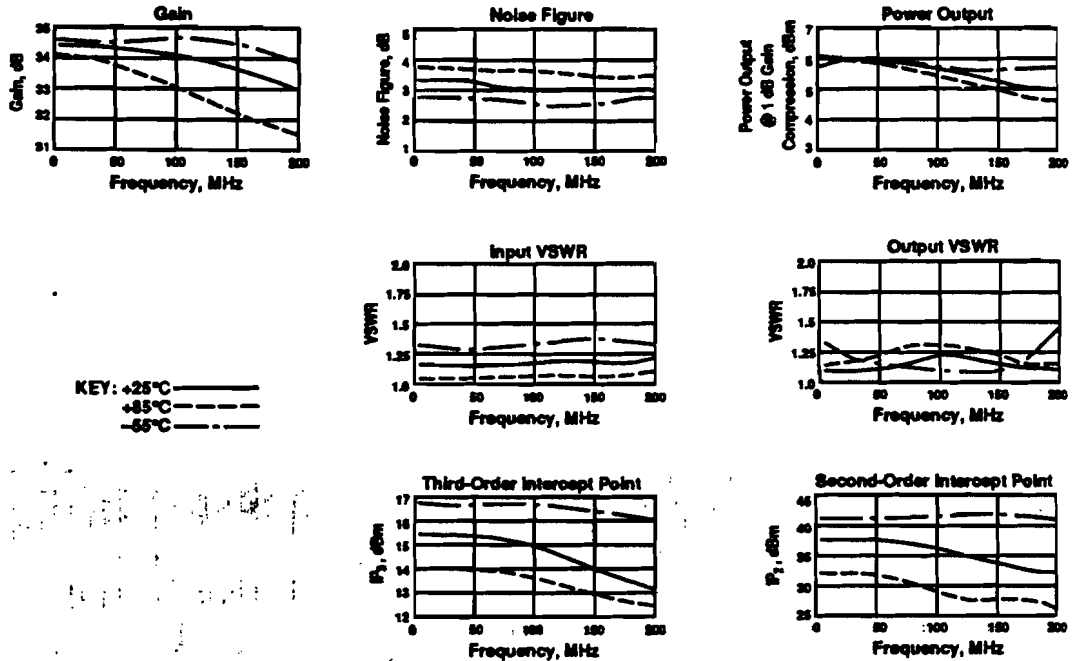
NOTES: 1. Values refer to 1st and 2nd stage transistors respectively.
 2. For further information, see High Reliability section.



Thin-Film Cascadable
Amplifier Module
5 to 200 MHz

GPD-201

TYPICAL PERFORMANCE OVER TEMPERATURE (@ +15 VDC unless otherwise noted)



AUTOMATIC NETWORK ANALYZER MEASUREMENTS (Typical production unit @ +25°C ambient)

NUMERICAL READINGS BIAS = 15.00 VOLTS

FREQ MHz	VSWR IN	GAIN dB	PHASE DEG	PHASE DEV	GPDEL ns	VSWR OUT	ISOL dB
100.0	1.22	34.08	-21.48	.03	.00	1.38	45.05
150.0	1.24	33.83	-31.73	-.07	.58	1.35	42.53
200.0	1.30	33.08	-41.78	.03	.55	1.35	45.17
250.0	1.33	32.23	-51.68		.52	1.35	44.14
300.0	1.39	31.33	-60.39		.46	1.37	45.05
350.0	1.42	30.34	-68.41		.40	1.41	42.90
400.0	1.46	29.22	-74.90		.33	1.46	45.18
450.0	1.49	28.20	-80.20		.28	1.51	42.67
500.0	1.51	27.05	-84.95		.21	1.55	42.98
550.0	1.54	25.98	-87.93		.18	1.59	43.16
600.0	1.56	25.02	-91.38		.15	1.61	42.20
650.0	1.57	23.93	-93.28		.08	1.64	41.70

S-PARAMETERS, MAGNITUDES AND ANGLES BIAS = 15.00 VOLTS

FREQ MHz	S ₁₁		S ₂₁		S ₁₂		S ₂₂	
	Mag	Ang	dB	Ang	dB	Ang	Mag	Ang
100.00	.089	-160.8	34.037	-21.5	-42.871	20.2	.172	-8
150.00	.105	-151.2	33.599	-31.7	-45.907	38.9	.153	8
200.00	.128	-152.8	33.063	-41.8	-45.886	28.4	.150	6.5
250.00	.144	-153.4	32.220	-51.8	-44.028	30.1	.148	13.7
300.00	.162	-156.8	31.300	-60.1	-43.385	56.8	.159	19.8
350.00	.173	-159.8	30.270	-68.4	-43.056	78.0	.171	22.8
400.00	.187	-163.8	29.200	-74.7	-41.723	80.0	.186	22.8
450.00	.199	-167.2	28.195	-80.2	-43.575	79.7	.204	21.9
500.00	.206	-170.2	27.005	-84.7	-43.475	100.7	.216	20.4
550.00	.214	-174.7	25.949	-87.7	-42.361	109.1	.227	17.7
600.00	.218	-177.3	24.986	-91.3	-41.874	113.8	.235	15.0
650.00	.224	-179.3	23.911	-93.2	-41.737	124.4	.242	11.7

Appendix E.3: The data sheets of the HSCH schottky diode.



**ZERO BIAS SCHOTTKY
DIODES FOR MIXERS
AND DETECTORS**

**HSCH-3206/07
HSCH-3486**

Features

- HIGH VOLTAGE SENSITIVITY**
- NO BIAS REQUIRED**
- CHOICE OF HIGH OR LOW VIDEO IMPEDANCE**

Description/Applications

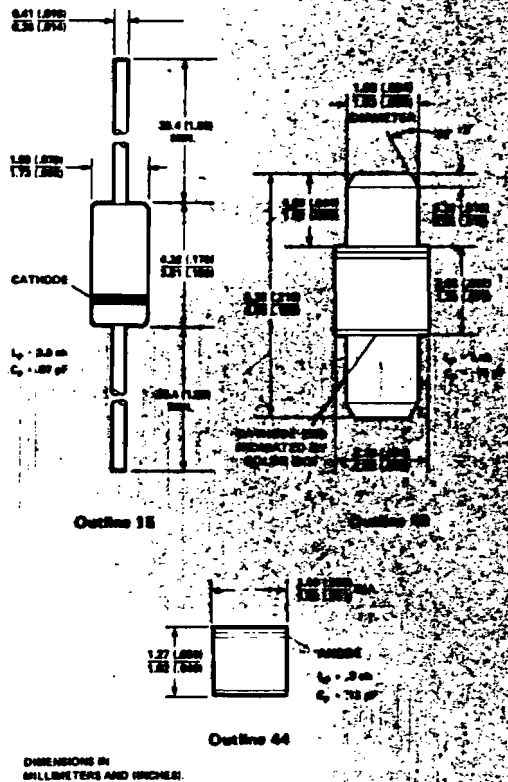
The high zero bias voltage sensitivity of these Schottky Barrier diodes makes them ideally suitable for narrow bandwidth video detectors, ECM receivers, and measurement equipment. These diodes also make excellent mixers for use with low power LO.

Maximum Ratings

Operating and Storage
 Temperature Range -65° C to -150° C
 CW Power Dissipation at T_{case} = 25° C
 HSCH-3206, -3207 200 mW
 HSCH-3486 300 mW
 Derate Linearly to 0 W at 150° C
 Pulse Power Dissipation at T_{case} = 25° C
 Peak power incident
 1 μs pulse, Du = 0.001 1 W
 These diodes are ESD sensitive. Handle with care to avoid static discharge through the diode.

Package Characteristics

The HP Outline 15 package has a glass hermetic seal with gold plated Dumet leads which should be restricted so that the bend starts at least 1/16" (1.6 mm) from the glass body. With this restriction, it will meet MIL-STD-750, Method 2036.
 Conditions A (4 lb. [1.8 kg] tension for 30 minutes). The maximum soldering temperature is 230°C for 5 seconds. Marking is by digital coding with a cathode band.



Electrical Specifications at $T_A = 25^\circ\text{C}$

Part Number	Package Outline	Maximum Tangential Sensitivity TSS (dBm)	Minimum Voltage Sensitivity γ ($\mu\text{V}/\mu\text{W}$)	Video Resistance R_v (K Ω)		Typical Total Capacitance C_T (pF)
				Min.	Max.	
HSCH-3207	44	-42	8	60	300	0.30
HSCH-3206	48	-42	8	80	300	0.30
HSCH-3486	15	-54	7.5	2	8	0.30
Test Conditions		Video Bandwidth = 2 MHz $f_{\text{max}} = 10 \text{ GHz}$	Power in = -30 dBm $f_{\text{test}} = 10 \text{ GHz}$ $R_L = 10 \text{ M ohm}$			$V_R = 0 \text{ V}$ $f = 1 \text{ MHz}$

Note
For HSCH-3207, -3206. $I_R = 10 \mu\text{A}$ (max) at $V_R = 3 \text{ V}$ at $T_A = 25^\circ\text{C}$. For reverse characteristics of HSCH-3486 see Figure 3

Typical Characteristics

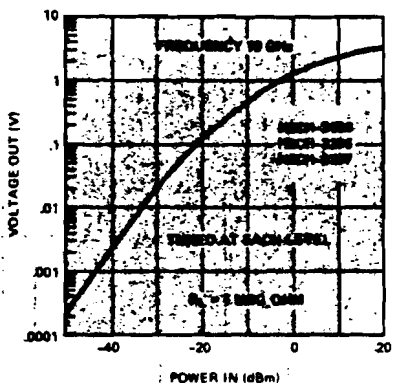


Figure 1. Typical Dynamic Transfer Characteristics

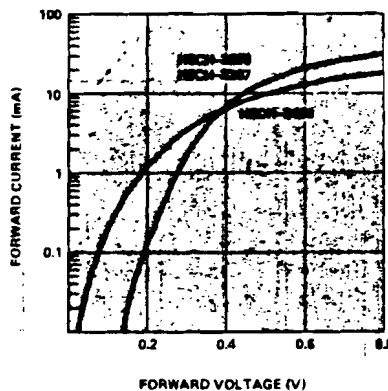


Figure 2. Typical Forward Characteristics at $T_A = 25^\circ\text{C}$.

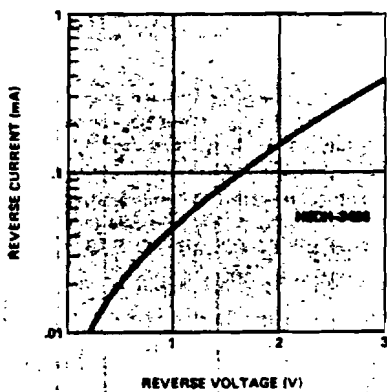


Figure 3. Typical Reverse Characteristics at $T_A = 25^\circ\text{C}$

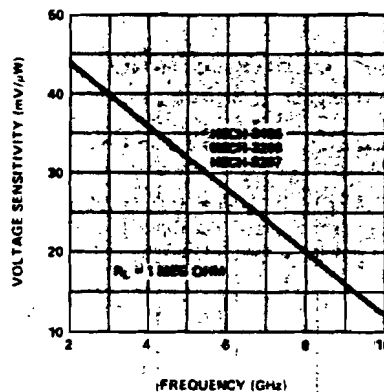


Figure 4. Typical Voltage Sensitivity vs Frequency

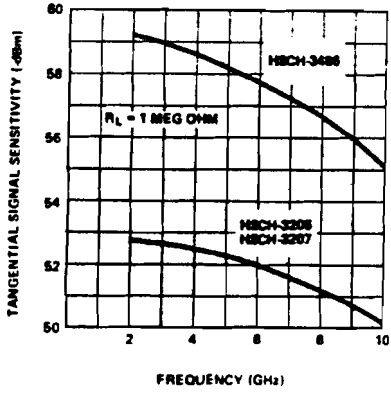


Figure 5 Typical Tangential Sensitivity vs Frequency

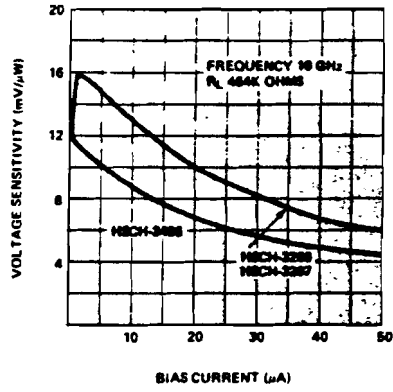


Figure 6 Typical Voltage Sensitivity vs. Bias Current.

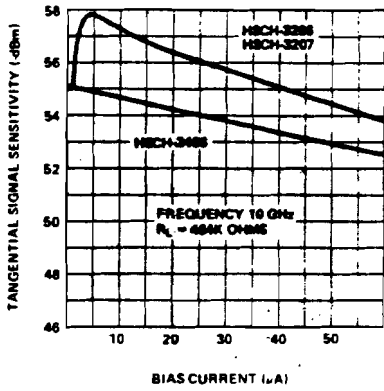


Figure 7 Typical Tangential Sensitivity vs. Bias Current

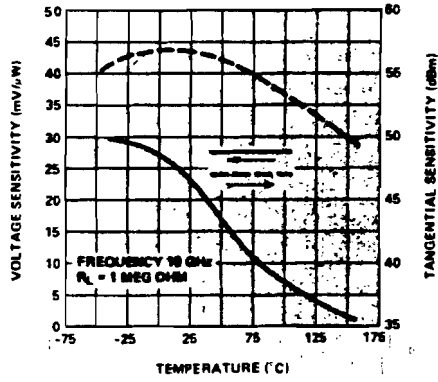


Figure 8 Effect of Temperature on HSC-3486.

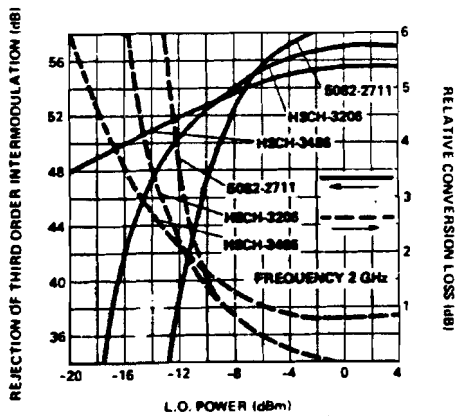


Figure 9. Mixer Performance.



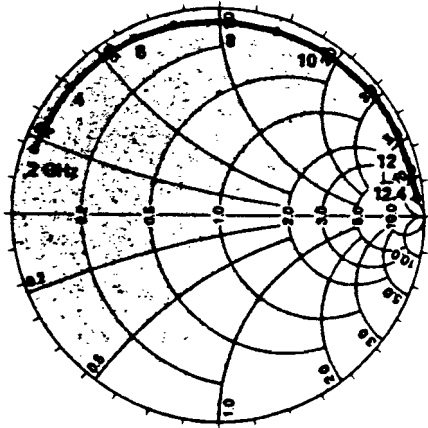


Figure 10. Typical Admittance Characteristics. HSCH-3206

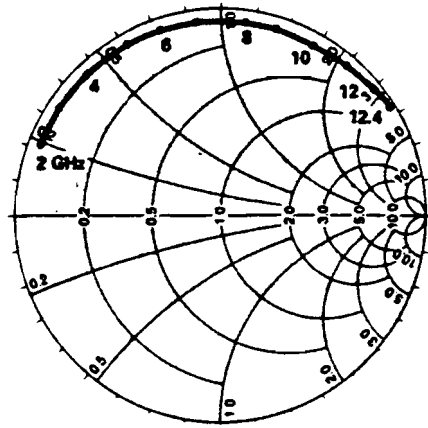


Figure 11. Typical Admittance Characteristics. HSCH-3207

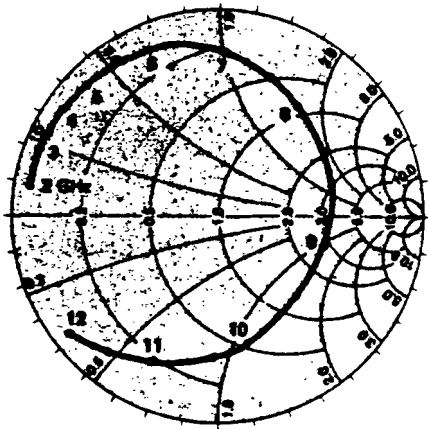


Figure 12. Typical Admittance Characteristics. HSCH-3486

Appendix E.4: The data sheets of the video amplifier.

OPA27 OPA37

MILITARY & DIE
VERSIONS
AVAILABLE

Ultra-Low Noise Precision OPERATIONAL AMPLIFIERS

FEATURES

- LOW NOISE: 100% tested, $3.8\text{nV}/\sqrt{\text{Hz}}$ max at 1kHz
- LOW OFFSET: $25\mu\text{V}$ max
- LOW DRIFT: $0.6\mu\text{V}/^\circ\text{C}$ max
- HIGH OPEN-LOOP GAIN: 120dB min
- HIGH COMMON-MODE REJECTION: 114dB min
- HIGH POWER SUPPLY REJECTION: 100dB min
- FITS OP-07, OP-05, AD510, AD517 SOCKETS

APPLICATIONS

- PRECISION INSTRUMENTATION
- DATA ACQUISITION
- TEST EQUIPMENT
- PROFESSIONAL AUDIO EQUIPMENT
- TRANSDUCER AMPLIFIER
- RADIATION HARD EQUIPMENT

DESCRIPTION

The OPA27/37 is an ultra-low noise, high precision monolithic operational amplifier.

Laser-trimmed thin-film resistors provide excellent long-term voltage offset stability and allow superior voltage offset compared to common zener-zap techniques.

A unique bias current cancellation circuit allows bias and offset current specifications to be met over the full -55°C to $+125^\circ\text{C}$ temperature range.

The OPA27 is internally compensated for unity-gain stability. The decompensated OPA37 requires a closed-loop gain ≥ 5 .

The Burr-Brown OPA27/37 is an improved replacement for the industry-standard OP-27/OP-37.

OPA27/37 AMPLIFIER CIRCUIT

International Airport Industrial Park • P.O. Box 11400 • Tucson, Arizona 85734 • Tel. (602) 746-1111 • Telex: 910-952-1111 • Cable: BURBROF • Telex: 06-5401

OPA27/37

OPERATIONAL AMPLIFIERS

PDS-466H

SPECIFICATIONS

ELECTRICAL

All $V_{CC} = \pm 15\text{VDC}$ and $T_A = +25^\circ\text{C}$ unless otherwise noted.

PARAMETER	CONDITIONS	OPA27/STA, OPA37/STE			OPA27/STB, OPA37/STF			OPA27/STC, OPA37/STG			UNITS
		MIN	TYP	MAX	MIN	TYP	MAX	MIN	TYP	MAX	
INPUT											
NOISE Voltage, $f_o = 10\text{Hz}$ $f_o = 30\text{Hz}$ $f_o = 1\text{kHz}$ Current, ⁽¹⁾ $f_o = 10\text{Hz}$ $f_o = 30\text{Hz}$ $f_o = 1\text{kHz}$	100% tested, (A, E)		3.1	5.5		3.5	5.5		3.8	8.0 ⁽²⁾	nV/ $\sqrt{\text{Hz}}$
	100% tested, (A, E)		2.9	4.5		3.1	4.5		3.3	5.6 ⁽²⁾	nV/ $\sqrt{\text{Hz}}$
	100% tested, (A, E)		2.7	3.8		3.0	3.8		3.2	4.5 ⁽²⁾	nV/ $\sqrt{\text{Hz}}$
				0.07	0.18		0.08	0.18		0.08	0.25 ⁽²⁾
OFFSET VOLTAGE⁽³⁾ Input Offset Voltage Average Drift ⁽⁴⁾ Long Term Stability ⁽⁴⁾ Supply Rejection	$T_A \text{ min to } T_A \text{ max}$		± 6	± 25		± 12	± 60		± 25	± 100	μV $\mu\text{V}/^\circ\text{C}$ $\mu\text{V}/\text{mo}$ dB
	$\pm V_{CC} = 4 \text{ to } 18\text{V}$	100	0.2	1	100	0.3	1.5	84	0.4	2.0	
	$\pm V_{CC} = 4 \text{ to } 18\text{V}$		134			125			120		
			± 0.2	± 10		± 0.6	± 10		± 1	± 20	
BIAS CURRENT Input bias Current			± 11	± 40		± 13	± 55		± 15	± 60	nA
OFFSET CURRENT Input Offset Current			6	35		8	50		10	75	nA
IMPEDANCE Common-Mode			3			2.5			2		Ω
VOLTAGE RANGE Common-Mode Input Range Common-Mode Rejection	$V_{CM} = \pm 11\text{VDC}$	± 11	± 12.3		± 11	± 12.3		± 11	± 12.3		V
		114	126		106	125		100	122		dB
OPEN-LOOP GAIN, DC											
Open-Loop Voltage Gain	$R_L \geq 2\text{k}\Omega$ $R_L \geq 1\text{k}\Omega$	120 118	126 125		120 118	125 125		117 124	124 124		dB dB
FREQUENCY RESPONSE											
Gain-Bandwidth Product ⁽⁵⁾	OPA27 OPA37	5 46	6 63		5 45	6 63		5 ⁽⁶⁾ 45 ⁽⁶⁾	6 63		MHz MHz
Slew Rate ⁽⁶⁾	$V_o = \pm 10\text{V}$ $R_L = 2\text{k}\Omega$	1.7	1.9		1.7	1.9		1.7 ⁽⁶⁾ 11 ⁽⁶⁾	1.9 11.9		V/ μs V/ μs
Setting Time, 0.01%	OPA27, G = +1 OPA37, G = +5 OPA27, G = +1 OPA37, G = +5	11 11	11.9 11.9		11 11	11.9 11.9		11 ⁽⁶⁾ 11 ⁽⁶⁾	11.9 11.9		μs μs
RATED OUTPUT											
Voltage Output	$R_L \geq 2\text{k}\Omega$	± 12	± 13.8		± 12	± 13.8		± 12	± 13.8		V
Output Resistance	$R_L \geq 600\Omega$	± 10	± 12.8		± 10	± 12.8		± 10	± 12.8		V
Short Circuit Current	DC, open loop $R_L = 0\Omega$		70	60		70	60		70	60 ⁽⁶⁾	Ω mA
POWER SUPPLY											
Rated Voltage			± 15			± 15			± 15		VDC
Voltage Range, Derated Performance Current, Quiescent	$I_o = 0\text{mA}$	± 4	3	± 22 4.7	± 4	3	± 22 4.7	± 4	3.3	± 22 5.7	VDC mA
TEMPERATURE RANGE											
Specification											$^\circ\text{C}$
A, B, C (J, Z)		-55		+125	-55		+125	-55		+125	$^\circ\text{C}$
E, F, G (J, Z)		-25		+85	-25		+85	-25		+85	$^\circ\text{C}$
G (P) (U)							0			+70	$^\circ\text{C}$
Operating: J, Z		-55		+125	-55		+125	-55		+125	$^\circ\text{C}$
P, U							-25			+85	$^\circ\text{C}$

NOTES: (1) Measured with industry-standard noise test circuit (Figures 1 and 2). Due to errors introduced by this method, these current noise specifications should be used for comparison purposes only. (2) Offset voltage specifications on grades A, and E are also guaranteed with units fully warmed up. Grades B, C, F, and G are measured with automatic test equipment after approximately 0.5 second from power turn-on. (3) Unruffled or ruffled with 8k Ω to 20k Ω potentiometer. (4) Long-term voltage offset vs time trend line does not include warm-up drift. (5) Typical specification only on plastic package units. Slew rate varies on all units due to differing test methods. Minimum specification applies to open-loop test. (6) This parameter not guaranteed in SOIC "U" package.

ELECTRICAL (FULL TEMPERATURE RANGE SPECIFICATIONS)

All $V_{CC} = \pm 15VDC$ and $T_A = T_{MIN}$ to T_{MAX} unless otherwise noted.

PARAMETER	CONDITIONS	OPA27/37A, OPA27/37E			OPA27/37B, OPA27/37F			OPA27/37C, OPA27/37G			UNITS
		MIN	TYP	MAX	MIN	TYP	MAX	MIN	TYP	MAX	
TEMPERATURE RANGE											
Specification Range											
A, B, C (J, Z)		-55		+125	-55		+125	-55		+125	°C
E, F, G (J, Z)		-25		+85	-25		+85	-25		+85	°C
G (P)							0			+70	°C
INPUT											
OFFSET VOLTAGE⁽¹⁾											
Input Offset Voltage											
A, B, C			±24	±80		±45	±200		±80	±300 ⁽³⁾	µV
E, F, G			±17	±50		±33	±140		±48	±220 ⁽³⁾	µV
Average Drift ⁽²⁾	$T_A \text{ min to } T_A \text{ max}$		±0.2	±0.6		±0.3	±1.3		±0.4	±1.8 ⁽³⁾	µV/°C
Supply Rejection											
A, B, C	$\pm V_{CC} = 4.5 \text{ to } 18V$	96	130		94	127		96 ⁽³⁾	122		dB
E, F, G	$\pm V_{CC} = 4.5 \text{ to } 18V$	97	130		96	127		90 ⁽³⁾	122		dB
BIAS CURRENT											
Input Bias Current											
A, B, C			±16	±80		±22	±95		±29	±150 ⁽³⁾	nA
E, F, G			±13	±60		±16	±95		±21	±150 ⁽³⁾	nA
OFFSET CURRENT											
Input Offset Current											
A, B, C			23	50		25	85		35	135 ⁽³⁾	nA
E, F, G			12	50		14	85		20	135 ⁽³⁾	nA
VOLTAGE RANGE											
Common-Mode Input Range											
A, B, C		±10.3	±11.5		±10.3	±11.5		±10.3 ⁽³⁾	±11.5		V
E, F, G		±10.5	±11.8		±10.5	±11.8		±10.5 ⁽³⁾	±11.8		V
Common-Mode Rejection	$V_{in} = \pm 11VDC$										
A, B, C		106	124		100	122		94 ⁽³⁾	120		dB
E, F, G		110	126		102	124		96 ⁽³⁾	122		dB
OPEN-LOOP GAIN, DC											
Open-Loop Voltage Gain	$R_L \geq 2k\Omega$										
A, B, C		116	121		114	120		110 ⁽³⁾	116		dB
E, F, G		118	123		117	122		113	120		dB
RATED OUTPUT											
Voltage Output	$R_L = 2k\Omega$										
A, B, C		±11.5	±13.7		±11.0	±13.5		±10.5 ⁽³⁾	±13.3		V
E, F, G		±11.7	±13.8		±11.4	±13.6		±11.0 ⁽³⁾	±13.4		V
Short Circuit Current	$V_O = 0VDC$		25			25			25		mA

NOTES (1) Offset voltage specifications on grades A and E are also guaranteed with the units fully warmed up. Grades B, C, F, and G are measured with automatic equipment after approximately 0.5 second. (2) Unrouted or routed with 8kΩ to 20kΩ potentiometer. (3) This parameter not guaranteed in SOIC "U" package.

ABSOLUTE MAXIMUM RATINGS

Supply Voltage	±22V
Internal Power Dissipation ⁽¹⁾	500mW
Input Voltage	±V _{CC}
Output Short-Circuit Duration ⁽²⁾	Indefinite
Differential Input Voltage ⁽³⁾	±0.7V
Differential Input Current ⁽³⁾	±25mA
Storage Temperature Range:	
J, Z	-65°C to +150°C
P	-55°C to +125°C
Operating Temperature Range:	
A, B, C, E, F, G (J, Z)	-55°C to +125°C
G (P, U)	-25°C to +85°C
Lead Temperature (Soldering, 60s)	+300°C
SOIC Package (3s)	+260°C

Package Type	Maximum Ambient Temperature for Rating	Derate Above Maximum Ambient Temperature
TO-99 (J)	80°C	7.1mW/°C
8-Pin Hermetic DIP (Z)	75°C	6.7mW/°C
8-Pin Plastic DIP (P)	82°C	5.8mW/°C
8-Pin SOIC (U)	85°C	—

NOTES:
 (1) Maximum package power dissipation vs ambient temperature.
 (2) To common with $\pm V_{CC} = 15V$.
 (3) The inputs are protected by back-to-back diodes. Current limiting resistors are not used in order to achieve low noise. If differential input voltage exceeds ±0.7V, the input current should be limited to 25mA.

OPA27/37

OPERATIONAL AMPLIFIERS

2

MECHANICAL

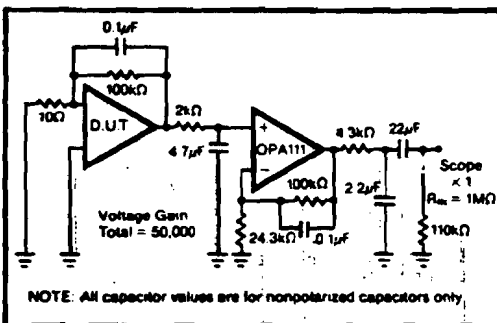
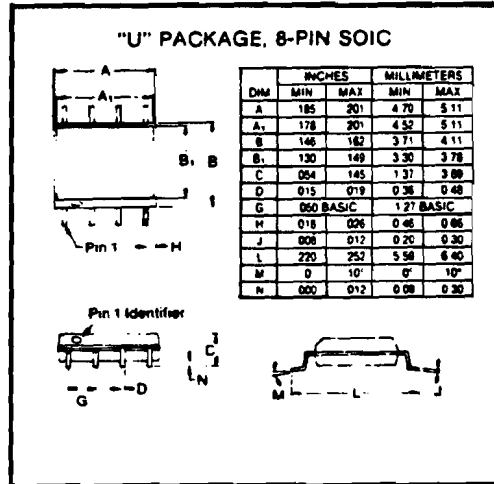
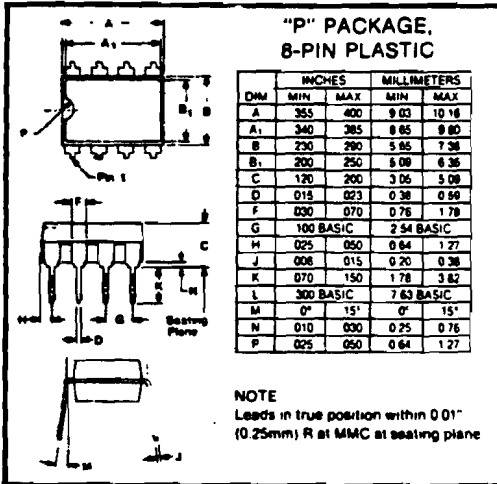


FIGURE 1. 0.1Hz to 10Hz Noise Test Circuit.

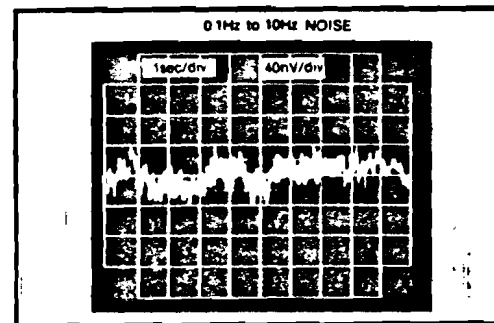


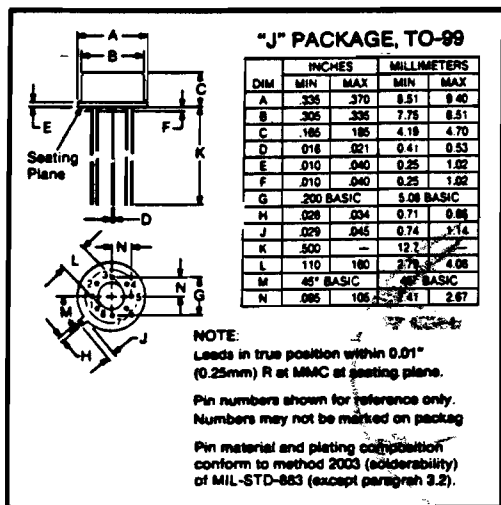
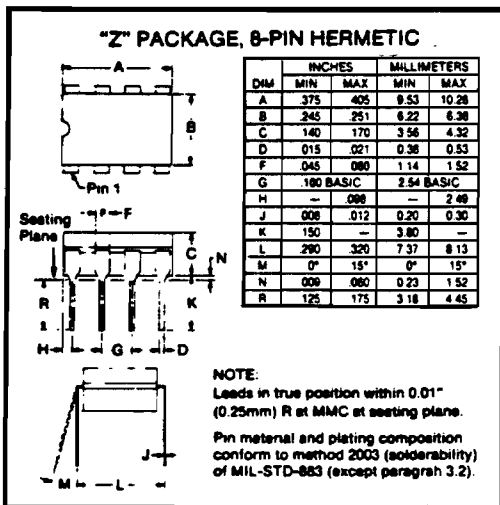
FIGURE 2. Low Frequency Noise.

ORDERING INFORMATION

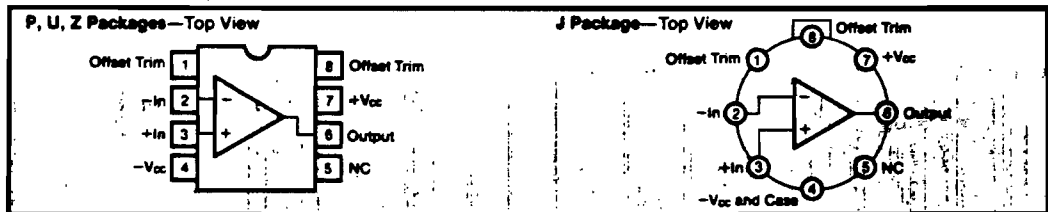
Model ⁽¹⁾	Package	Temperature Range	Offset Voltage max (µV), 25°C
OPA27AJ	TO-99	-55°C to +125°C	±25
OPA27BJ	TO-99	-55°C to +125°C	±80
OPA27CJ	TO-99	-55°C to +125°C	±100
OPA27EJ	TO-99	-25°C to +85°C	±25
OPA27FJ	TO-99	-25°C to +85°C	±80
OPA27GJ	TO-99	-25°C to +85°C	±100
OPA27AZ	Ceramic	-55°C to +125°C	±25
OPA27BZ	Ceramic	-55°C to +125°C	±80
OPA27CZ	Ceramic	-55°C to +125°C	±100
OPA27EZ	Ceramic	-25°C to +85°C	±25
OPA27FZ	Ceramic	-25°C to +85°C	±80
OPA27GZ	Ceramic	-25°C to +85°C	±100
OPA27GP	Plastic	0°C to +70°C	±100
OPA27GU	SOIC	0°C to +70°C	±100

BURN-IN SCREENING OPTION			
Model ⁽¹⁾	Package	Temperature Range	Burn-In Temp. (100h) ⁽²⁾
OPA27AJ-BI	TO-99	-55°C to +125°C	+125°C
OPA27EJ-BI	TO-99	-25°C to +85°C	+125°C
OPA27GJ-BI	TO-99	-25°C to +85°C	+125°C
OPA27AZ-BI	Ceramic	-55°C to +125°C	+125°C
OPA27EZ-BI	Ceramic	-25°C to +85°C	+125°C
OPA27GP-BI	Plastic	0°C to +70°C	+85°C
OPA27GU-BI	SOIC	0°C to +70°C	+85°C

NOTE: (1) Packages and prices for OPA37 are the same as for OPA27.
(2) Or equivalent combination of time and temperature.

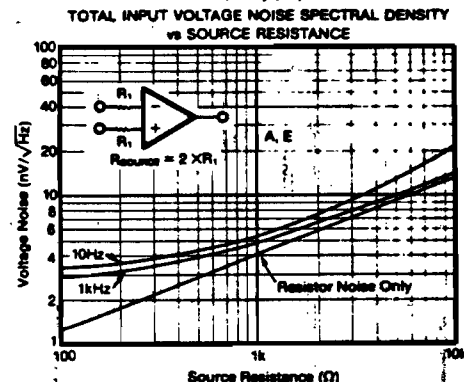
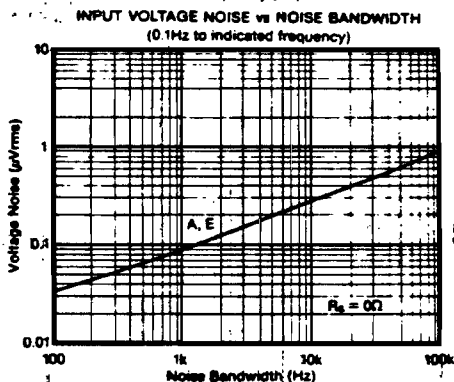
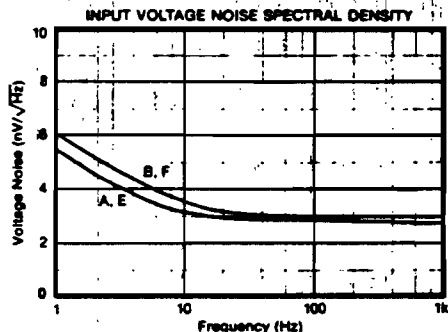
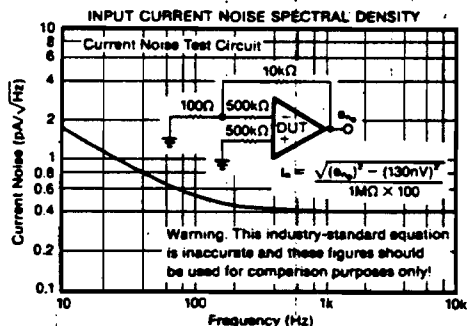


CONNECTION DIAGRAMS



TYPICAL PERFORMANCE CURVES

T_a = +25°C, ±V_{cc} = ±15VDC unless otherwise noted.

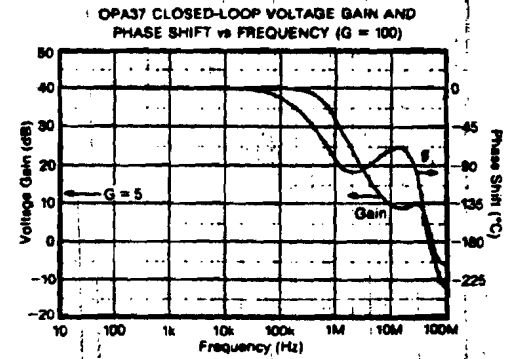
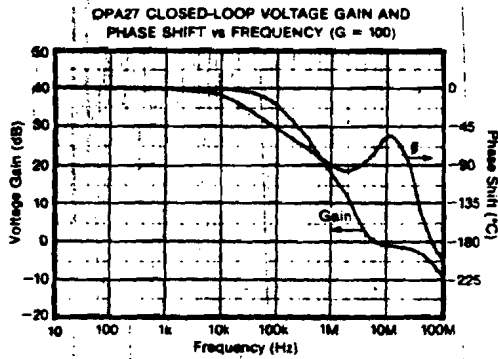
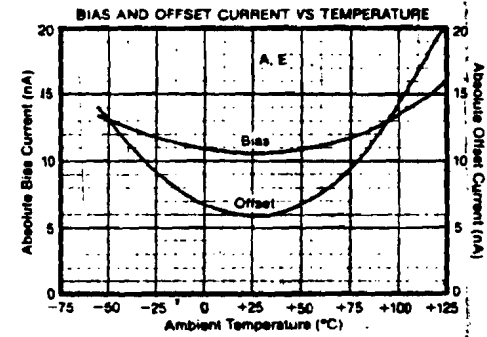
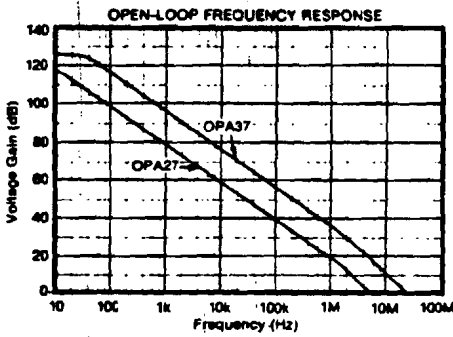
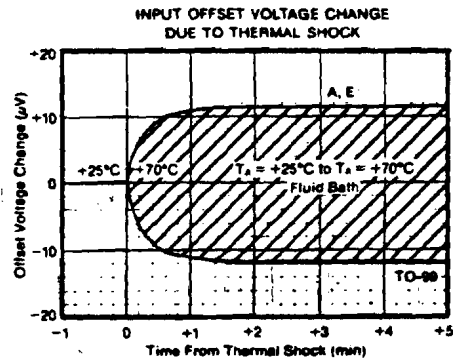
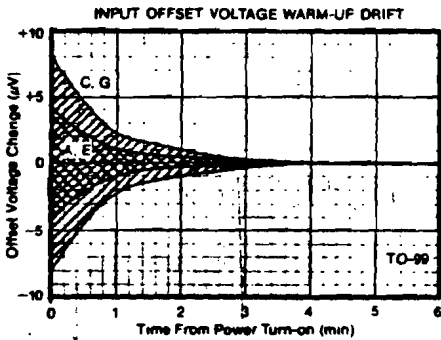
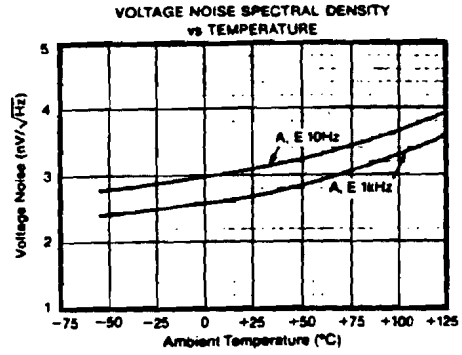
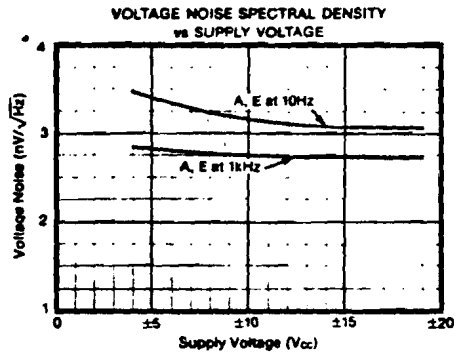


OPA2737

OPERATIONAL AMPLIFIERS

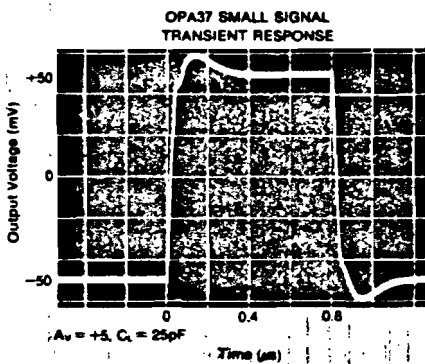
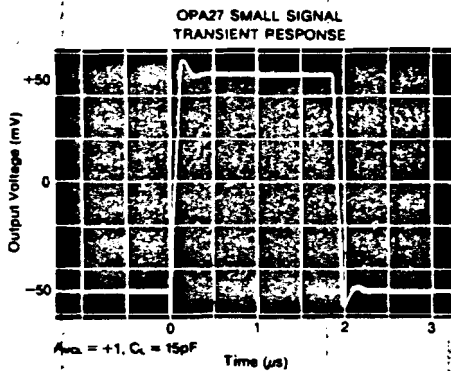
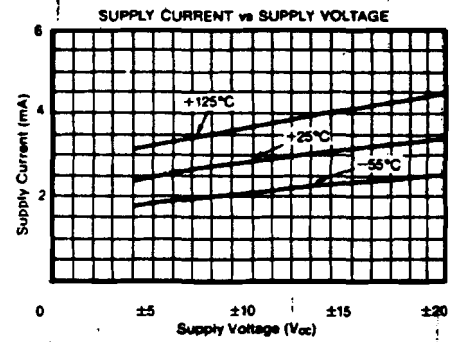
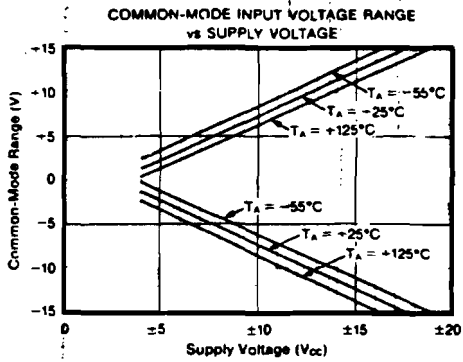
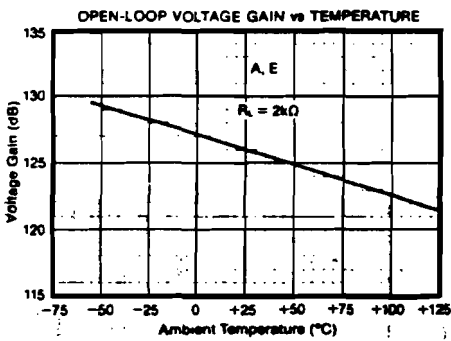
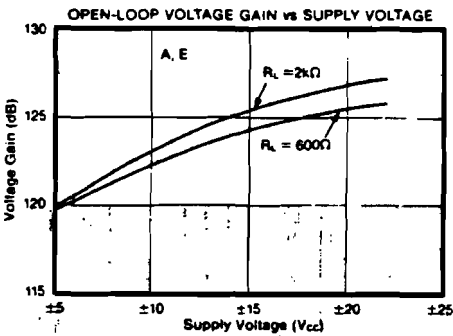
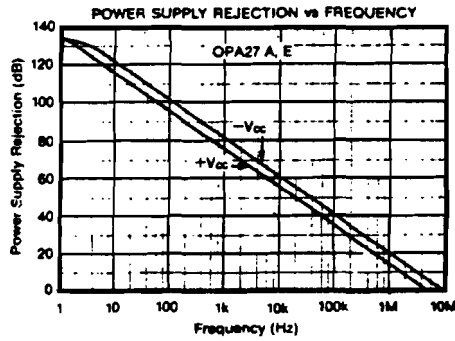
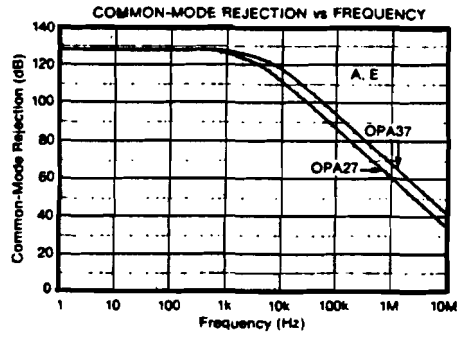
TYPICAL PERFORMANCE CURVES (CONT)

$T_A = +25^\circ\text{C}$, $\pm V_{CC} = \pm 15\text{VDC}$ unless otherwise noted.



TYPICAL PERFORMANCE CURVES (CONT)

$T_A = -25^\circ\text{C}$, $\pm V_{CC} = \pm 15\text{VDC}$ unless otherwise noted



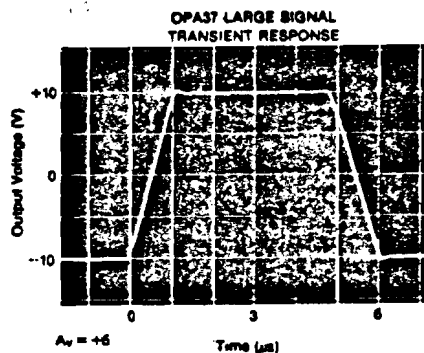
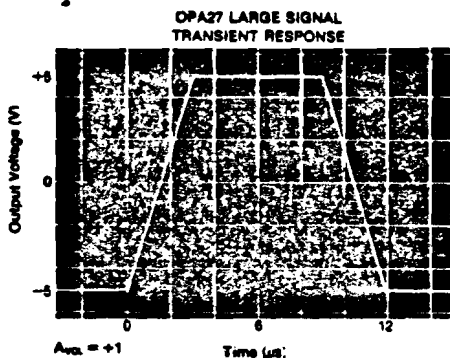
OPA27/37

2

OPERATIONAL AMPLIFIERS

TYPICAL PERFORMANCE CURVES (CONT)

$T_A = +25^\circ\text{C}$, $\pm V_{CC} = \pm 15\text{VDC}$ unless otherwise noted.



APPLICATIONS INFORMATION

OFFSET VOLTAGE ADJUSTMENT

The OPA27/37 offset voltage is laser-trimmed and will require no further trim for most applications. Offset voltage drift will not be degraded when the input offset is nulled with a $10\text{k}\Omega$ trim potentiometer. Other potentiometer values from $1\text{k}\Omega$ to $1\text{M}\Omega$ can be used but V_{OS} drift will be degraded by an additional 0.1 to $0.2\mu\text{V}/^\circ\text{C}$. Nulling large system offsets by use of the offset trim adjust will degrade drift performance by approximately $3.3\mu\text{V}/^\circ\text{C}$ per millivolt of offset. Large system offsets

can be nulled without drift degradation by input summing.

The conventional offset voltage trim circuit is shown in Figure 3. For trimming very-small offsets, the higher resolution circuit shown in Figure 4 is recommended.

The OPA27/37 can replace 741-type operational amplifiers by removing or modifying the trim circuit.

THERMOELECTRIC POTENTIALS

The OPA27/37 is laser-trimmed to microvolt-level input offset voltage and for very-low input offset voltage drift.

Careful layout and circuit design techniques are necessary to prevent offset and drift errors from external thermoelectric potentials. Dissimilar metal junctions can generate small EMFs if care is not taken to eliminate either their sources (lead-to-PC wiring, etc.) or their temperature difference. See Figure 1.

Short, direct mounting of the OPA27/37 with close spacing of the input pins is highly recommended. Poor layout can result in circuit drifts and offsets which are an order of magnitude greater than the operational amplifier alone.

NOISE: BIPOLAR VERSUS FET

Low-noise circuit design requires careful analysis of all noise sources. External noise sources can dominate in many cases, so consider the effect of source resistance on overall operational amplifier noise performance. At low source impedances, the lower voltage noise of a bipolar operational amplifier is superior, but at higher impedances the high current noise of a bipolar amplifier becomes a serious liability. Above about $15\text{k}\Omega$ the Burr-Brown OPA111 low-noise FET operational amplifier is recommended for lower total noise than the OPA27 (see Figure 5).

COMPENSATION

Although internally compensated for unity-gain stability, the OPA27 may require a small capacitor in parallel with a feedback resistor (R_f) which is greater than $2\text{k}\Omega$. This capacitor will compensate the pole generated by R_f and C_{IN} and eliminate peaking or oscillation.

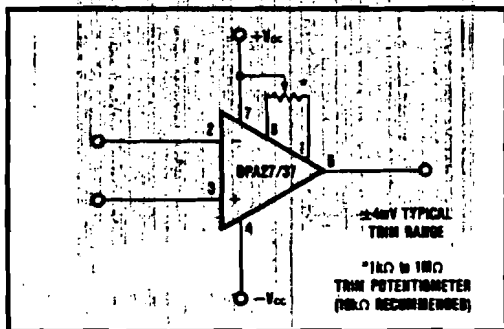


FIGURE 3. Offset Voltage Trim.

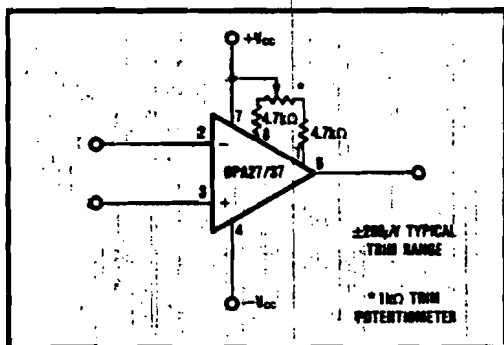


FIGURE 4. High Resolution Offset Voltage Trim.

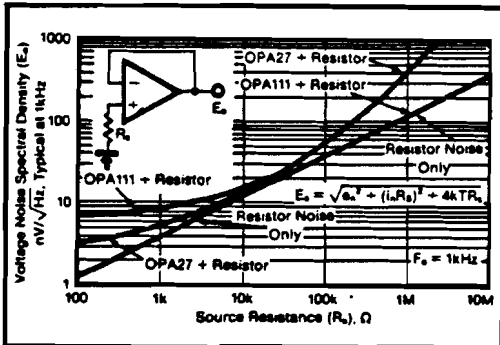


FIGURE 5. Voltage Noise Spectral Density Versus Source Resistance.

INPUT PROTECTION

Back-to-back diodes are used for input protection on the OPA27/37. Exceeding a few hundred millivolts differential input signal will cause current to flow and without external current limiting resistors the input will be destroyed.

Accidental static discharge as well as high current can damage the amplifier's input circuit. Although the unit may still be functional, important parameters such as input offset voltage, drift, and noise may be permanently damaged if any precision operational amplifier is subjected to abuse.

Transient conditions can cause feedthrough due to the amplifier's finite slew-rate. When using the OP-27 as a unity-gain buffer (follower) a feedback resistor of 1kΩ is recommended (see Figure 6).

BURN-IN SCREENING

Burn-in screening is an option available for the models indicated in the Ordering Information table. Burn-in duration is 160 hours at the maximum specified grade operating temperature (or equivalent combination of time and temperature).

All units are tested after burn-in to ensure that grade specifications are met. To order burn-in, add "-BI" to the base model number.

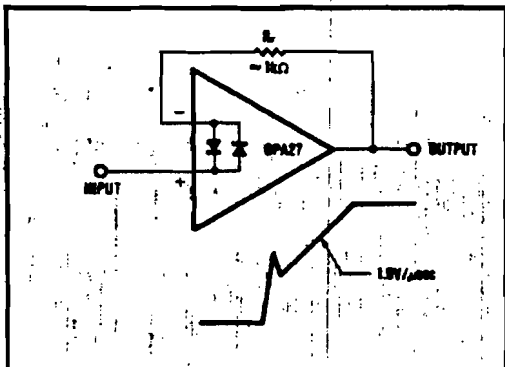


FIGURE 6. Pulsed Operation.

APPLICATIONS CIRCUITS

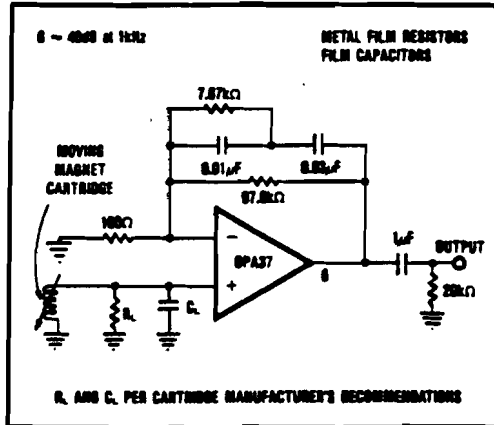


FIGURE 7. Low-Noise RIAA Preamplifier.

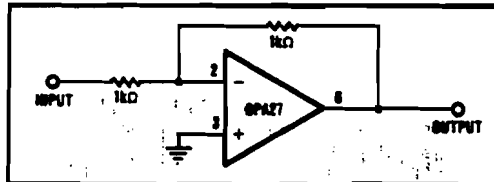


FIGURE 8. Unity-Gain Inverting Amplifier.

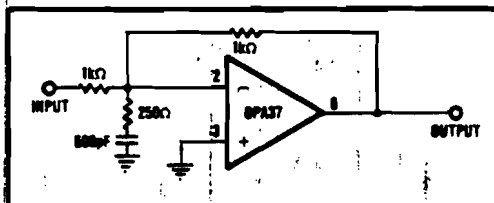


FIGURE 9. High Slew Rate Unity-Gain Inverting Amplifier.

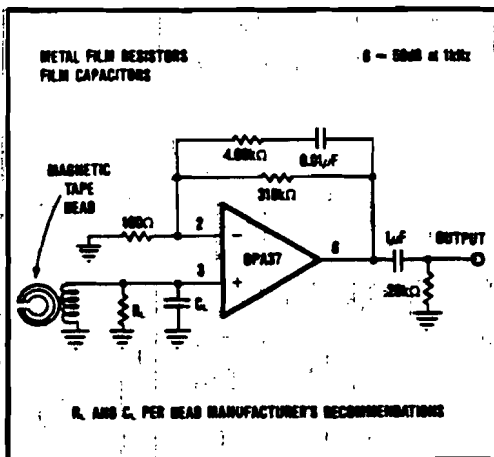


FIGURE 10. NAB Tape Head Preamplifier.

OPA27/37

OPERATIONAL AMPLIFIERS

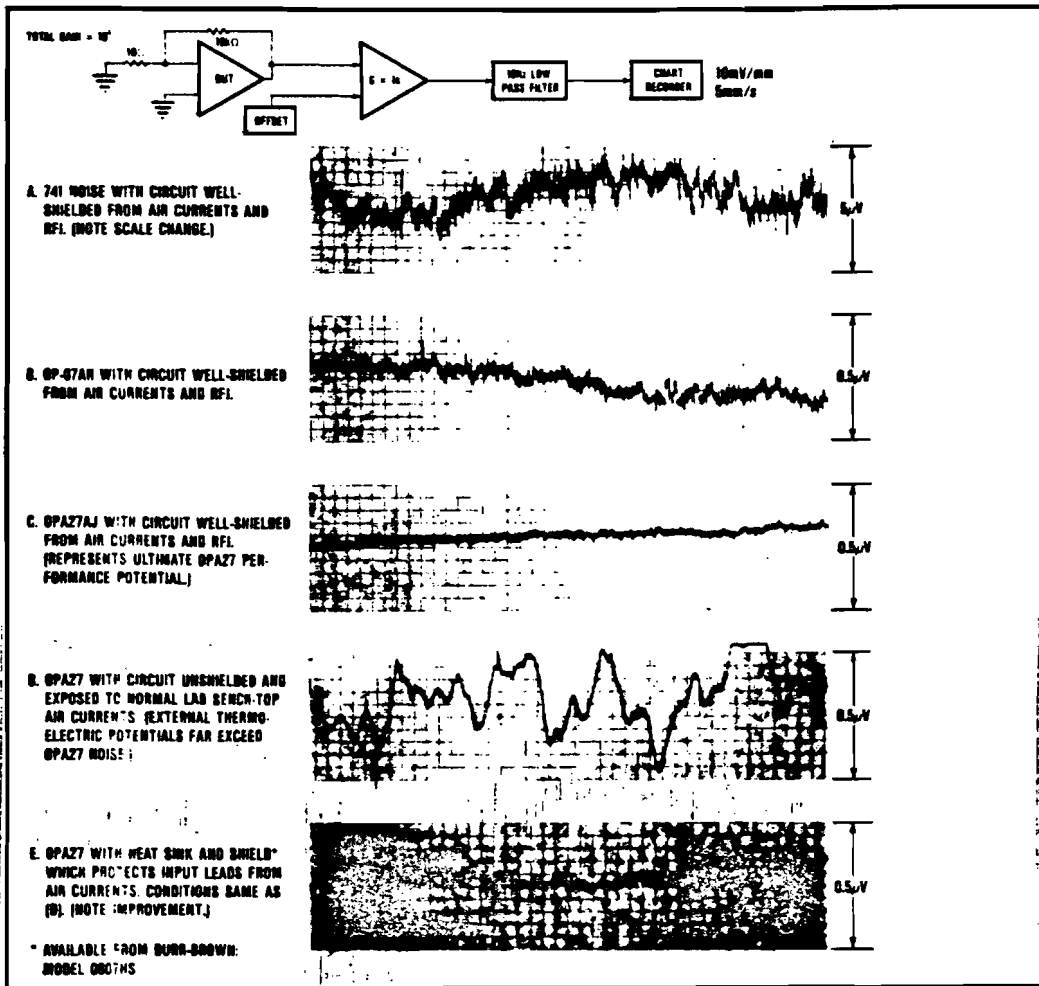


FIGURE 11. Low Frequency Noise Comparison.

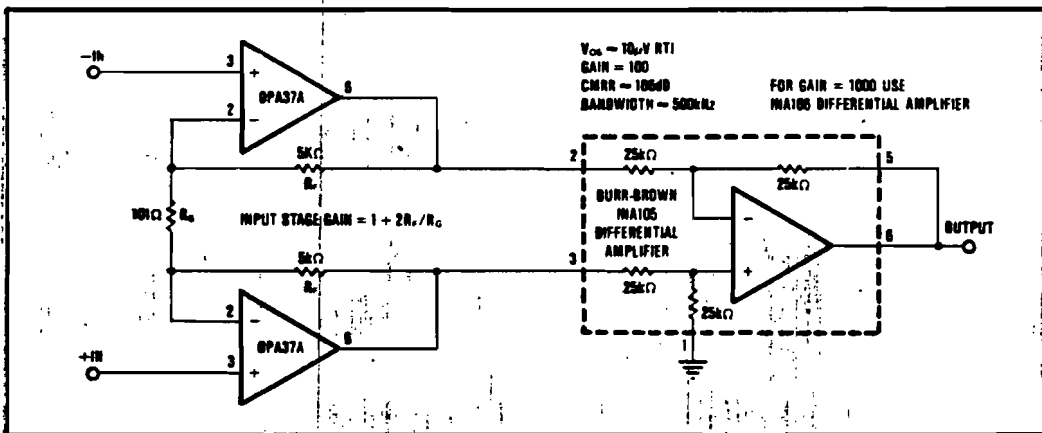


FIGURE 12. Low Noise Instrumentation Amplifier.

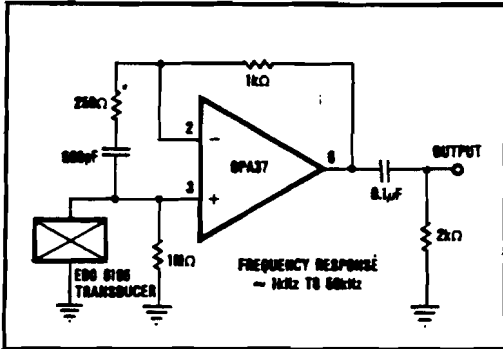


FIGURE 13. Hydrophone Preamplifier.

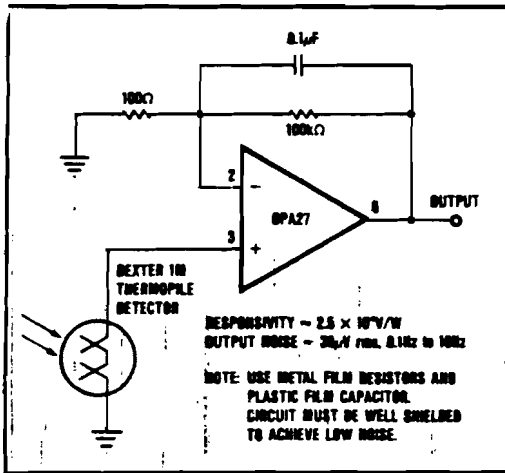


FIGURE 14. Long-wavelength Infrared Detector Amplifier.

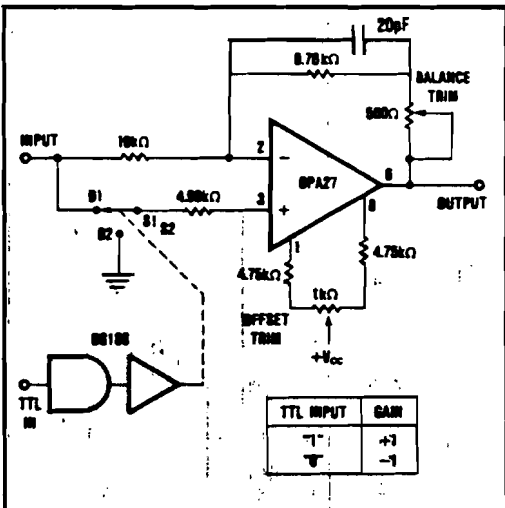


FIGURE 15. High Performance Synchronous Demodulator.

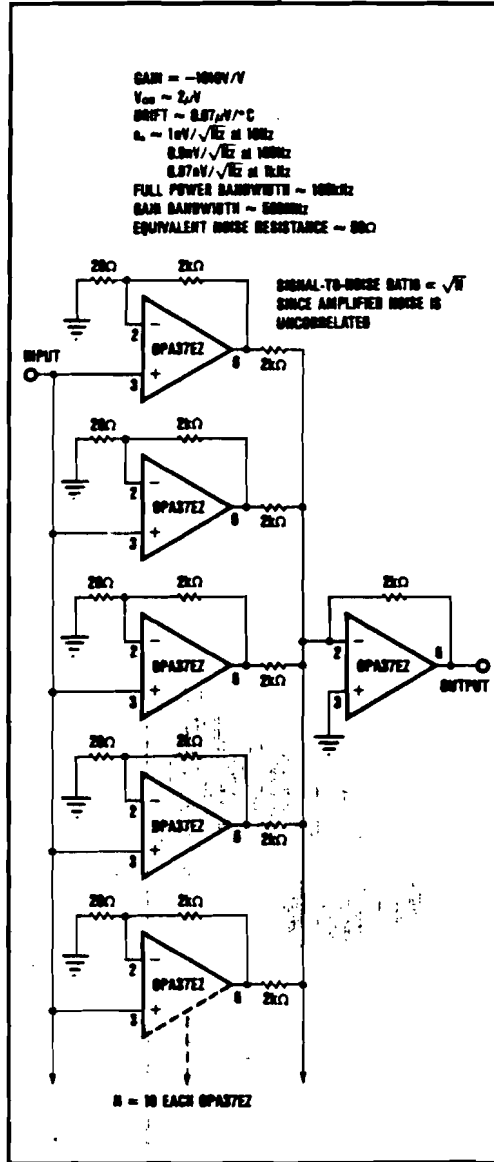


FIGURE 16. Ultra-low Noise "N" Stage Parallel Amplifier.

OPA27/37

2

OPERATIONAL AMPLIFIERS

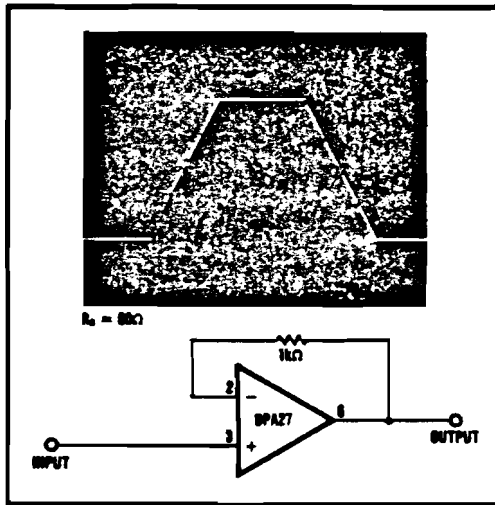


FIGURE 17. Unity-Gain Buffer.

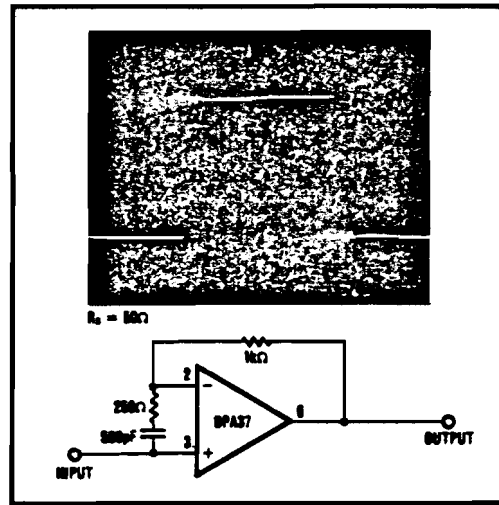


FIGURE 18. High Slew Rate Unity-Gain Buffer.

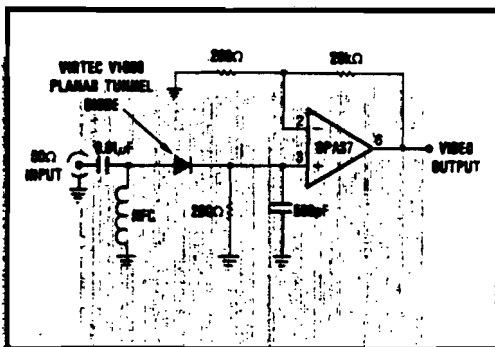


FIGURE 19. RF Detector and Video Amplifier.

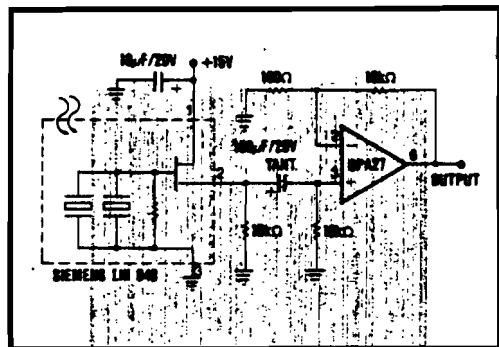


FIGURE 20. Balanced Pyroelectric Infrared Detector.

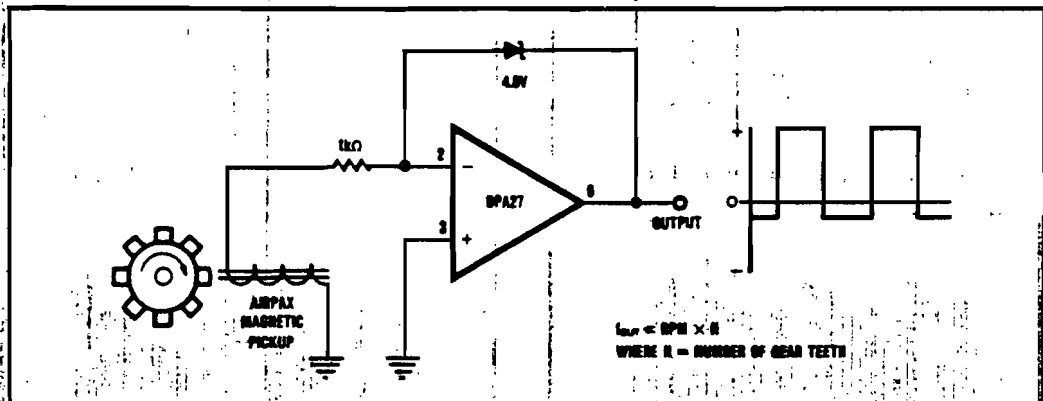


FIGURE 21. Magnetic Tachometer.